



**NTNU – Trondheim**  
Norwegian University of  
Science and Technology

# Development of Cross Cart Front Suspension

**Magnus Fløttum Bjerkaker**  
**Thomas Christiansen**

Master of Science in Product Design and Manufacturing

Submission date: June 2012

Supervisor: Terje Rølvåg, IPM

Norwegian University of Science and Technology  
Department of Engineering Design and Materials



THE NORWEGIAN UNIVERSITY  
OF SCIENCE AND TECHNOLOGY  
DEPARTMENT OF ENGINEERING DESIGN  
AND MATERIALS

**MASTER THESIS SPRING 2012  
FOR  
STUD. TECHN. MAGNUS FLØTTUM BJERKAKER  
OG THOMAS CHRISTIANSEN**

**UTVIKLING AV FORHJULOPPHENG TIL CROSS CART  
Development of Cross Cart front suspension**

The Cross Cart project is a part of an ongoing collaboration between Revolve NTNU and Petter Solberg Engineering (PSE). PSE is establishing the framework for production of Cross Carts, starting with the development of a prototype. The project is an important part of a common goal of Revolve NTNU and Petter Solberg; to promote motorsport engineering in Norway.

Cross Cart as a motorsport has been driven in most Nordic countries since the early 90's, and is becoming bigger every year. Due to a relatively open set of rules there exists few standards for the design of the carts. Such a standard is part of what PSE wishes to establish, while helping to popularize cross carting as an entrance sport for potential rally drivers.


The main task of this master's thesis is to develop a front suspension concept for a Cross Cart by using state-of-the-art software and prototyping techniques to evaluate and improve on knowledge collected from earlier testing.

1. Define a requirement specification for the front suspension.
2. Evaluate different front suspension concepts (double A-arms/Mc Pherson etc) with respect to the requirement specification.
3. Select and optimize a front suspension concept based on virtual testing.
4. If there is time and resources; implement the solution on a cross cart.

The thesis should include the signed problem text, and be written as a research report with summary both in English and Norwegian, conclusion, literature references, table of contents, etc. During preparation of the text, the candidate should make efforts to create a well arranged and well written report. To ease the evaluation of the thesis, it is important to cross-reference text, tables and figures. For evaluation of the work a thorough discussion of results is appreciated.

Three weeks after start of the thesis work, an A3 sheet illustrating the work is to be handed in. A template for this presentation is available on the IPM's web site under the menu "Undervisning". This sheet should be updated when the Master's thesis is submitted.

The thesis shall be submitted electronically via DAIM, NTNU's system for Digital Archiving and Submission of Master's thesis.

  
Torgeir Welo  
Head of Division

  
Terje Rølvåg  
Professor/Supervisor

 NTNU  
Norges teknisk-  
naturvitenskapelige universitet  
Institutt for produktutvikling  
og materialer

# CONTENTS

1	List of Figures.....	V
2	List of Tables.....	VII
3	Preface.....	1
4	Abstract .....	2
6	Revolve NTNU.....	3
7	Petter Solberg and Petter Solberg Engineering .....	4
8	Cross Cart .....	5
9	Software .....	7
10	Coordinate System .....	7
11	Suspension geometry design aspects: .....	8
11.1	Wheelbase: .....	8
11.2	Track width.....	9
11.3	Camber.....	9
11.3.1	Kinematic camber alteration.....	10
11.4	Toe.....	11
11.5	Kingpin og Scrub Radius.....	11
11.6	Caster and Mechanical Trail.....	12
11.7	Instant Centers and Roll Center .....	12
11.8	Effects of the Suspension Variables .....	13
11.9	Steering rod location.....	14
11.10	Anti features.....	15
11.11	Ackermann steering geometry .....	16
12	Product Requirements .....	17
13	Short-Long-arm Front suspension modeling.....	19
13.1	Front View Geometry.....	19
13.2	Side view geometry.....	20
13.3	Control Arm geometry .....	21
13.4	Steering Rod Location and Ackermann Geometry .....	23
14	Base Design Development.....	25
14.1	Wheel Base .....	25
14.2	Track Width.....	25

14.3	Roll center .....	25
14.4	Roll camber .....	25
14.5	Front View Geometry.....	26
14.6	Side View Geometry.....	26
14.7	Base geometry .....	27
15	Spring and Damper Actuation .....	28
16	Optimizing Kinematics.....	33
16.1	Motions.....	33
16.1.1	Roll.....	33
16.1.2	Pitch.....	33
16.1.3	Heave.....	34
16.1.4	Steering .....	34
16.1.5	Heave and Bump test .....	34
16.1.6	Turn and Heave test .....	34
16.2	Optimizing Control Arm Geometry .....	36
16.2.1	Turn and heave test .....	36
16.2.2	Heave test.....	48
16.3	Optimizing Steering Rack and Tie Rod Placements .....	50
17	Final Front Suspension Geometry .....	57
18	Kinematics; New vs. Old .....	59
19	Suspension Dynamics.....	64
19.1	Springs.....	64
19.2	Damping.....	66
19.3	FEDEM .....	71
20	Anti-Roll Bar.....	81
21	Results .....	87
22	Future work .....	88
23	Summary .....	89
24	Sammendrag .....	90
25	Bibliography.....	91

# 1 LIST OF FIGURES

Figure 1 – Oliver Solberg racing his cross cart .....	5
Figure 2 – Coordinate system.....	7
Figure 3 – Wheelbase .....	8
Figure 4 – Camber in relation to slip angle .....	9
Figure 5 – Camber change rate .....	10
Figure 6 – Key geometric features .....	11
Figure 7 – Front view.....	12
Figure 9 – Tie rod location.....	14
Figure 8 – Wheel tracking due to scrub radius .....	14
Figure 10 – Anti dive explained .....	15
Figure 11 – Ackermann.....	16
Figure 12 – Front view geometry .....	20
Figure 13 – Side view geometry .....	21
Figure 14 – Numbering of points for constructing control arm geometry .....	22
Figure 15 – Tie rod placement from above .....	23
Figure 16 – %Ackermann formula .....	24
Figure 17 – Front view.....	26
Figure 18 – Pull rod vs push rod .....	29
Figure 19 – Push rod option .....	30
Figure 20 – Ariel Atom front suspension detail .....	30
Figure 21 – Longitudinal push rod.....	31
Figure 22 – Longitudinal pull rod .....	31
Figure 23 – Final spring/damper concept, optimumK .....	32
Figure 24 – Final spring/damper concept, NX 7.5.....	32
Figure 25 – Pitch center.....	33
Figure 26 – Heave and bump test, heave.....	34
Figure 27 – Turn and heave test, heave .....	35
Figure 28 – Turn and heave test, roll .....	35
Figure 29 – Turn and heave test, steering.....	36
Figure 30 – Visualisation of the turn and heave test at 50% motion completion .....	37
Figure 31 - Camber curve for base design.....	38
Figure 32 – Camber curve after Reduced caster, LBJ moved 10mm backwards. ....	39
Figure 33 – Camber curve, LBJ moved another 10 mm backwards.....	40
Figure 34 – Camber curve, LBJ pulled 10 mm inwards .....	41
Figure 35 – Camber curve, LBJ pulled another 10 mm inwards .....	42
Figure 36 – Camber curve, LBJ pulled another 10 mm inwards .....	43
Figure 37 – Camber curve, LCA inner mounts moved 20 mm outwards.....	44
Figure 38 – Camber curve, LCA inner mounts moved another 20 mm outwards .....	45
Figure 39 – Toe curve from heave test illustrating Bump steer .....	45
Figure 40 – Initial steering rack and tie rod placement .....	46

Figure 41 – Modified steering rack and tie rod placement.....	46
Figure 42 – Camber curve after replacment of steering rack .....	47
Figure 43 – Camber curve, shortened LCA 20 mm.....	47
Figure 44 – Camber curve, final control arm geometry .....	48
Figure 45 – Camber curve heave test, final control arm geometry .....	49
Figure 46 – Wheel steering angles at steering wheel lock.....	50
Figure 47 – Initial toe curve.....	51
Figure 48 – Toe curve after 10mm lowering rack 10mm .....	52
Figure 49 – Toe curve after shortening rack 5 on each side .....	53
Figure 50 – Toe curve after another 2 mm shortening on each side.....	54
Figure 51 – Toe curve after raising rack 0.5 mm.....	55
Figure 52 – Toe curve for final tie rod location .....	56
Figure 53 – Final geometry, front view .....	58
Figure 54 – Final geometry, isometric view .....	58
Figure 55 – Generic cross cart geometry, front view .....	60
Figure 56 – Commercially available cross cart geometry, front view .....	60
Figure 57 – Camber curve, heave test.....	61
Figure 58 – Toe curve, heave test .....	62
Figure 59 – Camber curve, turn and heave test.....	63
Figure 60 – Friction damping.....	67
Figure 61 – Velocity damping.....	68
Figure 62 – Damping types.....	68
Figure 63 – Types of damping .....	70
Figure 64 – Upper suspension arm .....	71
Figure 65 – Upper suspension arm detail .....	72
Figure 66 – Triad.....	72
Figure 67 – Ball joint.....	73
Figure 68 – Grounded suspension arms.....	74
Figure 69 – Rocker.....	74
Figure 70 – Mass reaction forces, front wheels. (Illustration) .....	75
Figure 71 – FEDEM suspension model .....	76
Figure 72 – Load application, static compression .....	77
Figure 73 – Underdamped system .....	78
Figure 74 – Calculated damping.....	79
Figure 75 – Critical damping.....	80
Figure 76 – Overdamped system .....	81
Figure 77 – Rocker geometry .....	84
Figure 78 – Rocker link and knife link in side view.....	85



## 2 LIST OF TABLES

Table 1 – Product requirements.....	17
Table 2 – Rack adjustment to eliminate bump steer .....	24
Table 3 – Front upright geometry coordinates, [mm] .....	27
Table 4 – Frame front suspension mounts, [mm].....	27
Table 5 – Front upright geometry coordinates, [mm] .....	36
Table 6 – Frame front suspension mounts, [mm].....	36
Table 7 – Key parameters, base design.....	38
Table 8 – Key parameters, reduced caster, LBJ moved 10mm backwards.....	39
Table 9 – Key parameters, LBJ moved another 10 mm backwards .....	40
Table 10 – Key parameters, LBJ pulled 10 mm inwards.....	41
Table 11 – Key parameters, LBJ pulled another 10 mm inwards.....	42
Table 12 – Key parameters, LBJ pulled another 10 mm inwards.....	43
Table 13 – Key parameters, LCA inner mounts moved 20 mm outwards .....	44
Table 14 – Key parameters, LCA inner mounts moved another 20 mm outwards .....	45
Table 15 – Front upright geometry coordinates, [mm] .....	48
Table 16 – Frame front suspension mounts, [mm].....	48
Table 17 – Tie rod mounts, [mm].....	51
Table 18 – Final tie rod location coordinates, [mm] .....	56
Table 19 – Cart dimensions, [mm] .....	57
Table 20 – Front upright geometry coordinates, [mm] .....	57
Table 21 – Frame front suspension mounts, [mm].....	57
Table 22 – Parameter specification.....	57
Table 23 – Front upright geometry coordinates, [mm] .....	59
Table 24 – Frame front suspension mounts, [mm].....	59
Table 25 – Parameter specification.....	59
Table 26 – Specified criterias vs. achieved values.....	87

### 3 PREFACE

This project report constitutes the 5th grade master thesis for the mechanical engineering study program Product Development and Materials at the Norwegian University of Science and Technology (NTNU).

So many days, so many nights. It has been a struggle, combining the thesis work and building an open wheeled race car with Revolve NTNU. It would not have been possible if not for the projects both being so interesting and rewarding.

The thesis was given by Revolve NTNU, our Formula Student organization, Petter Solberg Engineering and the Department of Product Development and Materials at NTNU. It would not have been possible if it weren't for our faculty advisor, Terje Rølvåg, who has given us the opportunity to work independently and manage our own progress on our master thesis. Thanks a lot.

Trondheim, June 11, 2012



Magnus F. Bjerkaker



Thomas Christiansen

## 4 ABSTRACT

The very core of motor racing is to *win*. It is a complex activity and at the heart of this activity is reaching the ultimate performance level for the driver-vehicle entity. The driver will always have an advantage when the best possible vehicle is at his disposal. The vehicle suspension is a crucial part that, when designed well, facilitates driver control. The suspension is made to keep the tires firmly planted on the ground so they can be used to the limit of their potential. A number of factors influence the design of a vehicle suspension, and most of them influence each other. Because of this vehicle suspension design is a fine art of finding the compromise that will function best for the given vehicle and its competitive environment.

## 6 REVOLVE NTNU

Revolve NTNU is an independent, non-profit, student organization founded in 2010 aiming to represent the Norwegian University of Science and Technology (NTNU) in Formula Student events every year from 2012. The 2012 team consist of 35 students from different departments at NTNU.

The objective of the Formula Student competition is to build a one seated, open wheeled, race car. The competition evaluates environmental, economical and engineering aspects of the car, as well as its performance.

No Norwegian team has yet competed at a Formula Student or Formula SAE event. Revolve NTNU will compete at both Formula Student UK (Silverstone) and Formula Student Germany (Hockenheim) in 2012.

## 7 PETTER SOLBERG AND PETTER SOLBERG ENGINEERING

Petter Solberg is a professional rally driver from Spydeberg, Norway. He started his career in the World Rally Championship driving for Ford, before he became the lead driver for Subaru World Rally Team from 2000 to 2008. His career highlight is victory in the WRC overall title in 2003. Before the 2009 season Subaru withdrew from rallying, and Solberg gathered the financial means to start his own private team which he ran until the 2012 season, where he is back in the Ford World Rally Team again.

Along with his own World Rally Team, Solberg started Petter Solberg Engineering (PSE) in 2010 in Torsby, Sweden. In the 2011 S2000 World Rally Championship PSE ran a team for the Norwegian driver Eyvind Brynildsen, and PSE signed in 2012 with tire manufacturer Hankook to run Patrik Flodin in the 2012 Intercontinental Rally Championship (IRC). PSE is also working on a car for competing in the legendary Pikes Peak Hill Climb rally.

In 2011, Revolve NTNU and Petter Solberg Engineering signed a collaboration agreement aiming to bring Norwegian motorsport and the Norwegian academic community closer together. This has led to members of Revolve NTNU developing a cross cart for PSE, a project which this thesis is a part of. Petter Solberg hopes to make cross cart to rally what go-kart is to Formula 1, a stepping stone for developing driving talents.

## 8 CROSS CART

Cross carting is one of the newest branches of motorsport to take hold in Scandinavia, and is rising greatly in popularity in Norway, Sweden, Denmark, Estonia, Latvia and Lithuania. The sport was developed in the early 1980's in Sweden, inspired by similar vehicles in the US. The concept is driving go-carts on rally cross circuits. In short, cross carting is a kind of mini rally cross; the carts have proper suspensions and roll cages as well as regulated harnesses and safety gear specified in an international rulebook. The carts have steel space frames with motorcycle engines. Some kind of protective bodywork is also required.

The national Norwegian cross cart championship requires a valid cross cart license from Norway, Sweden or Denmark to participate in races (Norges Bilsportforbund, 2012). There are a couple of existing cross cart manufacturers in Norway, in addition to several international ones. Aspiring drivers have the choice of buying a complete cross cart, assembling it themselves with parts from pre-fabricated kits, or constructing a self-built cart from scratch. The races run on tracks with a mixture of gravel and tarmac surfaces with a length between 600 to 1200 meters. The drivers do 3 heats per race with 6 drivers starting in each heat, earning points for a good position in the final.



FIGURE 1 – OLIVER SOLBERG RACING HIS CROSS CART

There are 5 different classes:

- Mini
  - 270ccm, Honda GX 270 4-stroke.
  - Ages 6-11
  - Slip clutch

- No engine tuning
- Top speed limited to 60 km/h
- 85ccm
  - 1 cylinder, 2-stroke
  - Ages 9-13
  - Minimum weight of 230 kg, driver included
  - No engine tuning
  - Top speed limited to 80 km/h
  - Sequential gearbox
- 125ccm
  - 1 cylinder, 2-stroke
  - Ages 12-16
  - Minimum weight of 250 kg, driver included
  - Engine tuning allowed
- 250ccm:
  - 1 cylinder, 2-stroke
  - Ages 15 and up
  - Minimum weight of 270 kg, driver included
  - Engine tuning allowed
- 650ccm:
  - 1 cylinder, 4-stroke
  - Ages 16 and up
  - Braking on all 4 wheels
  - Minimum weight of 295 kg, driver included
  - Engine tuning allowed

The similarities in the different classes and the ease with which the carts can be upgraded enable the drivers to use the same cart throughout their whole career. Usually the only thing that needs to be done to move up a class is to change the engine and adding the required front brakes for the 650ccm class (Norges Bilsportforbund, 2012).

## 9 SOFTWARE

NX7.5, Siemens PLMS, 2009

OptimumK v1.1, Optimum G, 2008.

Fedem R5.0.1, Fedem Technology AS, 2010.

## 10 COORDINATE SYSTEM

The coordinate system used is from OptimumK, and consists of three axes to define the coordinates of the suspension points

- Longitudinal Axis – Points to the forward direction of the vehicle.
- Lateral Axis – Points to the left side of the vehicle.
- Vertical Axis – Points vertically upwards.

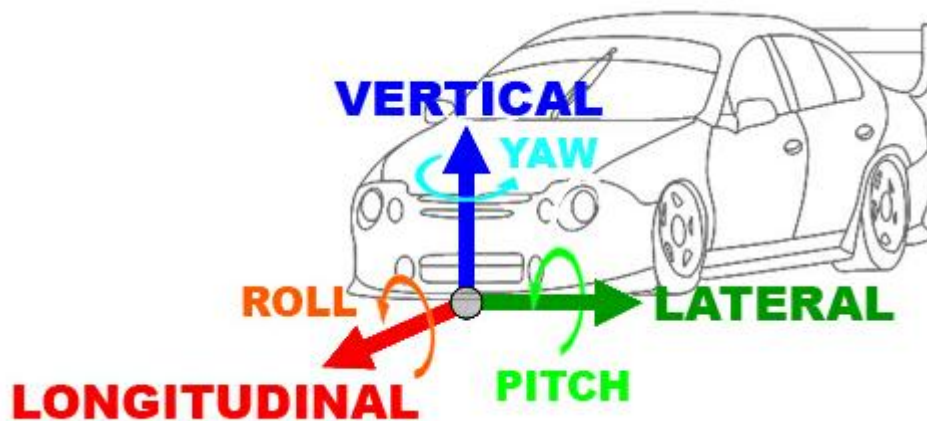


FIGURE 2 – COORDINATE SYSTEM



## 11 SUSPENSION GEOMETRY DESIGN ASPECTS:

This chapter will cover the kinematics required to develop an independent front suspension. Basically it covers how the unsprung mass of a vehicle is connected to the sprung mass. Connections that control the relative motions and the how the forces are transferred from sprung to unsprung mass. Every vehicle needs a specific suspension design depending on its area of use; there is no single best geometry (Milliken & Milliken, 1995).

### 11.1 WHEELBASE:

The length distance between the front and the rear axle of a car is called the wheel base. It is a distance measured from center to center on the two axles. This distance has a large impact on the axle load distribution. A long wheel base relative to the overall vehicle length will result in less load transfer between the axles during acceleration and braking, which in turn allows for softer springs and increased vehicle comfort.

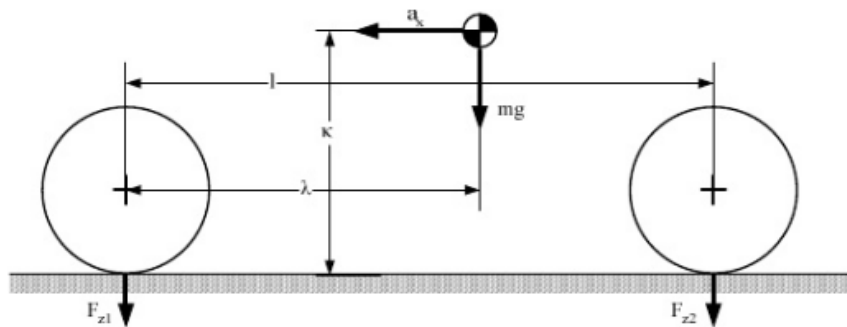


FIGURE 3 – WHEELBASE

The advantage of a smaller wheel base is the easier cornering, due to a smaller swept turning circle for at the same steering angle.

## 11.2 TRACK WIDTH

The front and rear track widths (TW) influence the vehicle's tendency to roll and the cornering behavior. A larger track width reduces the lateral load transfer in corners as shown by Equation 1 and increased stability. The increase in load transfer due to track width can be accommodated for through adjustment and/or fitment of an anti roll bar.

$$F_{z2} = \frac{\mu_{lat} \cdot h_{CG}}{tw_2}$$

EQUATION 1 – LATERAL LOAD TRANSFER

The wider track also requires more lateral movement to avoid obstacles. According to regulations the track cannot allow the outer walls of the tires to be more than 1500mm apart. (Norges Bilsportforbund, 2012)

## 11.3 CAMBER

The camber angle is the angle between a vertical axis and the tilted wheel plane (fig??). When the top of the wheel leans outward relative to the vehicle center axis, the camber is positive. A negative camber angle is measured when the wheel leans inwards. The camber angle affects the tires ability to generate lateral force due to friction. A cambered rolling pneumatic wheel generates a lateral force in the direction of the tilt. When the slip angle is zero, and this force occurs, it is referred to as *camber thrust*. A cambered wheel also contributes to an increase in the lateral forces produced by the wheel when cornering the vehicle.

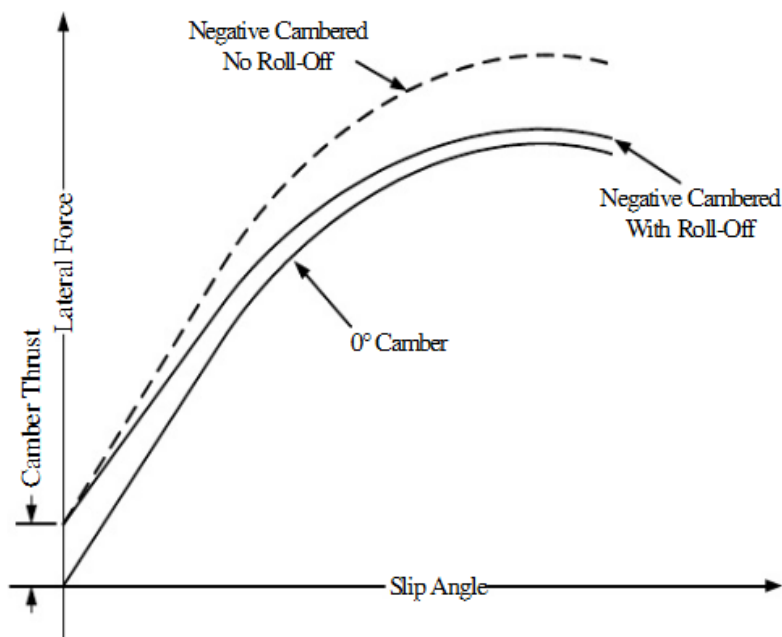


FIGURE 4 – CAMBER IN RELATION TO SLIP ANGLE

This is true as long as the tire shows linear behavior. If this linear range is exceeded the effects of the camber inclination will decrease, an effect called *Camber Roll-off*. Due to this roll-off effect the difference in lateral force is small when comparing a cambered and a non-cambered wheel at 5-10% of maximum slip angle. A difference which is much larger at zero slip angles due to the camber thrust.

### 11.3.1 KINEMATIC CAMBER ALTERATION

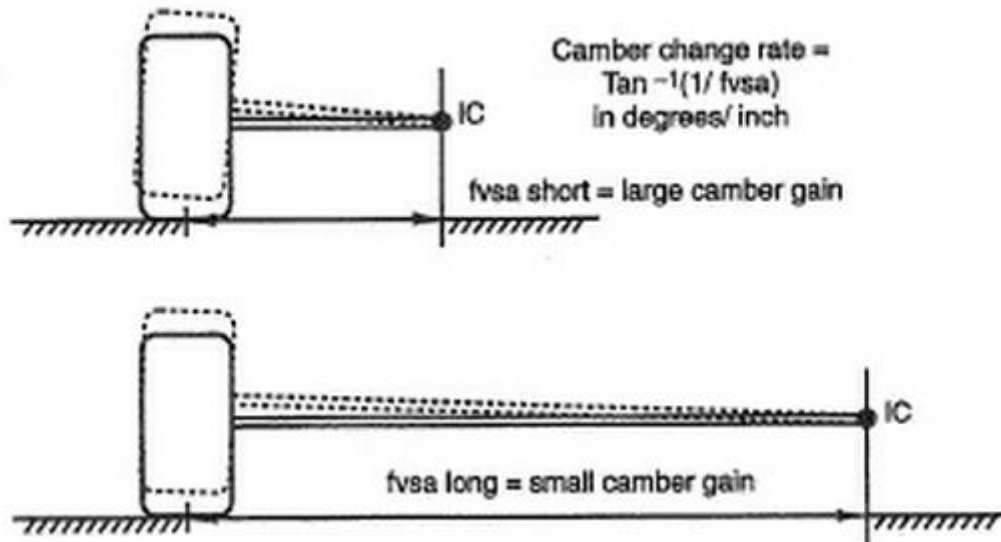


FIGURE 5 – CAMBER CHANGE RATE

Due to the geometry of independent wheel suspensions, the wheels incline with the body and the outer wheel tends to gain a positive camber alteration which in turn reduces the lateral grip of the tire. This kinematic effect is taken into account when designing the suspension model by designing for negative camber alteration at bump and positive at heave.

The lateral distance from the contact patch center to the IC in front view is called the *front view swing arm (fvsa)*. The *camber change rate* is a function of the fvsa length. In Figure 5 the upper and lower control arms are replaced with a single swing arm from the knuckle to the instant center. The camber change rate can then be calculated as a function of wheel travel:

$$\text{Camber change rate} = \tan^{-1} \frac{1}{fvsa}$$

EQUATION 2 – CAMBER CHANGE RATE

This means that a short fvsa results in large camber gains, while increasing the fvsa length decreases the camber gain. This linear relation can be altered to a more complex curve by

altering the length of the upper or lower control arm in relation to the other. This keeps the same fvs length at ride height, but shortens or lengthens it as the wheel travels.

## 11.4 TOE

Toe is measured as an angle between the longitudinal axis of the vehicle and the static angle of the wheel. If the front part of the wheels is closer to the center axis than the rear of the wheels, the vehicle has toe-in on that wheel axle. If the front of the wheel is further out, it is called toe-out. A minimum of static toe is desired to reduce unnecessary tire wear, uneven tire heating and rolling resistance due to the tires working against each other. The amount of static toe on the front axle depends on factors like camber, compliance in the steering, bump and roll steer, and implementation of Ackermann steering geometry.

Toe is adjusted to compensate for handling difficulties like over steer and under steer. Turn in can be improved by adding rear axle toe-out. As the car turns in the loads transfer to the outer wheel which in turn causes over steer.

## 11.5 KINGPIN OG SCRUB RADIUS

The kingpin in a solid front axle is the axis of which the wheel pivots. In modern independent suspension systems, the kingpin is replaced by two or more ball joints which define the steering axis. It is never vertical or centered on the tire contact patch for a number of reasons.

There are different parameters that define the kingpin location. In front view, the *Kingpin inclination* (KPI) is the angle between a vertical axis and the line drawn between centers of the upper (UBJ) and lower (LBJ) ball joints. *Spindle length* is defined as the distance between the kingpin axis and the wheel center plane at axle height. The distance between the steering axis intersecting the tire contact plane and center of the wheel is the *Scrub radius*. The scrub radius describes the amount of lateral motion on the tire relative to the ground that results from vertical motion of the wheel.

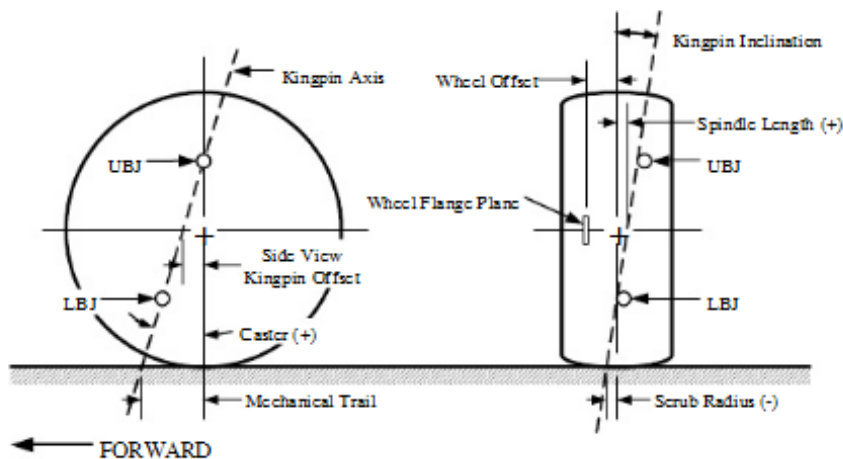


FIGURE 6 – KEY GEOMETRIC FEATURES

## 11.6 CASTER AND MECHANICAL TRAIL

In side view the kingpin angle is called *caster angle*. If the kingpin axis does not pass through the wheel center, *side view kingpin offset* is present. With the presence of *mechanical trail* the tire contact patch follows behind the steering axis in side view. The trail is the distance from the center of the tire contact patch to where the kingpin axis intersects the contact plane.

## 11.7 INSTANT CENTERS AND ROLL CENTER

An *instant center* (IC) is a momentary center of which the suspension linkages pivot around. The instant center moves as the suspension bumps or heaves and changes geometry.

“Instant” refers to a particular position of the suspension linkages, while “center” refers to the imaginary point that effectively is the pivot point of the linkages at that instant. The instant centers can be constructed in both front view and side view.

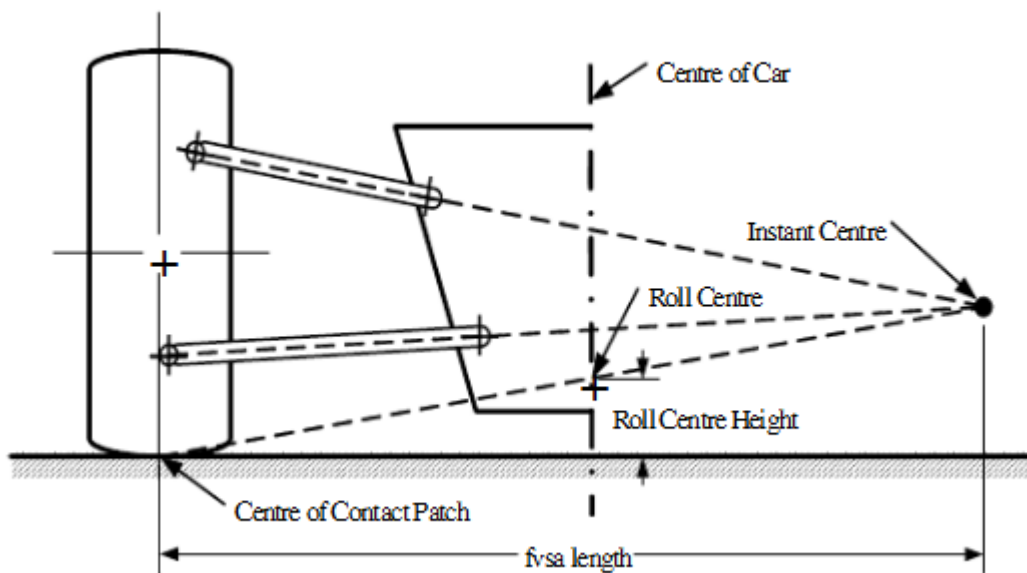


FIGURE 7 – FRONT VIEW

If an instant center is constructed by extending the lines that intersect the UBJ and the upper control arm (UCA) inner pivot point, and equivalent for the lower control arm (LCA). The instant center is where these two lines intersect. A line from the instant center to the center of the tire contact patch establishes the front view *roll center* height where it intersects the center line of the vehicle. The same procedure can be done for the other side of the front view, which then establishes the lateral position. The roll center doesn't need to be at the center of the vehicle, i.e. if there is unsymmetrical suspension or when evaluating the suspension during cornering. Consequently the roll center height is determined by the height of the instant centers.

The roll center is the location of the center of the *sprung mass* of the vehicle. It determines the force coupling between the sprung and unsprung mass of the vehicle. During cornering

centrifugal force acting on the vehicle's center of gravity (COG) can be translated down to the tires where the reactive lateral forces are built up according to Newton's 3<sup>rd</sup> law. This generates a rolling moment around the roll center, which causes the body of the vehicle to roll. A lower roll center will generate a larger rolling moment than for a high roll center. This rolling moment is ultimately counteracted by the springs. The height of the roll center determines the amount of roll resistance from the springs.

A roll center above ground level will allow the lateral force from the tires to generate a moment about the IC. This moment causes *jacking*, a phenomenon where the moment about the instant center lifts the sprung mass. Equally a roll center below ground causes the car to be pushed downwards. In either case the lateral force on the tires causes a vertical deflection of the sprung mass, the *horizontal-vertical coupling effect*.

## 11.8 EFFECTS OF THE SUSPENSION VARIABLES

Establishing KPI, spindle length, scrub and trail are usually subject to compromise between performance and packaging requirements. An understanding of how the different geometric measurements affect handling is therefore needed:

Positive spindle length will always raise the car up as the wheels are turned for cornering regardless of the direction steered, except when the KPI is zero. An increase in KPI away from vertical will increase the raising of the car when steering. Equally an increase in spindle length for a constant KPI This raising effect stimulates self centering steering at low speeds. KPI also affects the steer-camber characteristics. With a KPI inwards in the vehicle the wheel will lean outwards and generate positive camber when steered. The amount is small, but the effect is not neglectable if the track contains numerous tight corners. Traditionally the KPI has been around 12 degrees, now down to around 7 degrees (Dixon, 2009). Bumps on the road surface lead to longitudinal forces at the center of the wheel. This in turn causes kickback into the steering proportional to the spindle length, where a spindle length of zero will eliminate the kickback. For cross cart then, a fairly short spindle length is desirable.

An increase in mechanical trail causes an increase in the steering moment around the steering axis because of the increased moment arm for the lateral forces on the tire. This causes a self centering effect at speed. Larger trails results in larger steering forces required to turn the car. The mechanical trail should not be too large compared to the *pneumatic trail*, as the pneumatic trail approaches zero as the tire approaches its slip angle. This directly decreases the self centering torque, which gives a signal to the driver that the tire is near "breakaway" (initiation of under steer). This "breakaway signal" might be reduced in effect by too large mechanical trail compared to the pneumatic trail.

The caster angle will also the wheel to rise and fall with steer, but is (unlike the KPI/scrub effect) opposite from side to side. Following from this is both roll and weight transfer when cornering which leads to over steer. Caster angle also affects steer-camber. Positive caster

will cause negative camber on the outer wheel and positive on the inner will, consequently both wheels leans into the corner which is favorable.



FIGURE 8 – WHEEL TRACKING DUE TO SCRUB RADIUS

If there is scrub in the front suspension, the wheels will not follow a straight line on a rough road. This lateral motion will induce significant velocity components to the forward velocity and change the tire slip angle. This results in lateral disturbance of the handling. Hence scrub is highly relevant to a cross cart front suspension design, which is used on fairly rough grounds with lots of suspension travel. For rough road tracking it is preferable with negative scrub. The larger the scrub the stronger kickback in the steering wheel on rough terrain.

### 11.9 STEERING ROD LOCATION

The *steering rod* or *tie rod* is the linkage between the wheel and the steering rack. Its placement is crucial to avoid *bump steer* effects. Bump steer is a change in toe angle due to wheel travel. It can change a vehicles direction unexpectedly when riding over uneven ground, which is common in cross carting. Bump steer is eliminated through aligning the tie rod axis to intersect the front view instant center. The easiest way to assure this is to place the tie rod in the plane of the UCA or LCA. The grey areas in Figure 9 indicate a placement of the steering rack, and in turn the tie rod relative to the wheel center, which in turn will ensure a tendency towards under steer rather than over steer due to unavoidable camber compliance. A low placement in front of the wheel center, or high placement behind, also ensures toe-out due to lateral force deflection in the steering rack which leads to more stability when cornering. This might occur i.e. if the A-arms are insufficiently stiff.

The length of the lever arm between the outer tie rod end to the kingpin axis and the steering rack ratio determines the wheel steering angle in relation to the rotation of the steering wheel.

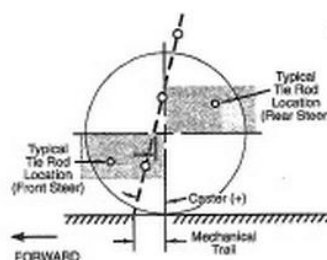


FIGURE 9 – TIE ROD LOCATION

## 11.10 ANTI FEATURES

*Anti features* refers to geometrical properties working against the longitudinal-vertical force coupling between the sprung and unsprung mass. The anti features are purely related to the slope of the *side view swing arm*. The anti features are only present during acceleration and braking; hence it does not affect the steady-state load transfer at the tire.

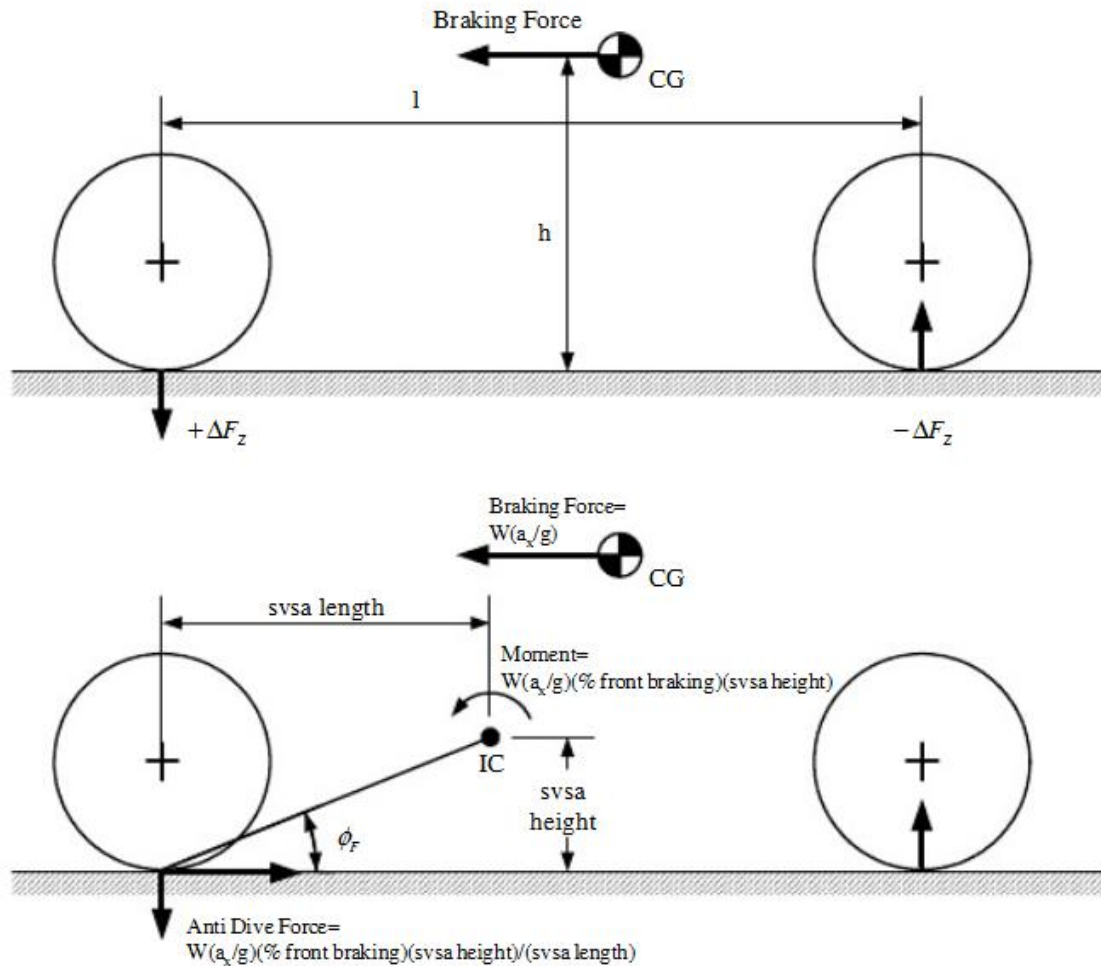


FIGURE 10 – ANTI DIVE EXPLAINED

The load transfer is a function of the wheelbase  $l$ , CG height  $h$ , and the acceleration or braking forces as seen in Figure 10. The anti features changes the amount of load transferred through the springs, and in turn the vehicles pitch behavior. Pro features are possible, but uncommon and not preferable for racing purposes. There are 3 different anti features for a rear wheel drive vehicle:

- Anti-dive – reduces bump deflection under forward braking.
- Anti-squat – reduces bump travel during forward acceleration.
- Anti-lift – reduces suspension droop in rear suspension during forward braking.



They are all measured in percent, i.e. will a front suspension set up with 100% anti-dive not deflect at all due to braking since no load will pass through the springs. With 0% anti-dive the front suspension will deflect according to spring stiffness since all of the transferred loads will pass through the springs.

The percentage of anti-dive can be calculated through the following equation:

$$\% \text{ anti dive} = \% \text{ front braking} \cdot \tan\theta_f \cdot \frac{l}{h}$$

EQUATION 3 – ANTI DIVE PERCENTAGE

11.11 ACKERMANN STEERING GEOMETRY

When cornering a vehicle the inner and outer wheel will have different distances to travel through the corner. During slow cornering, where forces due to accelerations are negligible, the steering angle  $\alpha$  needed to make a turn with radius R:

$$\alpha = \frac{l}{R}$$

EQUATION 4 – STEERING ANGLE

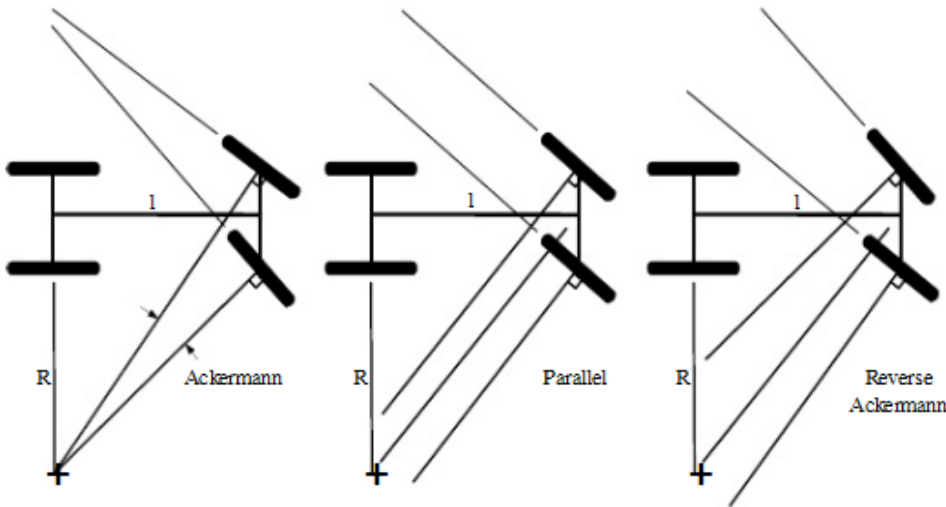


FIGURE 11 – ACKERMANN

If both wheels have concentric turning circles about the same center, the vehicle has *Ackermann steering geometry*. The kinematics of this results in toe-out on the outer wheel when cornering. With *Parallel steer* both wheels have the same steering angle  $\alpha$ . *Reverse Ackermann geometry* requires the outer wheel to have a larger steering angle than the inner wheel. Passenger cars usually have Ackermann steering to make low speed cornering easier for the driver. By accommodating this geometry feature in vehicles subject to low lateral accelerations the wheels are allowed to roll freely with low or no slip angle at all, because the wheels are steered about a coinciding turning centers. The high lateral accelerations of a race car results in significant slip angles, and in turn much higher loads on the outer wheels

due to lateral load transfer. Less slip angle is required to reach peak cornering force for a tire under low loads. In consequence, using Ackermann steering geometry on a race car would cause the inner tire to be dragged along at a higher slip angle than needed causing an increase in slip angle induced drag and an increase in tire temperature and tire wear. Hence the common practice to incorporate parallel steering or reverse Ackermann on race cars (Milliken & Milliken, 1995).

## 12 PRODUCT REQUIREMENTS

After talking to Petter Solberg Engineering and examining one of their cross carts, a product requirement specification for the front suspension was established. The specifications are set within the rules and regulations of cross cart racing (Norges Bilsportforbund, 2012) and with the intent of improving the performance of the cart. Some of the specifications originate from theoretical best practices and recommendations; others represent crucial design goals. Dynamic properties such as camber change and amounts of roll are difficult to specify to start with, specifications as these originate from analyses of previous designs.

TABLE 1 – PRODUCT REQUIREMENTS

Requirement	Specification
Max length (tire-tire)	2100 mm
Max outer width (tire-tire)	1500 mm
Bump steer/ Toe change	Less than 0.05 degree over the full suspension travel
Ackermann steering angle	Neutral or slightly reversed
Scrub radius	15 mm – 40 mm
Mechanical trail	0 mm – 20 mm
Kingpin inclination	3 deg – 15 deg
Caster angle	0 deg – 4 deg
Minimum suspension travel	Above +/- 70mm
Ground clearance	Above 100 mm
Roll steer	Less than 0.4 degrees per degree of body roll
Roll center	50 mm – 100 mm
Steering ratio	85 mm rack travel per steering wheel revolution
Static camber	0 degrees
Static toe	0 degrees
Wheel camber <sup>1</sup>	-0.5 deg – 0.5 deg
Steering angle	20 deg – 30 deg
Anti dive	40% – 50%
Rocker Motion ratio	Less than 1.2
Max roll angle	2 degrees

<sup>1</sup> At maximum turn with maximum bump

In addition there were several non-measurable concerns that needed addressing:

High loads directed through unfavorable paths in a structure result in bending moments and stress concentrations, particularly in joints and links in different parts of the vehicle. This is also the case in the cross cart, PSE have had problems with end rods breaking, especially on the lower a-arm, which is subject to high loads from the spring/damper unit. This problem will be addressed by carefully considering where loads travel through the suspension and into the car.

Minimizing unsprung mass is a key aspect of suspension design; the weight of the suspension components themselves is proportional to the forces directed into the vehicle's chassis. The cross cart suspension is not especially heavy, but one of the requirements is to increase the strength and lifespan of the components without increasing the unsprung mass.

To increase the roll stiffness and adjustability of the suspension system an anti roll bar concept needs to be evaluated.

A suspension design is not necessarily perfect from the start, which is why the central properties of the suspension need to be somewhat adjustable. Camber, caster and toe angles should be relatively easy to change within certain intervals.

The tires used on the front suspension are 165/70-10 Maxxis C9272, and the wheels are 10"x7" of unknown type. The inner diameter of the wheel available for suspension packaging is 235 mm. The offset of the wheel can be built to specification. The tire OD is 430 mm.

The cross cart weight is 260 kg, with a front-rear weight distribution of 42-58. This puts the Center of gravity (CoG) 908 mm rearwards of the front axle. It is assumed to be centered on the longitudinal axis of the cart, and 350 mm above ground.

## 13 SHORT-LONG-ARM FRONT SUSPENSION MODELING

The task of modeling any suspension development is primarily based on packaging constraints. Before establishing the positions of the UBJ and LBJ, the track width, wheel base, wheel size, tire size, brakes, springs, dampers, etc all need to be kept in mind. The cross cart front suspension design will be based on a short-long-arm design, referring to the different lengths of the upper and lower control arms. This is the design choice because of its ability to achieve desired performance objectives with minimum compromise. (Milliken & Milliken, 1995)

The SLA geometry is based on the position of the lower ball joint, which is given by the desired parameters in the preceding paragraph. The upper ball joint is then determined either by scrub radius or kingpin angle requirements. An additional design freedom is the knuckle length. A *short knuckle* means that the upper ball joint is located within the diameter of the wheel. To reduce the loads on the suspensions components it is desirable to increase the kingpin length by spacing the upper and lower ball joints further apart. Usually this leads to a *tall knuckle* design, where the upper ball joint is located outside the wheel diameter. This increases the ball joint span, thus reducing the reaction loads in the control arms and other suspension components. This allows for reasonable kingpin angles, while still allowing the preferred spindle length and scrub radius. The tall knuckle design has higher structural requirements to the knuckle design, but build errors will lead to smaller geometrical changes than with a short knuckle.

The current cross cart suspension design has trouble with high loads breaking the control arms. A tall knuckle design will be used to increase the life cycle for the suspension assembly without requiring greater dimensions on control arms and ball joints.

### 13.1 FRONT VIEW GEOMETRY

Reserving space for brakes define the left over space to fit the upper and lower ball joints. The front view instant center is determined by the desired roll center height and front swing arm length. Equation 5 defines the front swing arm length, to ensure proper roll camber characteristics.

$$fvsa = \frac{\frac{tw}{2}}{1 - roll\ camber} = \frac{\frac{tw}{2}}{1 - \frac{wheel\ camber\ angle}{chassis\ roll\ angle}}$$

EQUATION 5 – FRONT VIEW SWING ARM LENGTH

A line is projected from the center of the tire contact patch, through the roll center, and to

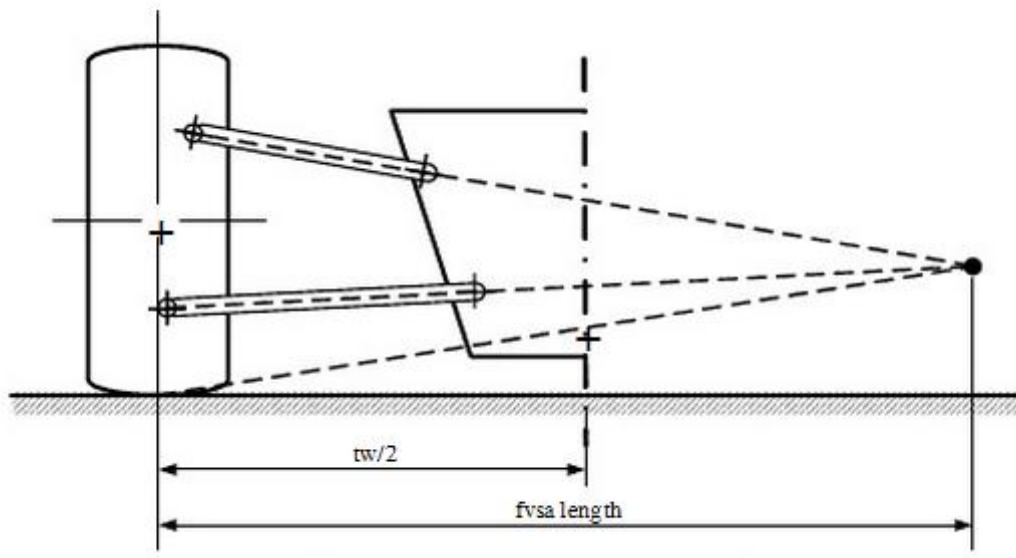


FIGURE 12 – FRONT VIEW GEOMETRY

the fvsa length. This determines the position of the front view instant center. Projected lines from the upper and lower ball joints to the instant center, defines the planes in which the control arms centerlines should lie. The length of the LCA should be as long as possible, but is limited by packaging requirements. In the traditional cross cart design the pedal box sits between the LCAs. The design also needs to take frame torsional stiffness into account. Too much deflection in the frame gives unwanted kinematic changes while driving. The UCA's length in relation to the LCA length now determines the camber change curve. If the UCA and LCA inner mounts are on the same vertical line, the camber/wheel travel curve will be a linear function. The desired camber change curve is progressive concave towards negative camber with much less camber change (even into positive cambers) in droop. This is achieved with a shorter UCA. The curvature increases, as the UCA gets shorter.

The front view geometry is finished by roughly placing the steering rack and rod. This should lie along a line through the tie rod outer point projecting into the front view instant center. A tie rod along this line ensures a linear ride toe curve, but doesn't indicate the final tie rod placement.

## 13.2 SIDE VIEW GEOMETRY

The side view geometry has its own instant center, which lies in the plane of the wheel centerline. The instant center is attended to first in side view, and depends on the desired anti features, the side view swing arm (svsa) length and wheel path under bump. The angle  $\phi$  in Figure 13 is calculated from the desired anti features by Equation 3. Side view swing arm length determines the longitudinal wheel travel during bump, and combine with the angle  $\phi$  to establish the side view instant center as seen in Figure 13.

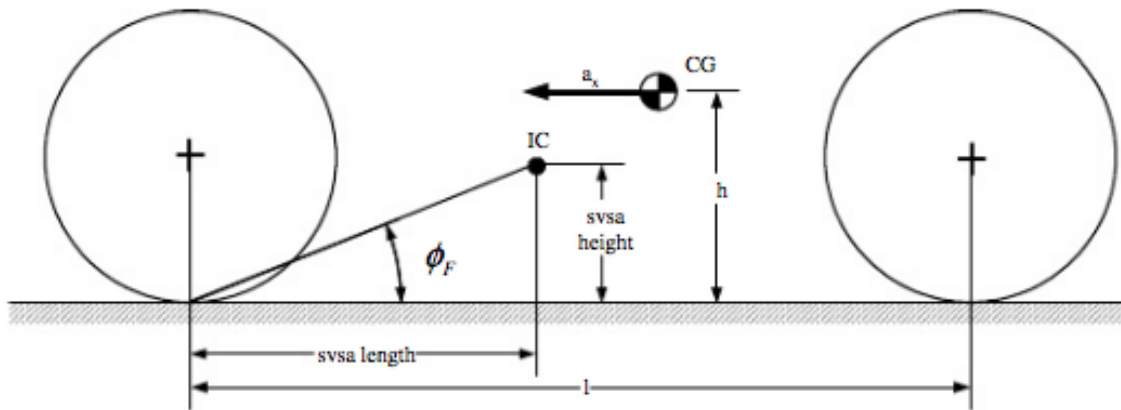


FIGURE 13 – SIDE VIEW GEOMETRY

### 13.3 CONTROL ARM GEOMETRY

To find the inner mounting points for the control arms, *Race car vehicle dynamics by Milliken/Milliken* describes a projection method to link up the front and side view geometries that has been established so far. The method builds on two geometrical cornerstones; three points determine a plane and the intersection of two planes forms a straight line. This will be used to determine the three dimensional geometry of the front suspension.

- #1 Upper control arm inner pivot point
- #2 Upper ball joint
- #3 Extension into the longitudinal plane
- #11 Lower control arm inner pivot point
- #12 Lower ball joint
- #13 Extension into the longitudinal plane

These points are transferred into the side view in Figure 14. Lines are projected from #3 and #13 to the instant center. A point #4 is established on this line a few inches from the instant center. Same procedure to determine point #14 before these two is projected into front view. A line is projected between point #2 and point #14 as far inboard as #1, and repeat for point #12 through point #14 until point# 11.

It is desirable to have inner pivot points of the control arms parallel to the centerline of the vehicle. A vertical line is therefore drawn in front view through point #1 to form the front projection of the UCA axis. A point #5 is placed on this line where the vertical axis intersects the extension of points #2 and #4, equally a point #15 for defined by #11, #12 and #14. Lines

projected between points #1 and #5, and #11 and #15, are where the control arm pivot points needs to be located. The opening between the pivot points can be varied.

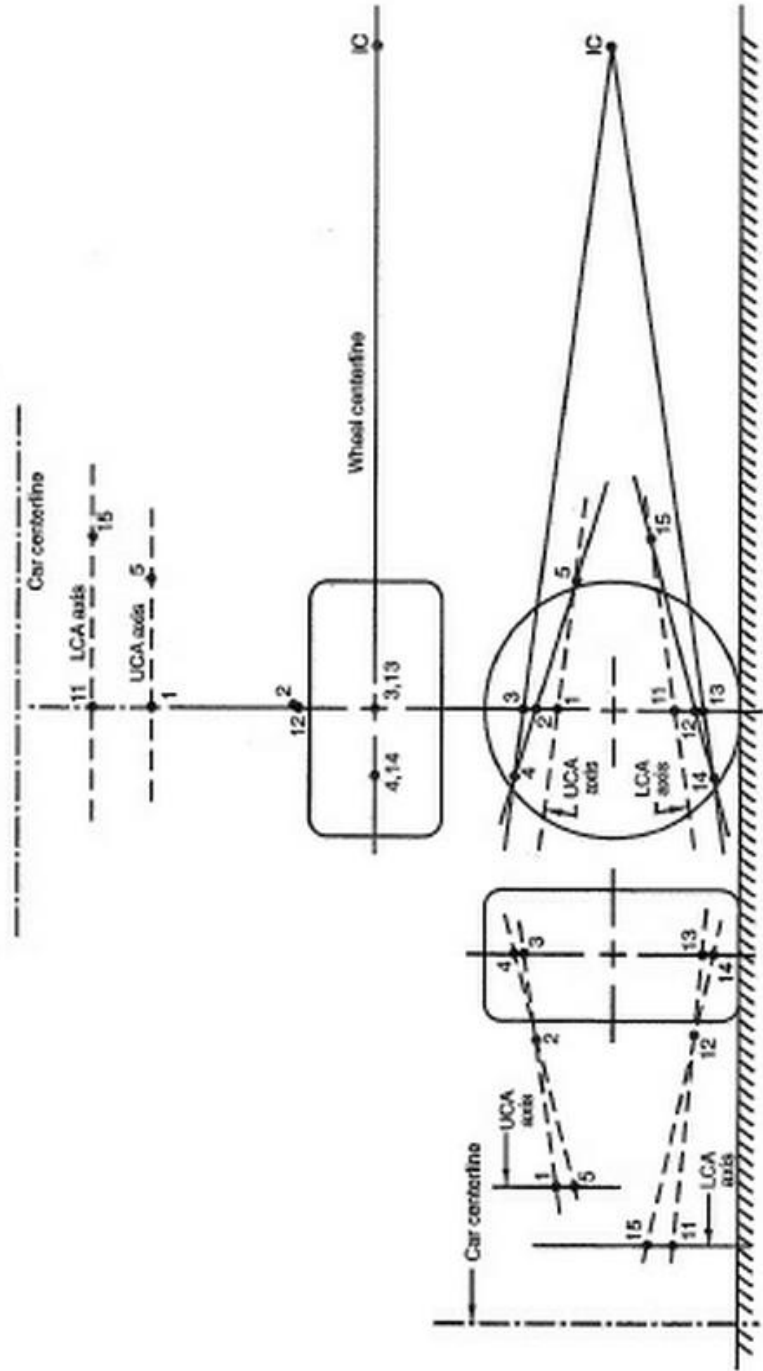


FIGURE 14 – NUMBERING OF POINTS FOR CONSTRUCTING CONTROL ARM GEOMETRY

## 13.4 STEERING ROD LOCATION AND ACKERMANN GEOMETRY

Bump steer affects the predictability of the vehicles handling, and should be reduced to an absolute minimum. The placement of the tie rod is crucial, but its placement is restricted by several packaging of requirements. To leave as much space as possible for the driver, the steering rack needs to be positioned in front of the frame. This determines the position of

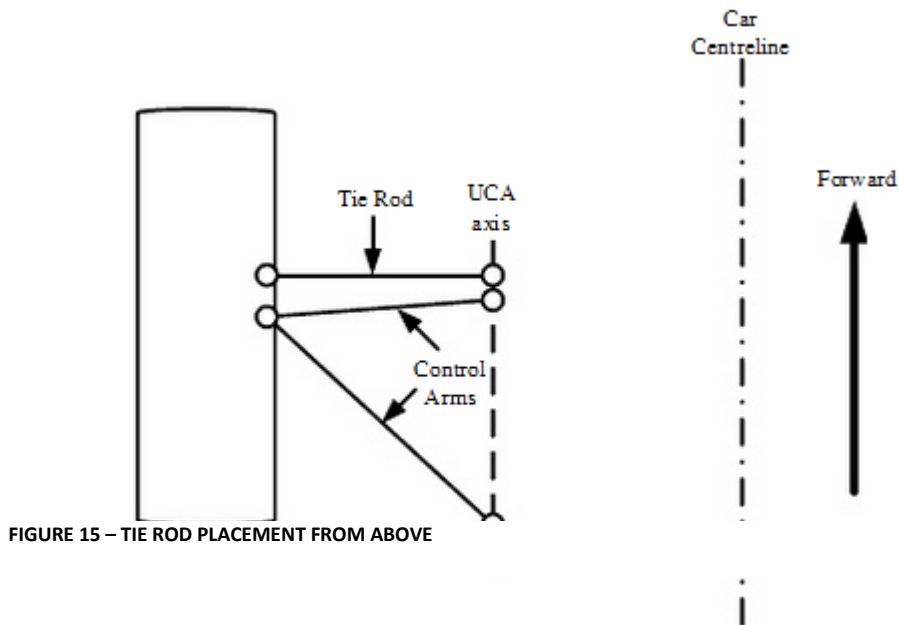


FIGURE 15 – TIE ROD PLACEMENT FROM ABOVE

the inner pivot points of the tie rod. The outer tie rod ball joint placement is dependant of the amount of Ackermann and the steering ratio wanted from steering wheel to wheel. For the cross cart it is desirable to have adjustable Ackermann geometry due to the varying track profiles it will be used on. Low speed, high grip, tight corners will have an advantage of 100% Ackermann, but at higher speeds Ackermann is not preferable at all. The cross cart will be set up with a base design with 0 % Ackermann. Adjustments from the baseline design will be built in the suspension components. The placement of the tie rods in front of the control arms will lead to the unwanted compliance effects. Placing the tie rod behind the control arms would change this around, but then the adjustability of the Ackermann geometry would be limited.

The Ackermann percentage is calculated as seen in Figure 16.



**%Ackerman**

%Ackerman is calculated using the following formula.

$$\delta_{\text{inside } 100} = \text{TAN}^{-1} \left[ \frac{\text{WB}}{\frac{\text{WB}}{\text{TAN}(\delta_{\text{outside}})} - \text{Tr}} \right] - \delta_{\text{outside}}$$

WB = Wheelbase  
Tr = Front Track

$\delta_{\text{inside } 100}$  = Inside Steer for 100% Ackerman  
 $\delta_{\text{inside}}$  = Inside Steer  
 $\delta_{\text{outside}}$  = Outside Steer

$$\% \text{ Ackerman} = \frac{\delta_{\text{inside}} - \delta_{\text{outside}}}{\delta_{\text{inside } 100\% \text{ Ackerman}}} \times 100$$

FIGURE 16 – %ACKERMANN FORMULA

When fine tuning bump steer, following table is useful (Staniforth, 2010):

TABLE 2 – RACK ADJUSTMENT TO ELIMINATE BUMP STEER

Bump	Droop	Rack adjustment
Toe-in	Toe-out	Raise forward mounted R&P
Toe-out	Toe-in	Lower forward mounted R&P
Toe-out	Toe-out	Lengthen forward mounted rack bar
Toe-in	Toe-in	Shorten forward mounted rack bar

## 14 BASE DESIGN DEVELOPMENT

The kinematic development of the cross cart front suspension was done in Optimum K kinematics software. A base setup was made using a tall knuckle lay out to reduce the loads on the a-arms due to brake torque.

### 14.1 WHEEL BASE

The NBF cross cart rules and regulations states a maximum length of 2100 mm between the extremities of the front and rear wheels. The wheel base is set to 1610 mm, which including wheels gives a length of 2080 mm. This results in the lowest amount of load transfer between the front and rear axles possible, and leaves as much room as possible for vehicle packaging, within the current regulations.

### 14.2 TRACK WIDTH

The track was chosen to be as wide as possible within the rules and regulations of cross cart. The rules state that the maximum allowable width of the cart including tire width is 1500 mm. Taking into account a 7 inch wide front wheel, the track width was set to 1305mm, which results in an overall width of 1483 mm. The track width was chosen as wide as possible to lower the camber change rate as much as possible since the cross cart suspension requires quite a lot of wheel travel. (Norges Bilsportforbund, 2012)

### 14.3 ROLL CENTER

A roll center height of 65 mm, right in the middle of the design specifications, was chosen as a design basis.

$$\text{roll stiffness, geometry} = \frac{\text{roll center height}}{\text{Center of Gravity height}} = \frac{65 \text{ mm}}{350 \text{ mm}} = 19 \%$$

EQUATION 6 – ROLL STIFFNESS

With a center of gravity assumed to be 350 mm above ground, it results in approximately 19 % roll stiffness due to geometry and 81% is due to ARB and springs.

### 14.4 ROLL CAMBER

It is preferred to have a roll camber close to 1, so that the camber gain due body roll is neutralized as much as possible. We chose a roll camber base of 0.95, since 1 gives an infinite fvsa length. The fvsa length with 0.95 roll camber is calculated in Equation 7:

$$\text{fvsa length} = \frac{\frac{1305 \text{ mm}}{2}}{1 - 0.95} = 13050 \text{ mm}$$

EQUATION 7 - FVSA LENGTH

## 14.5 FRONT VIEW GEOMETRY

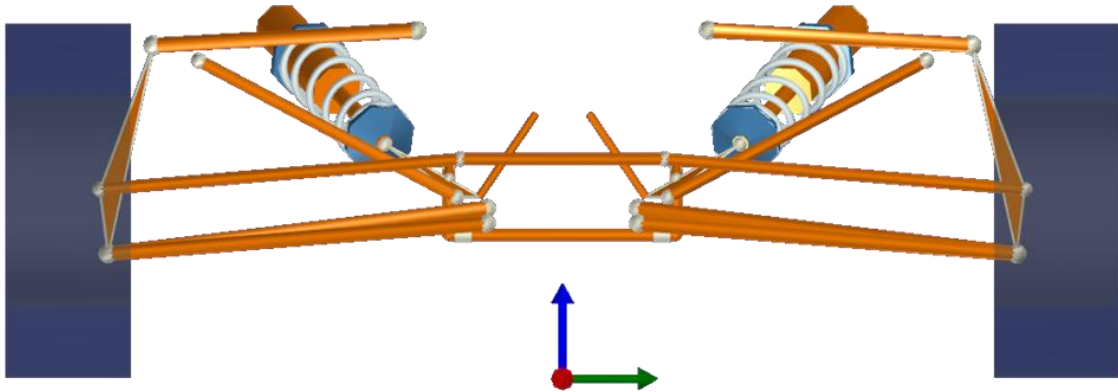


FIGURE 17 – FRONT VIEW

Figure 17 shows the planes on which the upper and lower control arms should lie. The LCA inner mounts are in-line and placed at +/- 100 mm in y-direction. This position allows a long LCA, while still leaving some space for the frame to have torsion-resistant cross section in the front. The upper arms are placed at +/- 200 mm in y-direction to start with. This position determines the camber curve, and will be optimized through kinematic analysis.

The tie rod and steering rack are roughly placed, but its position is also determined through kinematic analysis to avoid bump steer.

## 14.6 SIDE VIEW GEOMETRY

The traditional cross carts suffers from diving during braking, and talks with Petter Solberg indicate that the front suspension is bottoms out during hard braking. The first step of establishing side view geometry is creating an instant center, which is a function of side view swing arm length and anti features.

Since anti-dive is a function of front braking, the design specification states approximately 50% anti-dive for 50% front braking.

Frame design makes it preferable to have level mounts on the UCA, which puts the inner UCA mounts at 460mm above ground. Svsa was set to length of 4600 mm. The anti dive percentage is calculated below:

$$\theta_f = \tan^{-1} \frac{460}{4600} = 5.71^\circ$$

EQUATION 8 – SIDE VIEW ANGLE

$$\% \text{ anti dive} = 50\% \cdot \tan \theta_f \cdot \frac{l}{h} = 50\% \cdot \tan 5.71 \cdot \frac{4600}{460} = 50\%$$

EQUATION 9 – ANTI DIVE

## 14.7 BASE GEOMETRY

From the above mentioned dimensions, the base geometry was developed using the method described in section 10. It resulted in the suspension points in table??

TABLE 3 – FRONT UPRIGHT GEOMETRY COORDINATES, [MM]

Point of interest	X	Y	Z
Wheel center	805	652.5	235
Upper ball joint	800.5	540	440
Lower ball joint	822.5	625	165
Tie rod outer joint	882.5	611	230

TABLE 4 – FRAME FRONT SUSPENSION MOUNTS, [MM]

Point of interest	X	Y	Z
Upper control arm - front	872.5	200	460
Upper control arm - rear	600.5	200	460
Lower control arm - front	872.5	100	205
Lower control arm - rear	600.5	100	225
Tie rod inner joint	882.5	160	280

## 15 SPRING AND DAMPER ACTUATION

When designing a double-wishbone suspension system one has the liberty to locate the dampers and springs in a number of ways. The most common location, especially on road cars, is direct actuation. This means that the wheel's loads are transferred into the spring/damper directly, through being connected either on the wheel upright or one of the wishbones on one end and the car's frame on the other. The current PSE cross cart uses a direct actuation form of suspension. This kind of location is by far the simplest and most straightforward, but increases the unsprung mass of the suspension. Depending on the wheel base and type of vehicle, direct actuation can also be less favorable because of the need to place the spring/damper in an angle relative to the vertical movement of the wheel. The axis of the spring/damper should run as parallel to the wheel movement as possible, and preferably through the center of the contact patch between the wheel and the ground. This is mostly a problem on open-wheel race cars where the wishbones extend outwards of the car's body, and therefore lacks appropriate anchoring points for the springs/dampers. The steeper the angle in towards the frame, the less of the unit's potential deformation can be utilized, which should ideally be a 1:1 ratio of motion, meaning that for example 5 cm upwards (bump) motion on the wheel gives a 5 cm compression of the unit.

With higher performance in racing comes a need for better suspension designs, and an essential factor in the quest for better handling is reducing unsprung mass. The spring/damper unit, being one of the heaviest components of a car's suspension, should be moved in towards the centerline of the car. This also helps to concentrate more weight closer to the vehicle's center of gravity, which further improves handling and balance. There are two main ways to transfer the movement of the wheel into the now inboard spring/damper unit, push or pull rods. These concepts are illustrated in Figure 18.

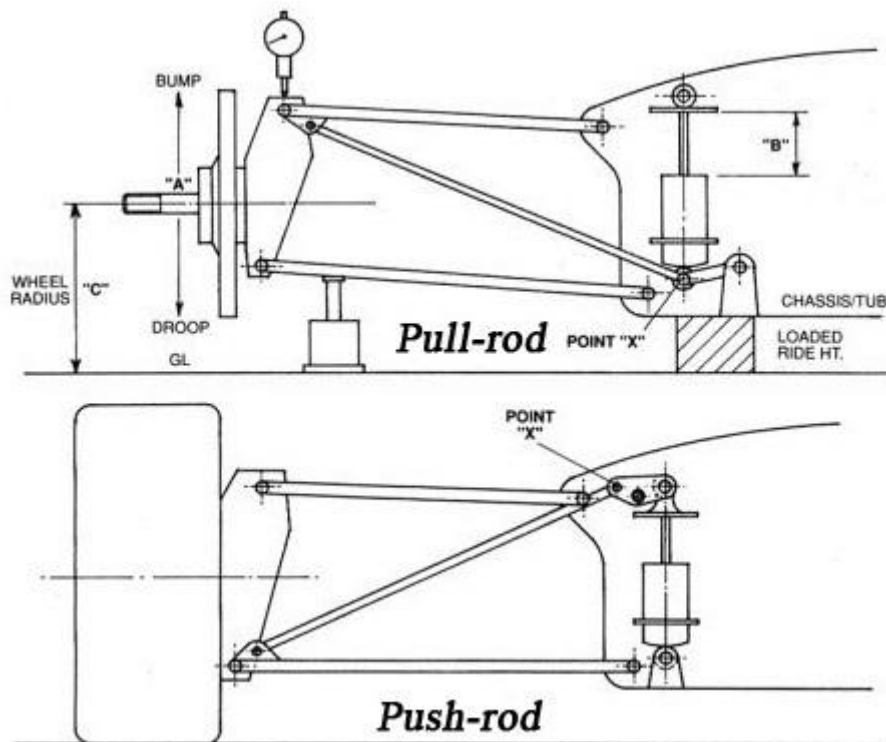


FIGURE 18 – PULL ROD VS PUSH ROD

They function in the same way, using a rod-link to transfer loads from the wheel to the spring/damper through a rocker with a pivot axis. This axis can be modified to enable rotation around almost any point, so that the spring/damper unit is not constricted to any particular location. By varying the geometry of the rocker unit, the desired ratio of motion as well as progressive or degressive spring behavior can be achieved.

Progressive springs are springs that increase their spring rate when they are compressed in such a way that the relationship between load applied and spring deformation is no longer linear. This means that the more a progressive spring is compressed, the harder it becomes compress further. A degressive spring behaves the opposite way. These spring characteristics can be mimicked in the rocker itself, by varying the geometry of the angles the forces go through around the rocker pivot axis.

The pushrod option is traditionally considered to be the best, mainly because of it being relatively simple and understandable. Pull rods are, dynamically speaking, preferred when possible because it improves the center of gravity by placing the spring/damper unit low in the body. In a cross cart, a pushrod suspension is difficult because of the pedal box and steering rack already taking up much space in the very narrow front section of the frame. This is especially the case with the typical vertical orientation of the very tall spring/damper. Such a setup means that the frame of the kart has to be raised in the front to accommodate a proper rocker attachment, as shown in Figure 19. Transversely mounted units are also out of the question because of their length.

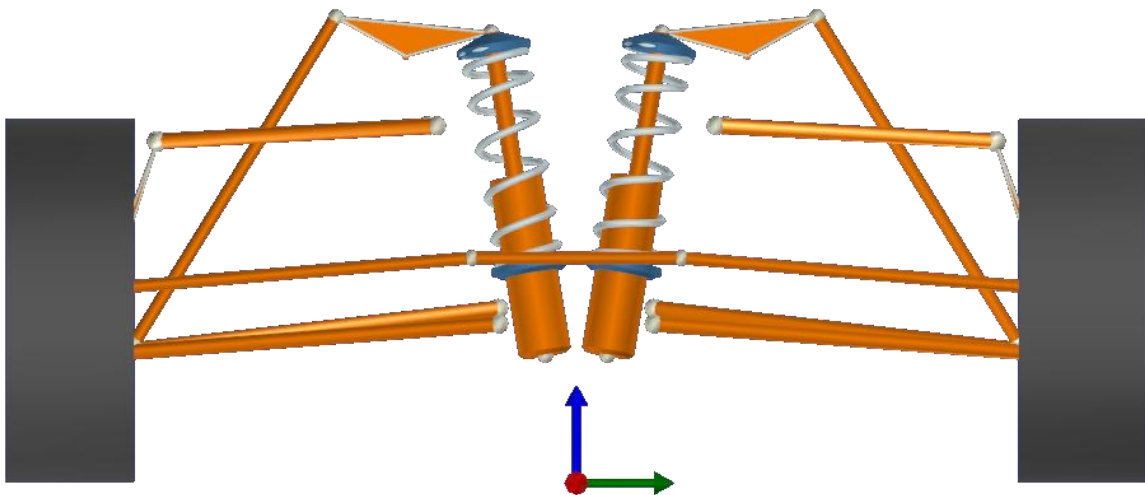


FIGURE 19 – PUSH ROD OPTION

Another option is longitudinally oriented springs/dampers, as seen on for example the Ariel Atom in Figure 20.



FIGURE 20 – ARIEL ATOM FRONT SUSPENSION DETAIL

A downside to the longitudinal setup is that the load path from the front springs has to end on a traversing tube, which exposes the tube to high moment and torque stresses. Another downside is that the 1:1 motion ratio requirement means that the spring/damper unit needed to be located high in the vehicle to make the necessary angle on the push rod possible. This is illustrated in Figure 21.

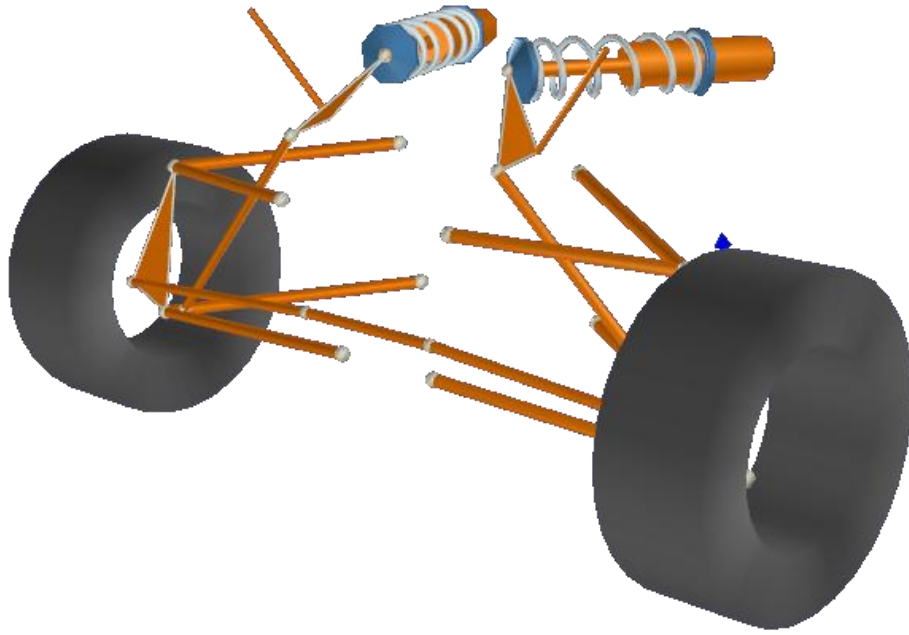


FIGURE 21 – LONGITUDINAL PUSH ROD

After considering several push rod options, focus was turned to pull rods. The first pull rod was placing the spring/damper unit along the bottom of the cart, placing the weight very low and feeding loads into the frame longitudinally. This setup is shown in Figure 22. It was however apparent that this setup would not work, due to packaging issues. The rocker pivot axis becomes unnatural in relation to the movement of the wheel, and the rocker collides with the lower a-arm when it is actuated.

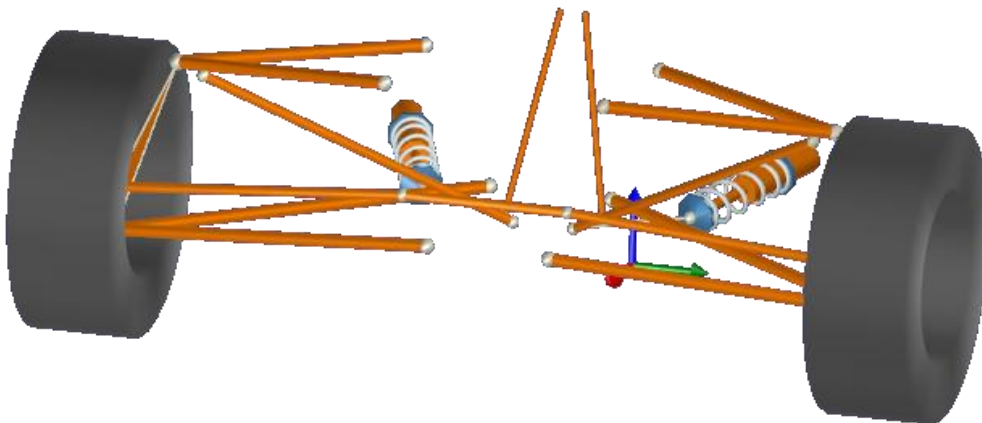


FIGURE 22 – LONGITUDINAL PULL ROD

Several iterations of this design finally resulted in the spring/damper unit slightly raised from the bottom of the frame, and attached at an angle up and out towards the top of the cart. This gave the required motion ratio with a steep enough pull rod, and makes attachment of



the rocker and spring/damper unit to the frame relatively easy. This setup is shown in Figure 23 and Figure 24 in Optimum K and NX 7.5 respectively. The NX model was made to able to visualize the system and to export meshed models to FEDEM for dynamic analysis.

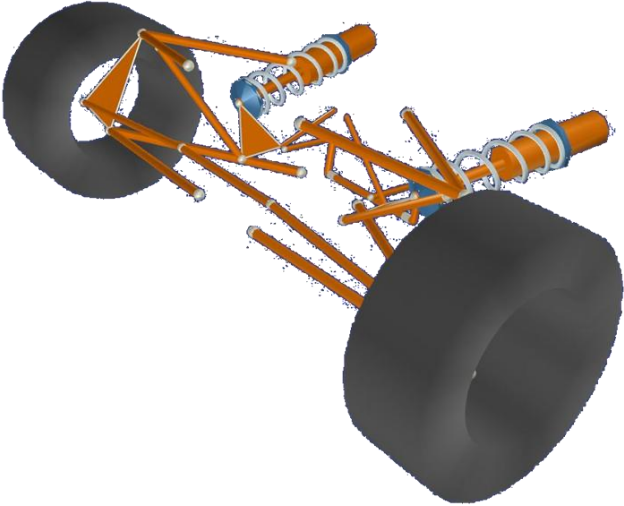


FIGURE 23 – FINAL SPRING/DAMPER CONCEPT, OPTIMUMK

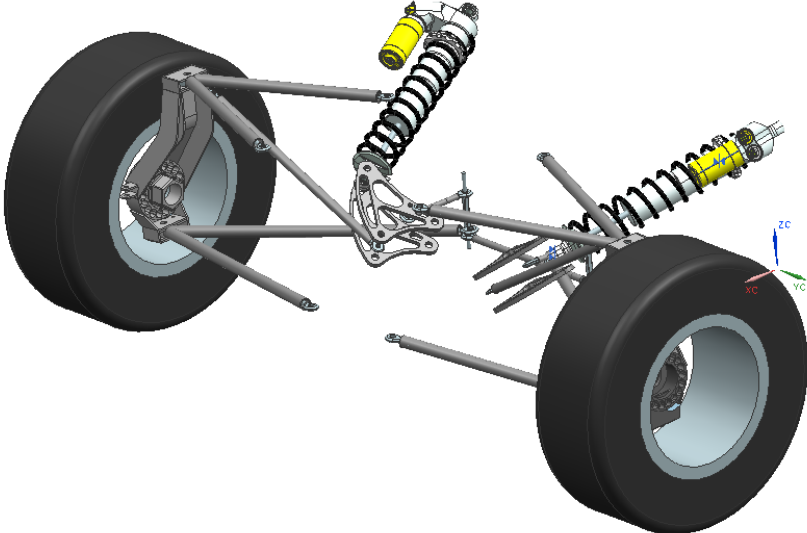


FIGURE 24 – FINAL SPRING/DAMPER CONCEPT, NX 7.5

This setup actuates the lightest end of the spring/damper unit, increasing the responsiveness of the system. With angling the units out from the center of the cart they follow the natural widening of the frame rearwards to the cockpit area.

## 16 OPTIMIZING KINEMATICS

Optimizing the kinematics is a game of compromises. The following objectives were prioritized when optimizing the kinematics using Optimum K:

- Toe-in/toe-out below 0.05 degrees during straight line driving over maximum bump, to eliminate bump steer.
- Wheel camber always between +/-1 degree; even during the sharpest turn with maximum body roll.

Two simple tests were used to optimize the kinematics, based on the 3 of the 4 motions defined in Optimum K.

### 16.1 MOTIONS

A simulation is defined by 4 different motions in Optimum K;

- Roll (deg)
- Pitch (deg)
- Heave (mm)
- Steering (deg)

The duration of the simulation is defined from 0% to 100% motion.

#### 16.1.1 ROLL

Roll motion is the motion where the vehicle chassis rotates around the roll axis. It is defined by the suspension geometry, and is the line between the front and rear roll center. The roll axis moves as the suspension moves. Positive roll is defined to the right when the vehicle is viewed from the rear.

#### 16.1.2 PITCH

Pitch is the motion where the chassis rotates around the pitch axis, which in 2D lies at the pitch center. The pitch center is formed by the intersection of the lines connecting the tire contact patches and the Instant Center at the opposite end, as seen in Figure 25 – Pitch center:

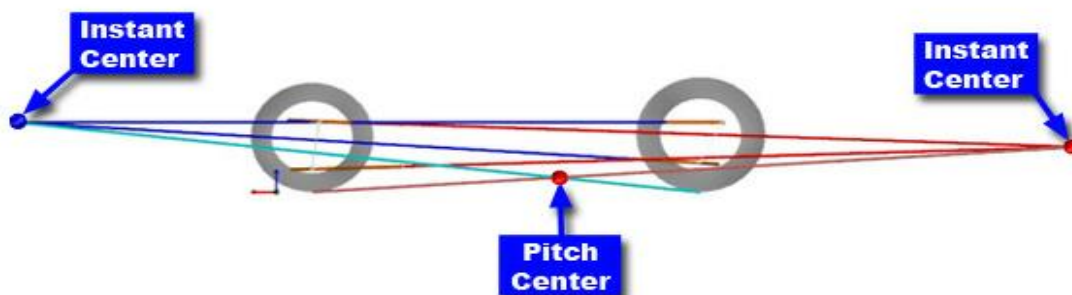


FIGURE 25 – PITCH CENTER

### 16.1.3 HEAVE

Heave is the vertical displacement of the chassis. This movement is described as heave when the chassis moves upwards compared to the wheels and bump when it moves downwards.

### 16.1.4 STEERING

Steering refers to the angular displacement of the wheels around the steering axis. The steering input is in rotation of the steering wheel, which translates into wheel steering angle through the selected steering ratio.

### 16.1.5 HEAVE AND BUMP TEST

The heave and bump test is a basic simulation in which the wheels were configured to hit both maximum heave and maximum bump over a set motion. The heave and bump test was configured as following:

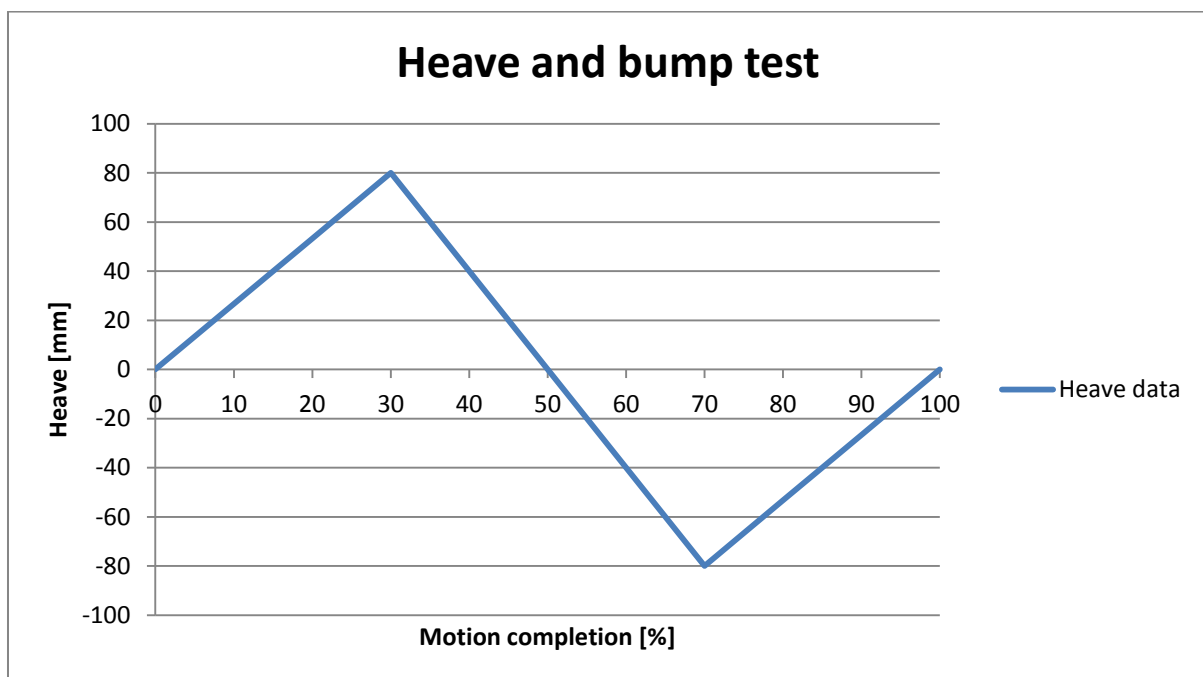


FIGURE 26 – HEAVE AND BUMP TEST, HEAVE

### 16.1.6 TURN AND HEAVE TEST

In the turn and heave test, the vehicle chassis is subjected to both heave and roll under maximum steering. The test reaches 80 mm bump, 2 degrees roll to right and 135 degrees steering lock to the left at 50% motion. This simulates a left hand turn while deflecting the suspension. The suspension is symmetric, so there is no use in simulating the equivalent right hand turn.

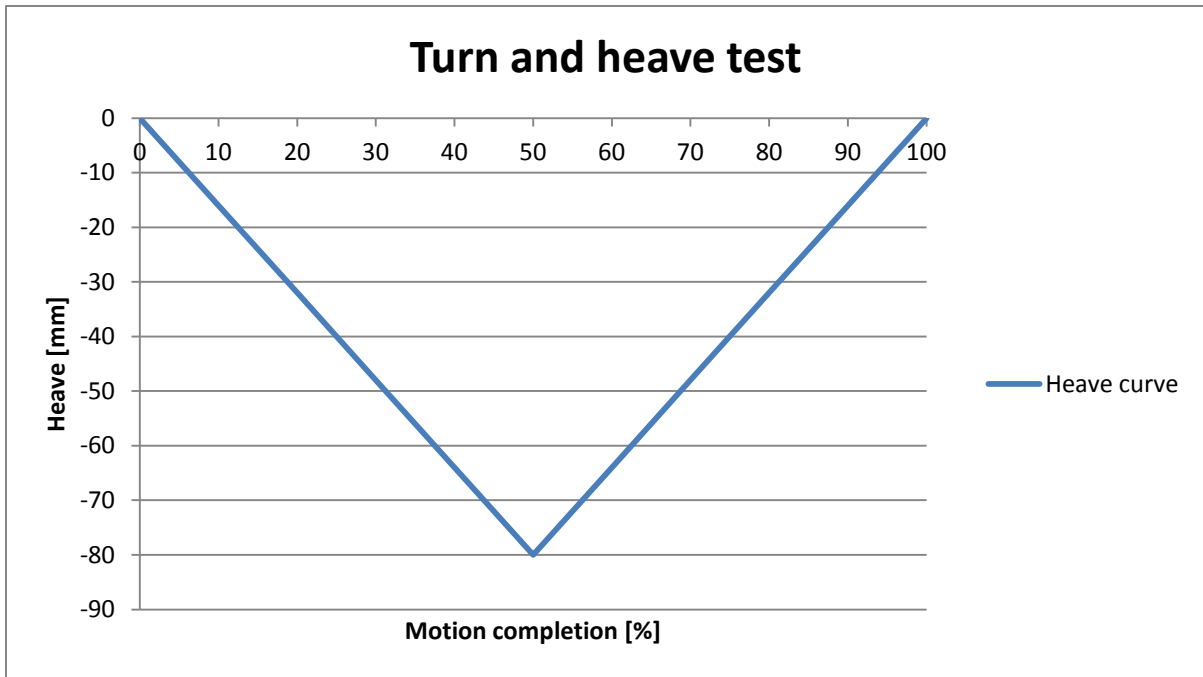


FIGURE 27 – TURN AND HEAVE TEST, HEAVE

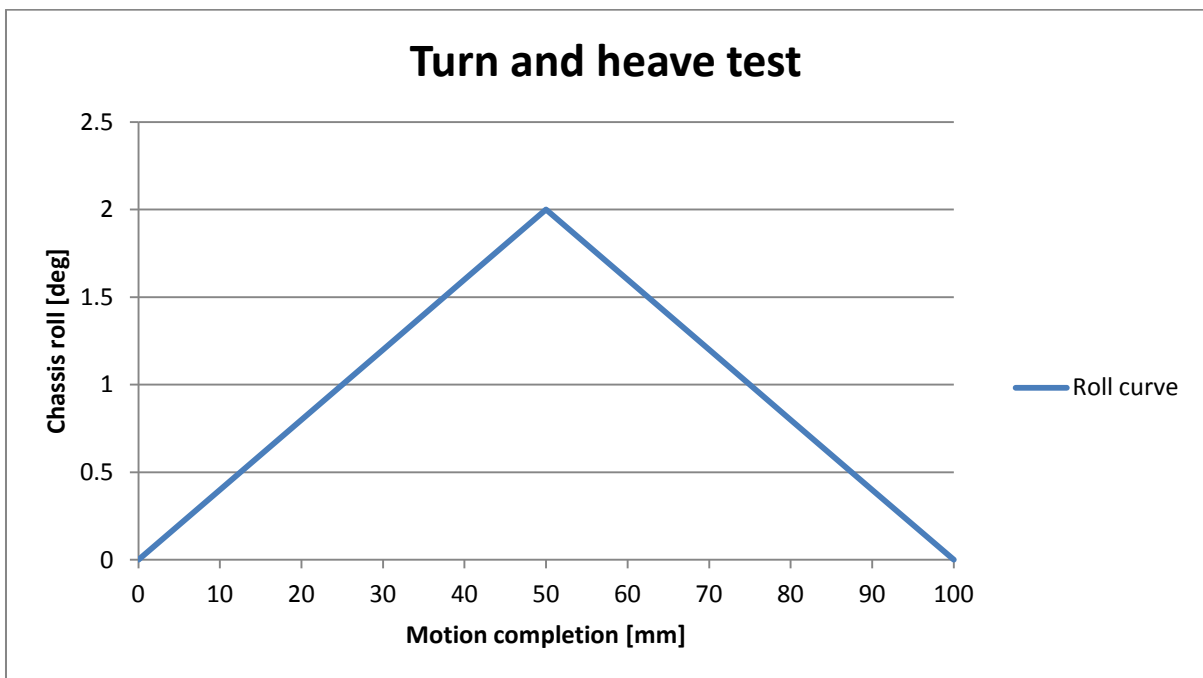


FIGURE 28 – TURN AND HEAVE TEST, ROLL

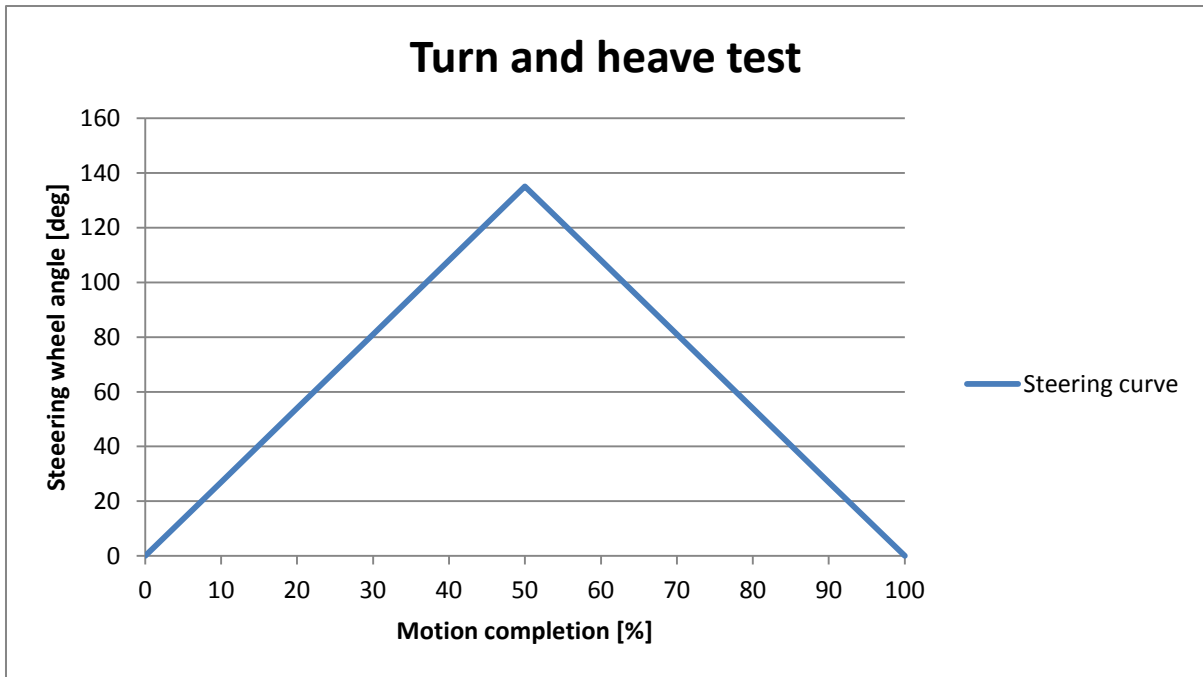


FIGURE 29 – TURN AND HEAVE TEST, STEERING

## 16.2 OPTIMIZING CONTROL ARM GEOMETRY

The optimizing was done stepwise, at first focusing on the turn and heave test. The goal was to keep the wheels as vertical as possible through the corner, with priority on the outer wheel. This way the tire contact patch is as large as possible, ensuring the highest level of grip possible. The process is time consuming and requires lots of iterations, to get the wanted result. The graphs and tables in this section is a selection of the most relevant iterations.

### 16.2.1 TURN AND HEAVE TEST

The process started with the base geometry from section 13, listed in Table 5 and Table 6. The spring and damper setup is a generic pull rod concept, as configured in section 15.

TABLE 5 – FRONT UPRIGHT GEOMETRY COORDINATES, [MM]

Point of interest	X	Y	Z
Wheel center	805	652.5	235
Upper ball joint	800.5	540	440
Lower ball joint	822.5	625	165
Tie rod outer joint	887.5	611	230

TABLE 6 – FRAME FRONT SUSPENSION MOUNTS, [MM]

Point of interest	X	Y	Z
Upper control arm - front	872.5	192.5	460
Upper control arm - rear	600.5	192.5	460
Lower control arm - front	872.5	100	205

Lower control arm - rear	600.5	100	225
Tie rod inner joint	887.5	160	280

Initial simulations and optimization was done using the turn and heave test described in section 16.1.6

Figure 30 displays the first simulation where the right (outer) wheel reaching -1.8 degrees of camber, while the left wheel reaches 2.9 degrees. This is not within specifications, and must be corrected.

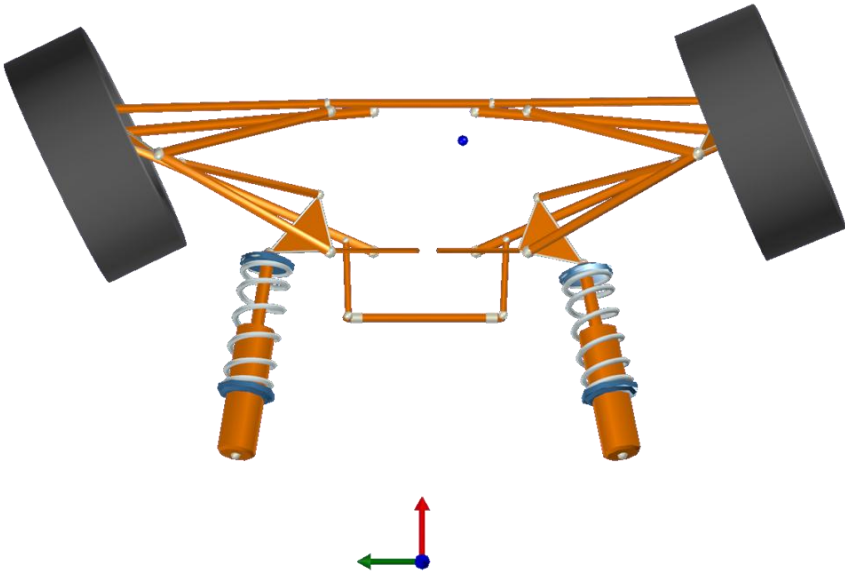


FIGURE 30 – VISUALISTION OF THE TURN AND HEAVE TEST AT 50% MOTION COMPLETION

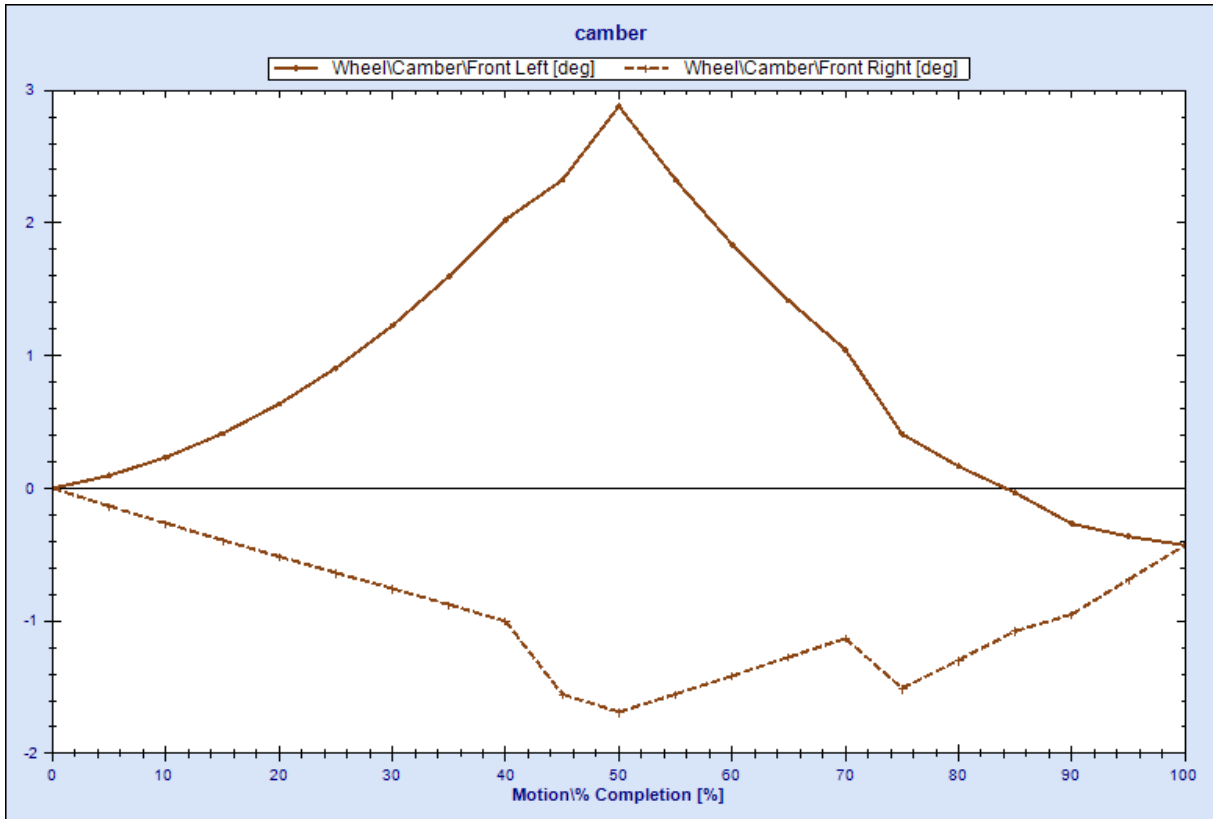


FIGURE 31 - CAMBER CURVE FOR BASE DESIGN

TABLE 7 – KEY PARAMETERS, BASE DESIGN

Parameter	Lower value	Unit
Kingpin inclination (KPI)	19.1	[degrees]
Scrub radius	-29.5	[mm]
Caster angle	6.8	[degrees]
Mechanical trail	37.3	[mm]
Roll center height (static)	59.4	[mm]

Table 7 shows a caster angle of 6.8 degrees and a KPI of 19.1 degrees. Both values are way higher than what is preferred. An increase in caster angle adds negative camber on the outside wheel and positive to the inside wheel. From Figure 31 there is indications of too much caster present in the geometry. The caster angle was reduced by moving the lower ball joint (LBJ) in millimeter increments backwards (negative x-direction). This would also reduce the trail, which was above specification. Figure 32 shows the results after moving the LBJ 10 mm.

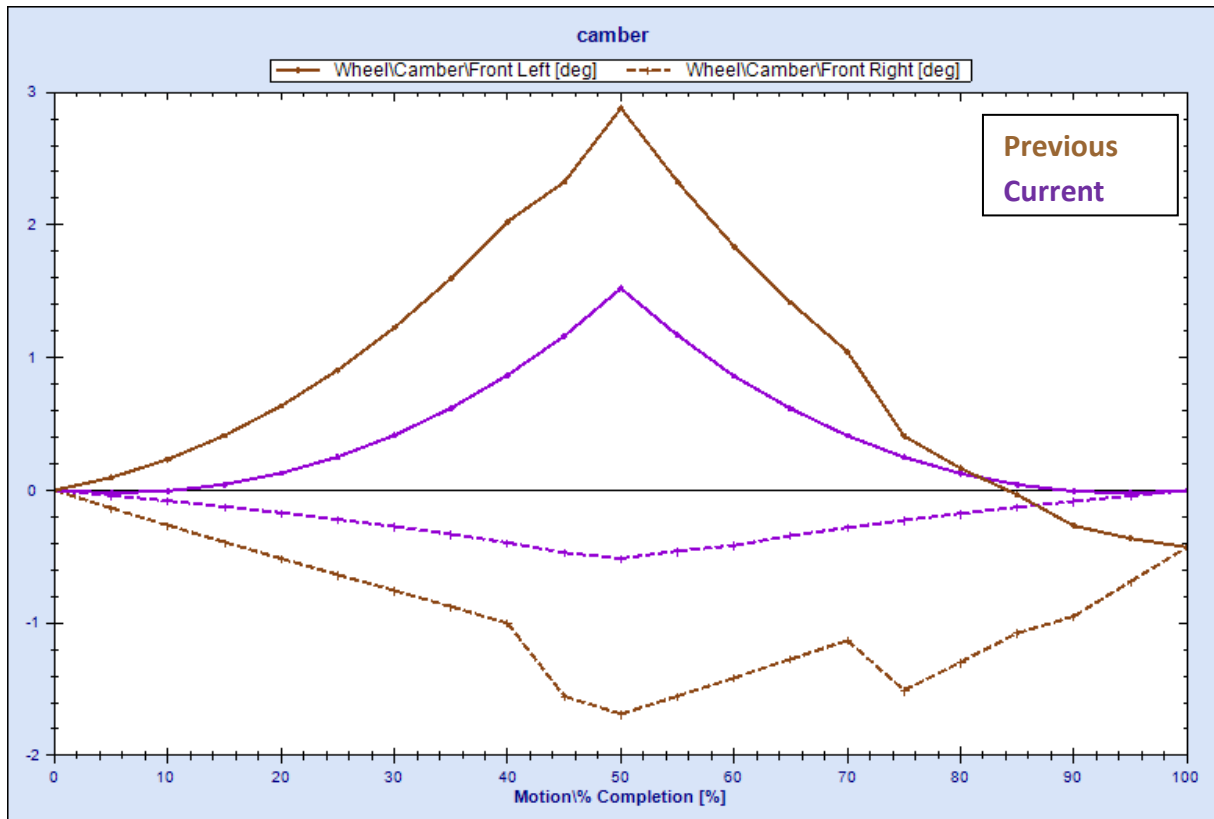


FIGURE 32 – CAMBER CURVE AFTER REDUCED CASTER, LBJ MOVED 10MM BACKWARDS.

TABLE 8 – KEY PARAMETERS, REDUCED CASTER, LBJ MOVED 10MM BACKWARDS

Parameter	Lower value	Unit
Kingpin inclination (KPI)	19.1	[degrees]
Scrub radius	-29.5	[mm]
Caster angle	4.8	[degrees]
Mechanical trail	21.3	[mm]
Roll center height (static)	63	[mm]

The camber curve is improved but there is still too much camber change, outer wheel reaches -0.45 degrees while the inner wheel reaches 1.5 degrees positive camber. The camber curve needs further improvement.

Some of the affected design specifications are listed in Table 8. KPI and scrub are unaffected, as expected, while caster is reduced to 4.8 degrees and mechanical trail to 21.3 mm. The trail is now within spec. An eye is also kept on the change in roll center height, which increased 3.6 mm.

The LBJ joint was incremented further backwards. Another 10 mm resulted in the camber curve displayed in Figure 33 below.



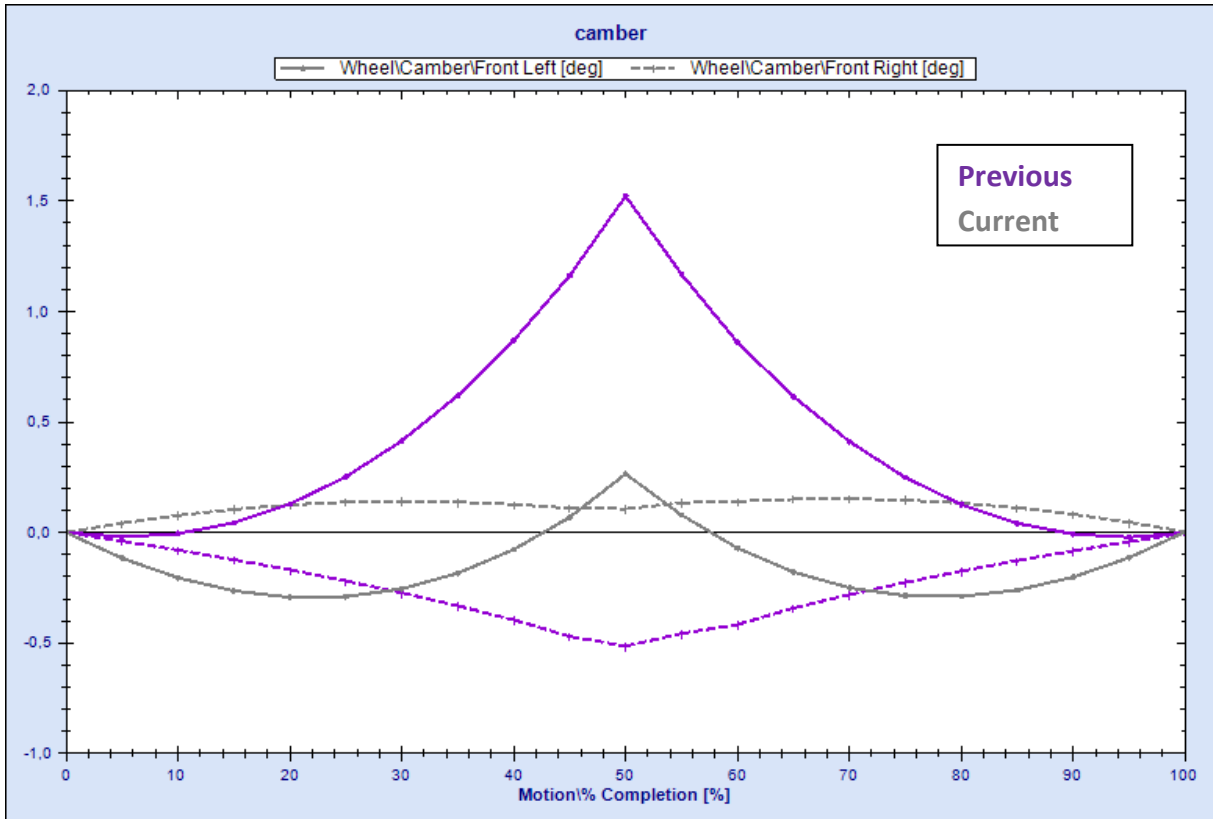


FIGURE 33 – CAMBER CURVE, LBJ MOVED ANOTHER 10 MM BACKWARDS

TABLE 9 – KEY PARAMETERS, LBJ MOVED ANOTHER 10 MM BACKWARDS

Parameter	Lower value	Unit
Kingpin inclination (KPI)	19.1	[degrees]
Scrub radius	-29.5	[mm]
Caster angle	2.7	[degrees]
Mechanical trail	5.3	[mm]
Roll center height (static)	66.1	[mm]

The camber change was now within the design specification. Other aspects of the geometry could now be investigated.

From Table 9 we see that the KPI and scrub radius are outside specification. Reducing KPI will increase the scrub, which is what we want, but it also affects the camber when steered. To reduce KPI, the lower ball joint (LBJ) is pulled inwards in 1 millimeter increments, where the first example given is at 10 inwards.

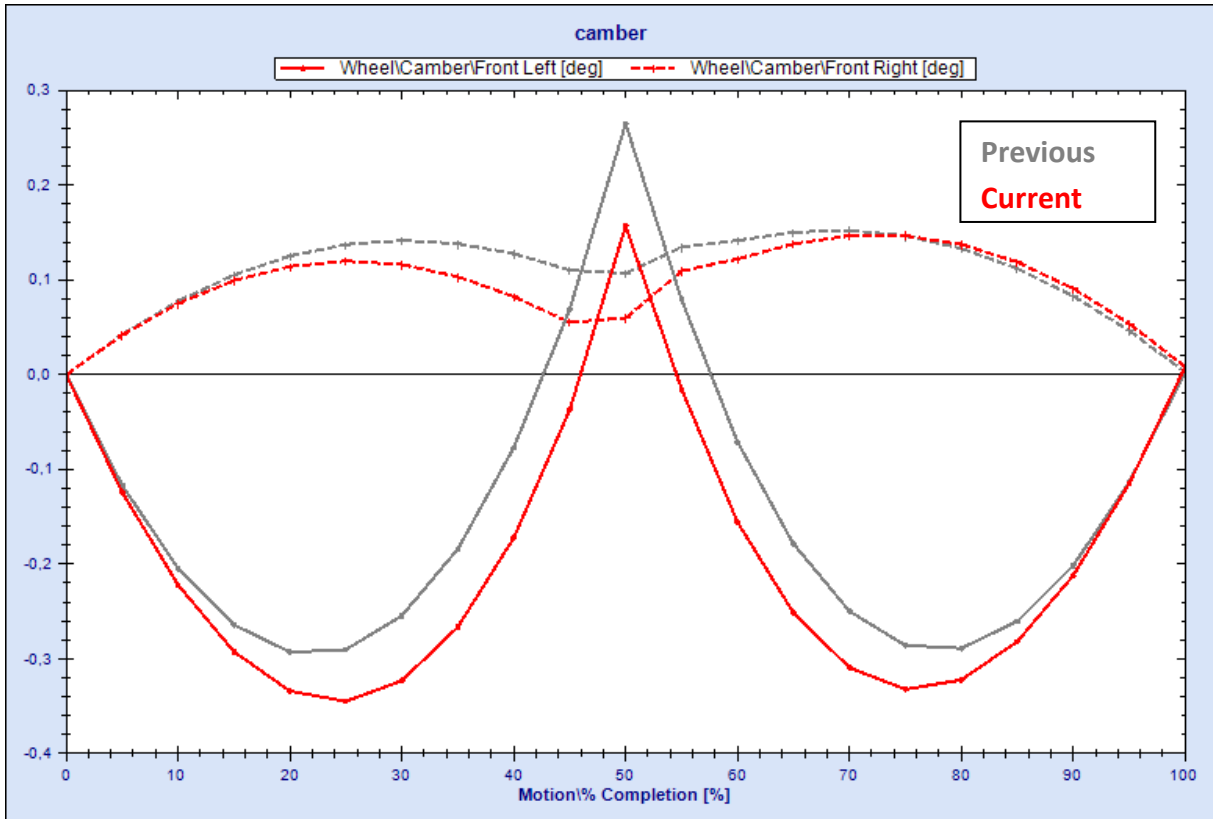


FIGURE 34 – CAMBER CURVE, LBJ PULLED 10 MM INWARDS

TABLE 10 – KEY PARAMETERS, LBJ PULLED 10 MM INWARDS

Parameter	Lower value	Unit
Kingpin inclination (KPI)	17.2	[degrees]
Scrub radius	-13.5	[mm]
Caster angle	2.6	[degrees]
Mechanical trail	5	[mm]
Roll center height (static)	67.8	[mm]

Figure 33 shows a camber curve still within spec, but the adjustment is not enough for KPI and scrub radius. The LBJ was incremented inwards, the results showed in Figure 34 and Table 11 are for a total of 10mm inwards.

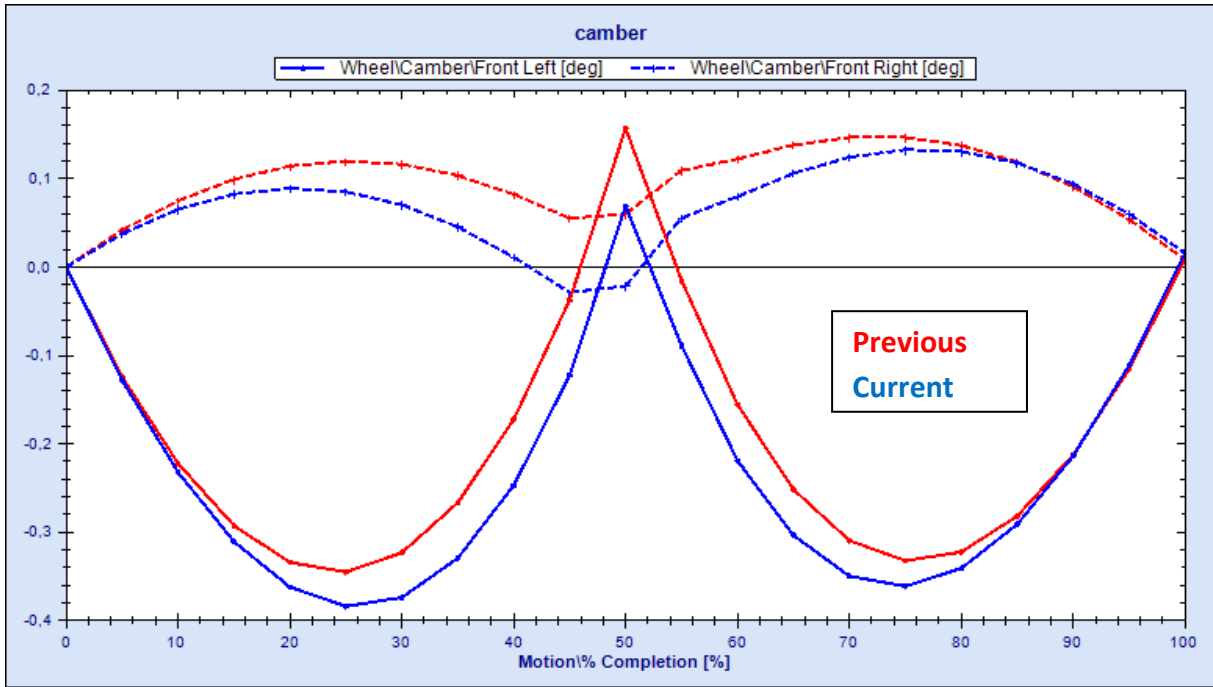


FIGURE 35 – CAMBER CURVE, LBJ PULLED ANOTHER 10 MM INWARDS

TABLE 11 – KEY PARAMETERS, LBJ PULLED ANOTHER 10 MM INWARDS

Parameter	Lower value	Unit
Kingpin inclination (KPI)	15.3	[degrees]
Scrub radius	5	[mm]
Caster angle	2.6	[degrees]
Mechanical trail	5	[mm]
Roll center height (static)	69.6	[mm]

The KPI is still marginally above desired specifications, and the scrub radius is too small. Another 10 mm was incremented inwards on the LBJ;

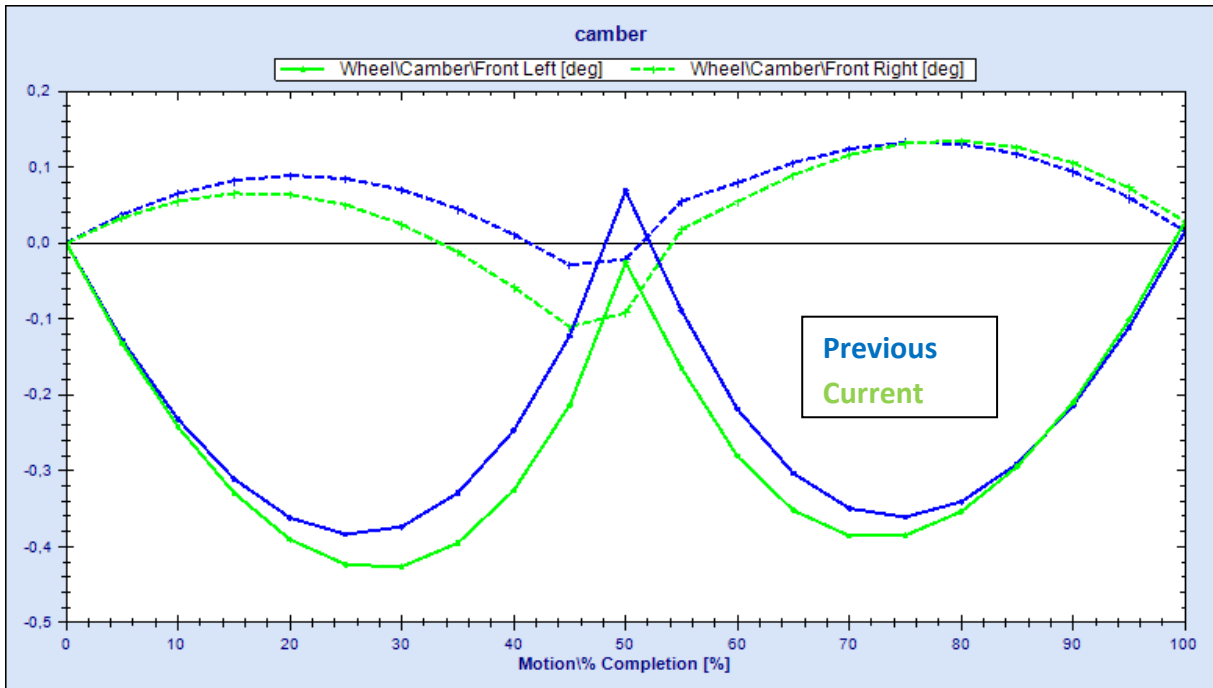


FIGURE 36 – CAMBER CURVE, LBJ PULLED ANOTHER 10 MM INWARDS

TABLE 12 – KEY PARAMETERS, LBJ PULLED ANOTHER 10 MM INWARDS

Parameter	Lower value	Unit
Kingpin inclination (KPI)	13.3	[degrees]
Scrub radius	18.5	[mm]
Caster angle	2.6	[degrees]
Mechanical trail	5	[mm]
Roll center height (static)	71.4	[mm]

The values are now within spec but the camber curves seem more concave and convex than they need to. The camber curves are controlled by the length ratio between the short upper and long lower control arm. One option is to shorten the lower arm. This would also free up some space between the control arm mounts for packaging inside the frame. A pedal box or radiator could fit in this area, depending on how much the control arm mounts are adjusted. At first the lower inner control arm mounts were moved 20 mm outwards.

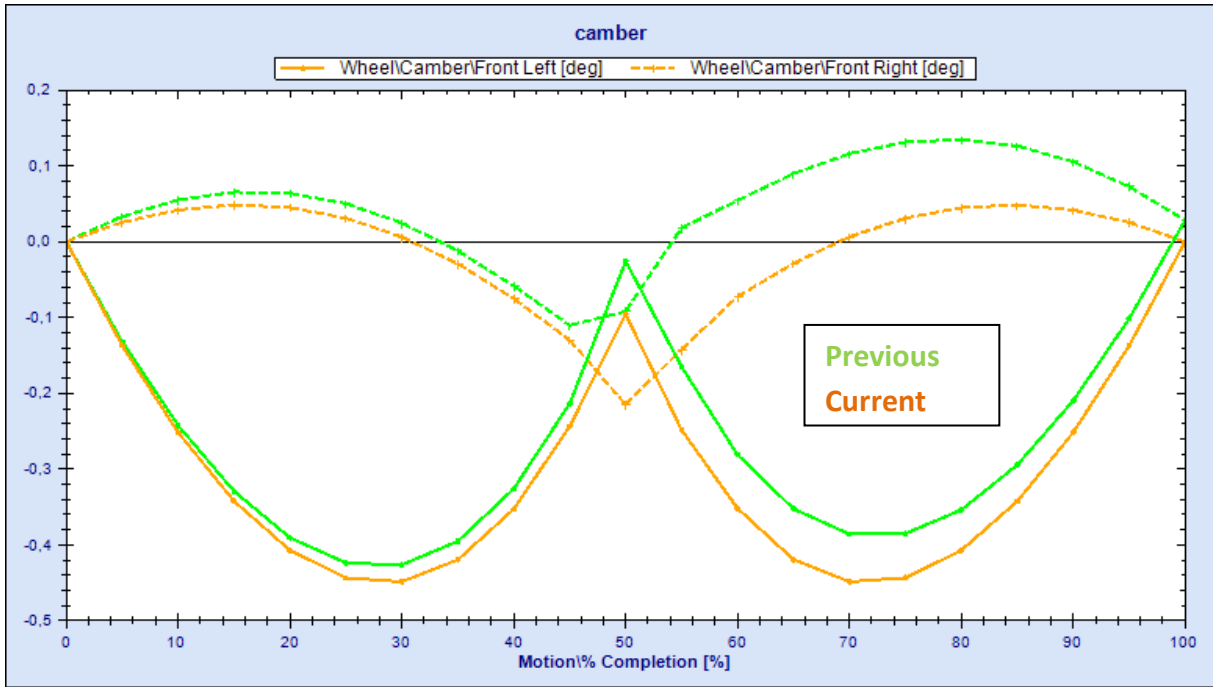


FIGURE 37 – CAMBER CURVE, LCA INNER MOUNTS MOVED 20 MM OUTWARDS

TABLE 13 – KEY PARAMETERS, LCA INNER MOUNTS MOVED 20 MM OUTWARDS

Parameter	Lower value	Unit
Kingpin inclination (KPI)	13.3	[degrees]
Scrub radius	18.5	[mm]
Caster angle	2.6	[degrees]
Mechanical trail	5	[mm]
Roll center height (static)	75.4	[mm]

The camber curve translated slightly towards negative camber, but a less curved camber change for the outer wheel was wanted. The LCA inner mounts were stepwise moved another 20 mm outwards, in addition to spacing out the inner UCA mounts 12.5 mm.

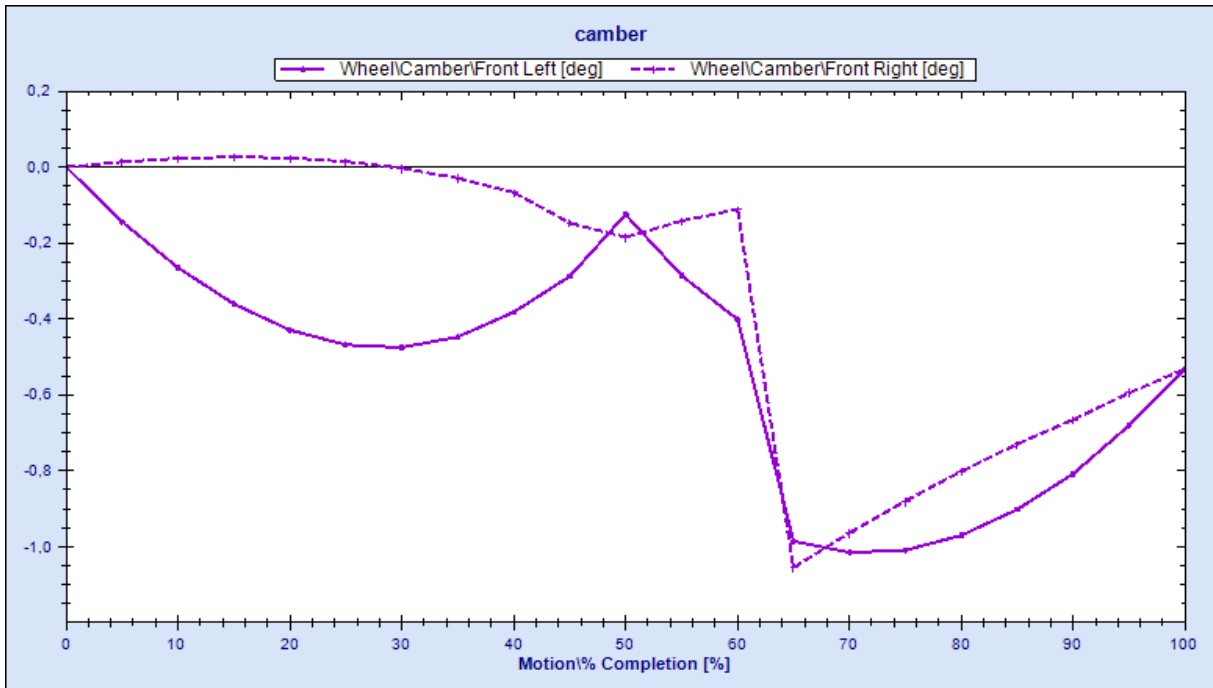


FIGURE 38 – CAMBER CURVE, LCA INNER MOUNTS MOVED ANOTHER 20 MM OUTWARDS

TABLE 14 – KEY PARAMETERS, LCA INNER MOUNTS MOVED ANOTHER 20 MM OUTWARDS

Parameter	Lower value	Unit
Kingpin inclination (KPI)	13.3	[degrees]
Scrub radius	18.5	[mm]
Caster angle	2.6	[degrees]
Mechanical trail	5	[mm]
Roll center height (static)	80.6	[mm]

The simulation shows a marginally high roll center, and there are irregularities in the camber change curve assumed to be caused by incorrect placement of the steering rack and tie rods. The bump steer was checked with the heave test.

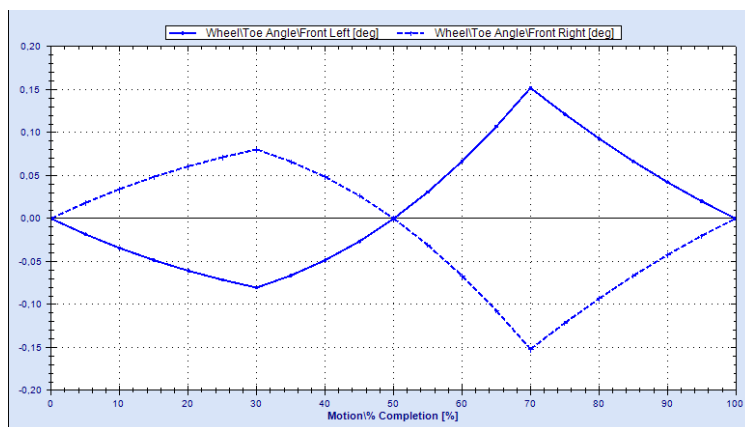


FIGURE 39 – TOE CURVE FROM HEAVETEST ILLUSTRATING BUMP STEER

Figure 39 shows some toe out in heave and toe in on bump. Reducing bump steer will probably remove irregularities in turn and heave simulation.

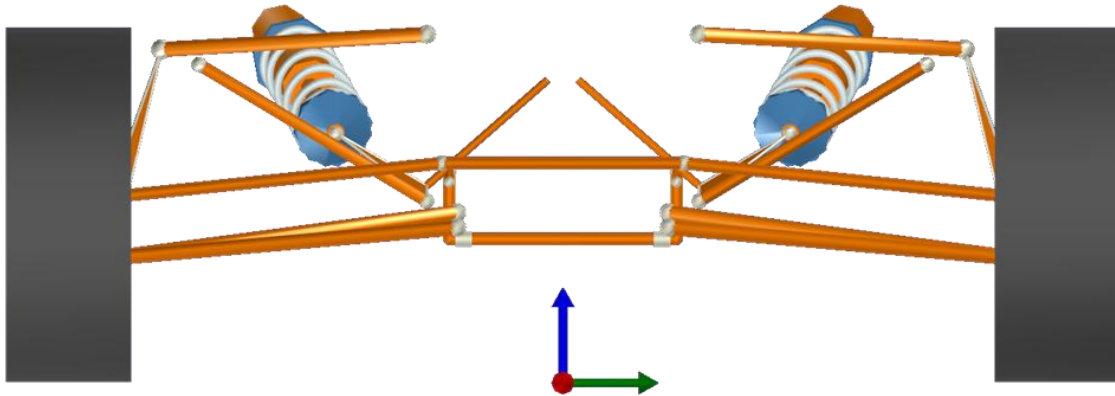


FIGURE 40 – INITIAL STEERING RACK AND TIE ROD PLACEMENT

Initially the steering rack was placed 280 mm above ground, with the tie rod at 230 mm. This was determined through the development of the front view geometry in section 12.1. The rack and rod were moved down 30 mm to try to compensate for the geometric disturbance from 60% motion completion in the previous simulation. It is easier to correct the bump steer effects when the steering rack and tie rods lie close to one of the control arm planes.

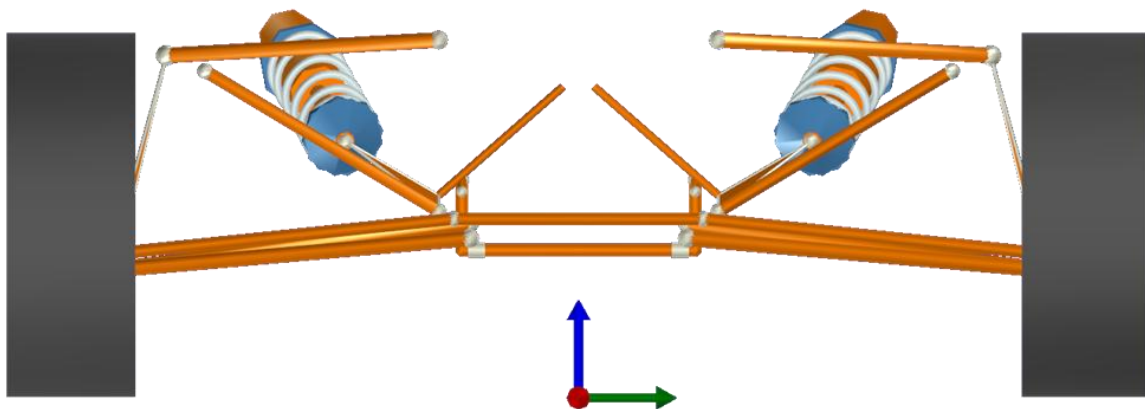


FIGURE 41 – MODIFIED STEERING RACK AND TIE ROD PLACEMENT

Results of the adjustment affected the camber a great deal, which indicate that the steering setup added steered camber as suspected. Further adjustments to rack and tie rods will be made when the control arm geometry is fixed.

The turn and heave test was run again.

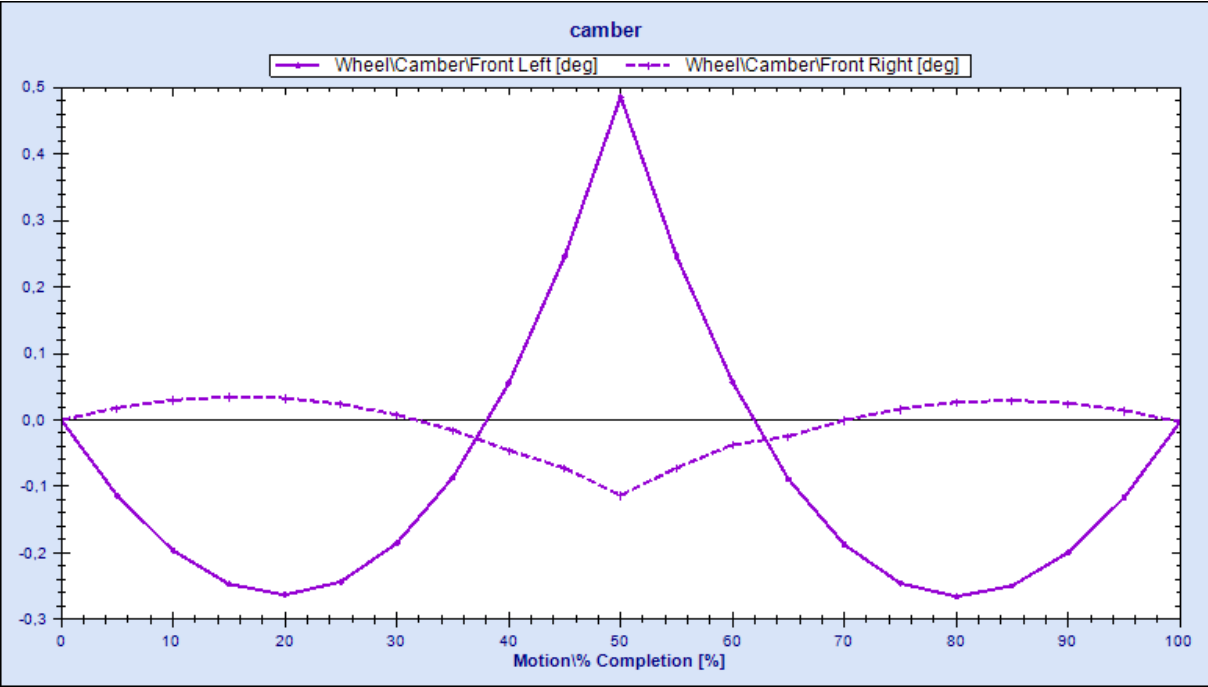


FIGURE 42 – CAMBER CURVE AFTER REPLACEMENT OF STEERING RACK

The camber curve for the inner wheel was now even more convex, due to removing the camber effects of bump steer. The LCA was shortened another 20 mm to compensate.

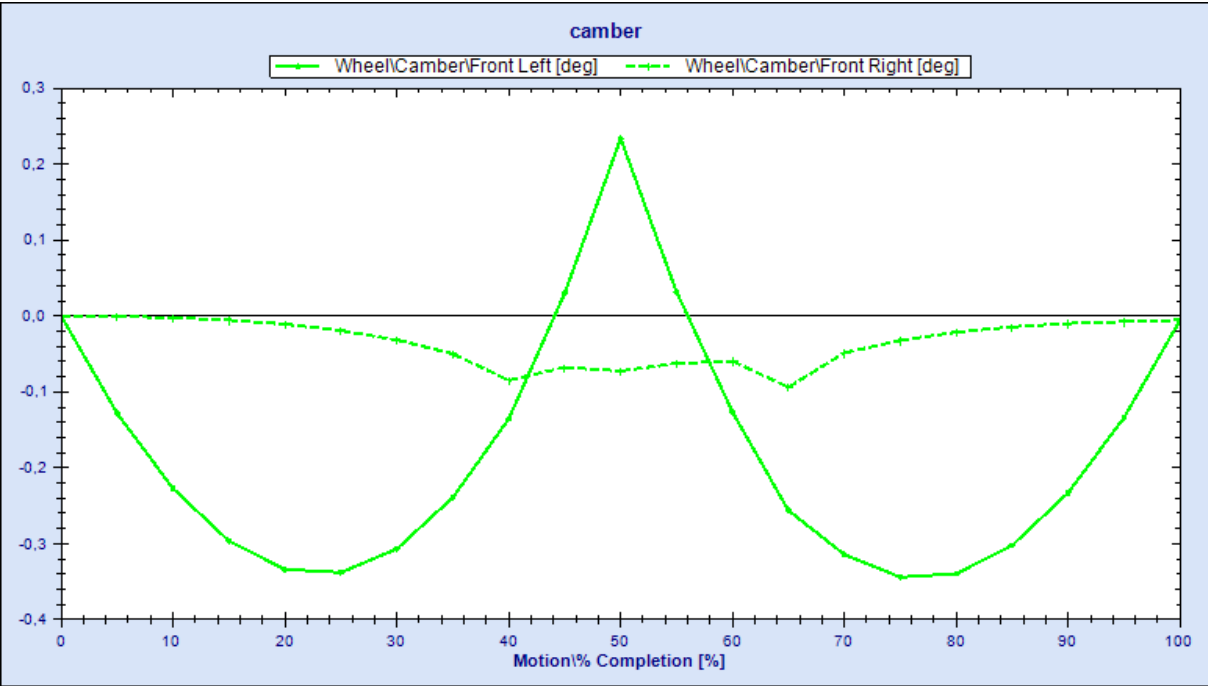


FIGURE 43 – CAMBER CURVE, SHORTENED LCA 20 MM



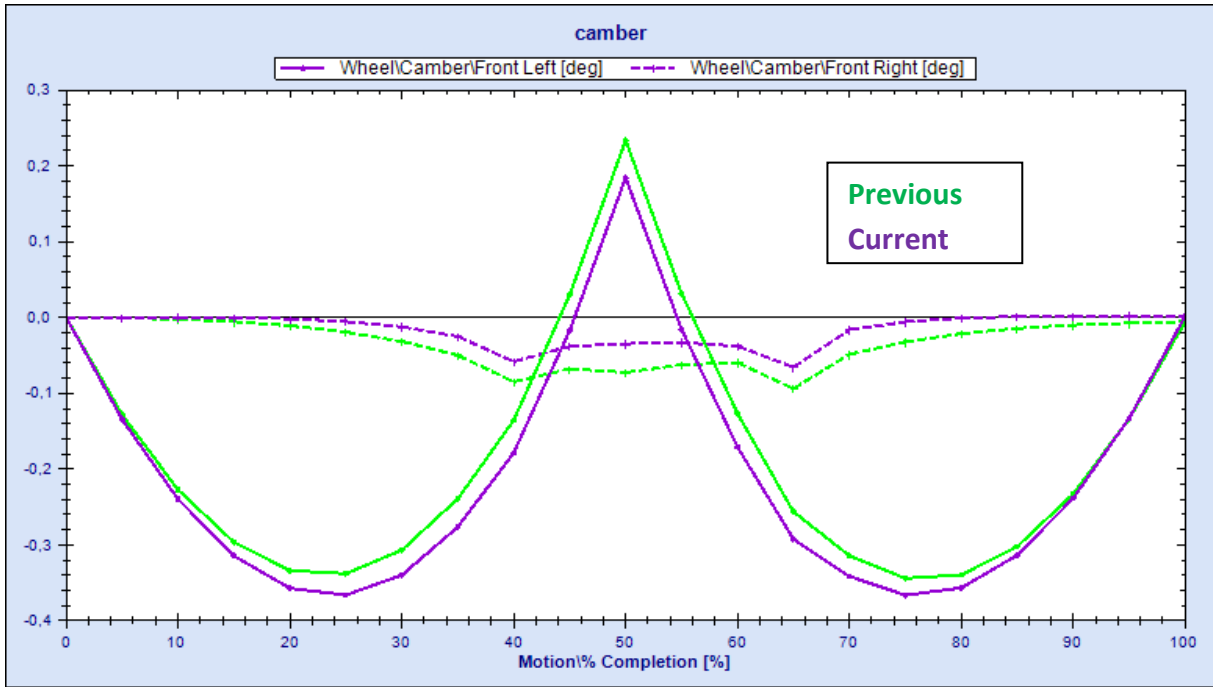


FIGURE 44 – CAMBER CURVE, FINAL CONTROL ARM GEOMETRY

A final tweak resulted in the camber curve seen in Figure 44. It allowed a bit more space, and marginally better camber for the inner wheel. Coordinates of the current control arm set up can be seen in Table 15 and Table 16:

TABLE 15 – FRONT UPRIGHT GEOMETRY COORDINATES, [MM]

Point of interest	X	Y	Z
Wheel center	805	652.5	235
Upper ball joint	800.5	540	440
Lower ball joint	822.5	625	165
Tie rod outer joint	900	611	230

TABLE 16 – FRAME FRONT SUSPENSION MOUNTS, [MM]

Point of interest	X	Y	Z
Upper control arm - front	860	178	460
Upper control arm - rear	585	178	460
Lower control arm - front	860	165	205
Lower control arm - rear	585	165	225
Tie rod inner joint	900	160	250

### 16.2.2 HEAVE TEST

Nest part of the optimization process is to examine the camber curves for straight line driving over rough terrain. This is checked using the heave test. The results of the heave test for the geometry in Table 15 and Table 16 can be seen in Figure 45.

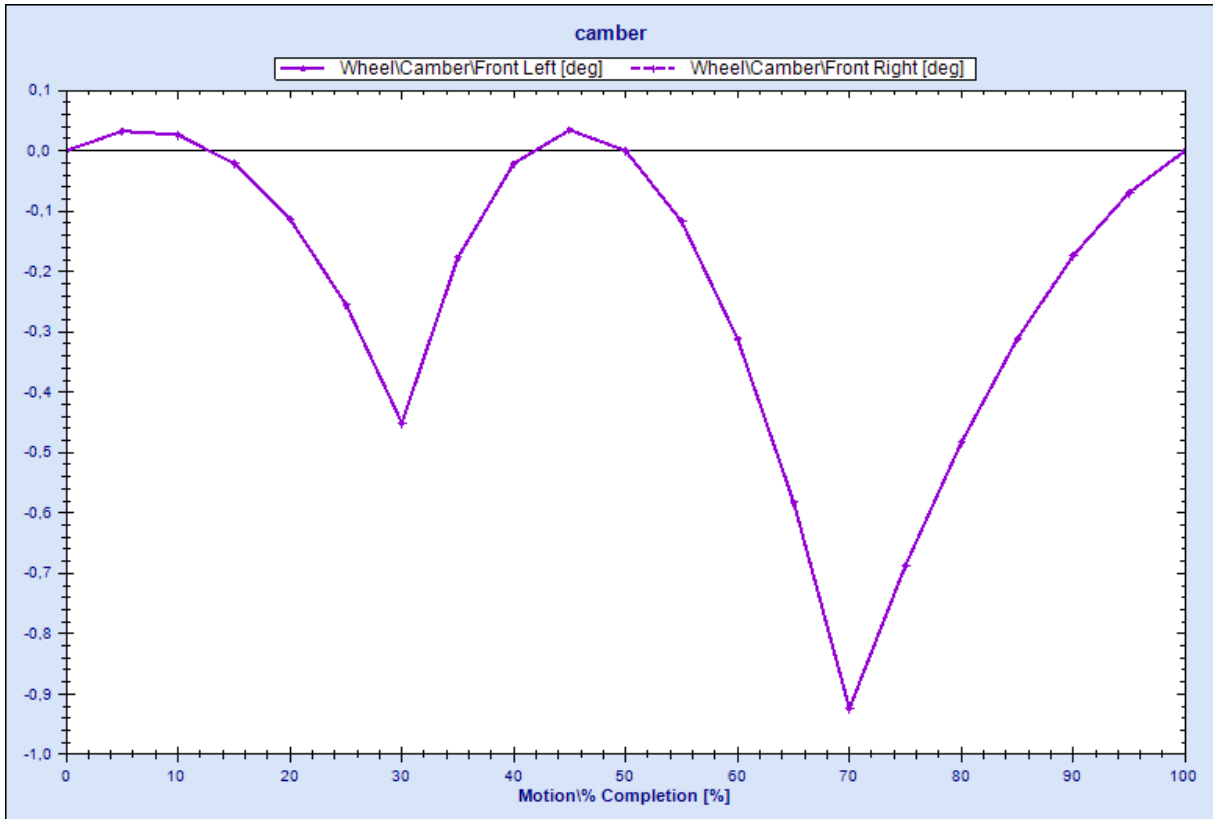


FIGURE 45 – CAMBER CURVE HEAVE TEST, FINAL CONTROL ARM GEOMETRY

The camber curve shows negative camber for both heave and bump, both below -1.0 degrees. This is within spec and required no more adjustment.

### 16.3 OPTIMIZING STEERING RACK AND TIE ROD PLACEMENTS

Next feature to address is the steering rack and tie rod placement. Crucial here is the bump steer, which is analyzed through the heave test and with toe angle as output.

To ensure the correct Ackermann geometry, the outer mounting point for the tie rod was moved inwards to 590 mm in y-direction to reduce the Ackermann percentage.

The Ackermann percentage was calculated based on steering angles from OptimumK:

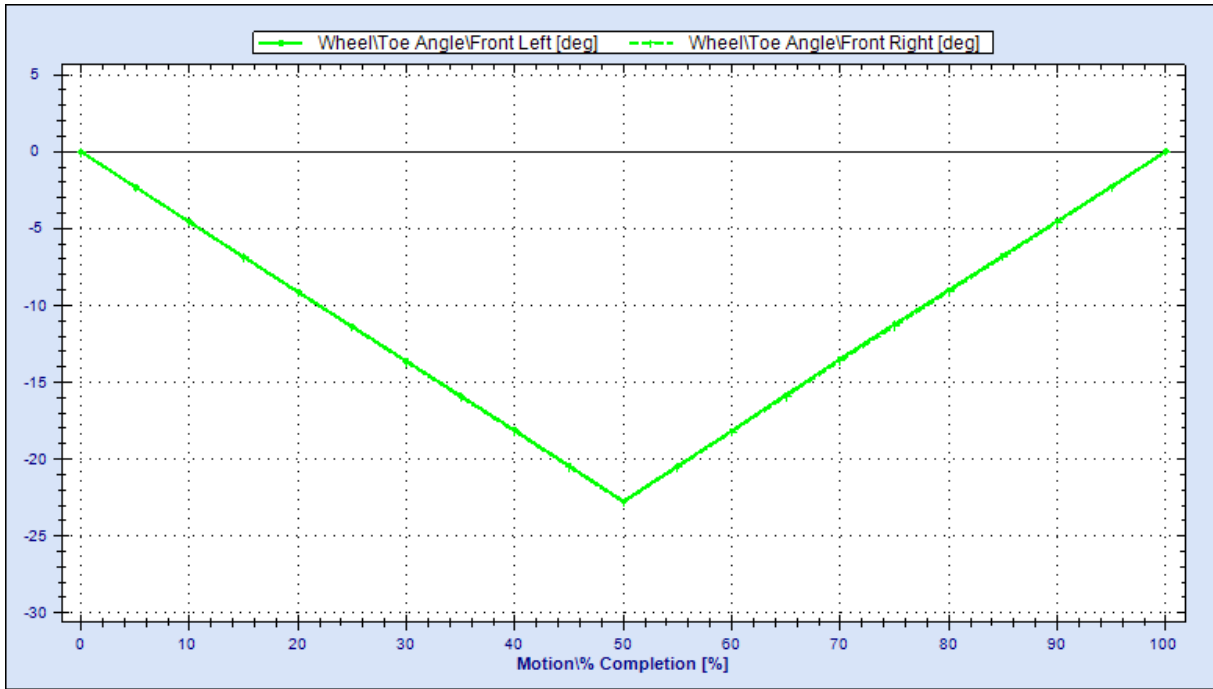


FIGURE 46 – WHEEL STEERING ANGLES AT STEERING WHEEL LOCK

$$\delta_{inside\ 100} = \tan^{-1} \left( \frac{WB}{\frac{WB}{\tan \delta_{outside}} - Tr} \right) - \delta_{outside}$$

$$\delta_{inside\ 100} = \tan^{-1} \left( \frac{1610}{\frac{1610}{\tan 22} - 1305} \right) - 22 = 9$$

$$\%Ackermann = \frac{\delta_{inside} - \delta_{outside}}{\delta_{inside\ 100}} \cdot 100$$

$$\%Ackermann = \frac{22 - 22}{9} \cdot \frac{22.5 - 22.5}{9} \cdot 100 = 0\%$$

The new tie rod outer mount resulted in a neutral Ackermann geometry.

The steering rack needed to be moved forwards to accommodate the frame members between the control arm mounts. The rack was moved to 900 mm in x-direction, which resulted in the tie rod coordinates listed in Table 17.

TABLE 17 – TIE ROD MOUNTS, [MM]

Point of interest	X	Y	Z
Tie rod inner joint	900	160	250
Tie rod outer joint	900	590	200

The first simulation with the heave test resulted in about than 1.6 degrees toe-in on heave, and 1.2 degrees toe out on bump. This is far from the specification of 0.05 degrees

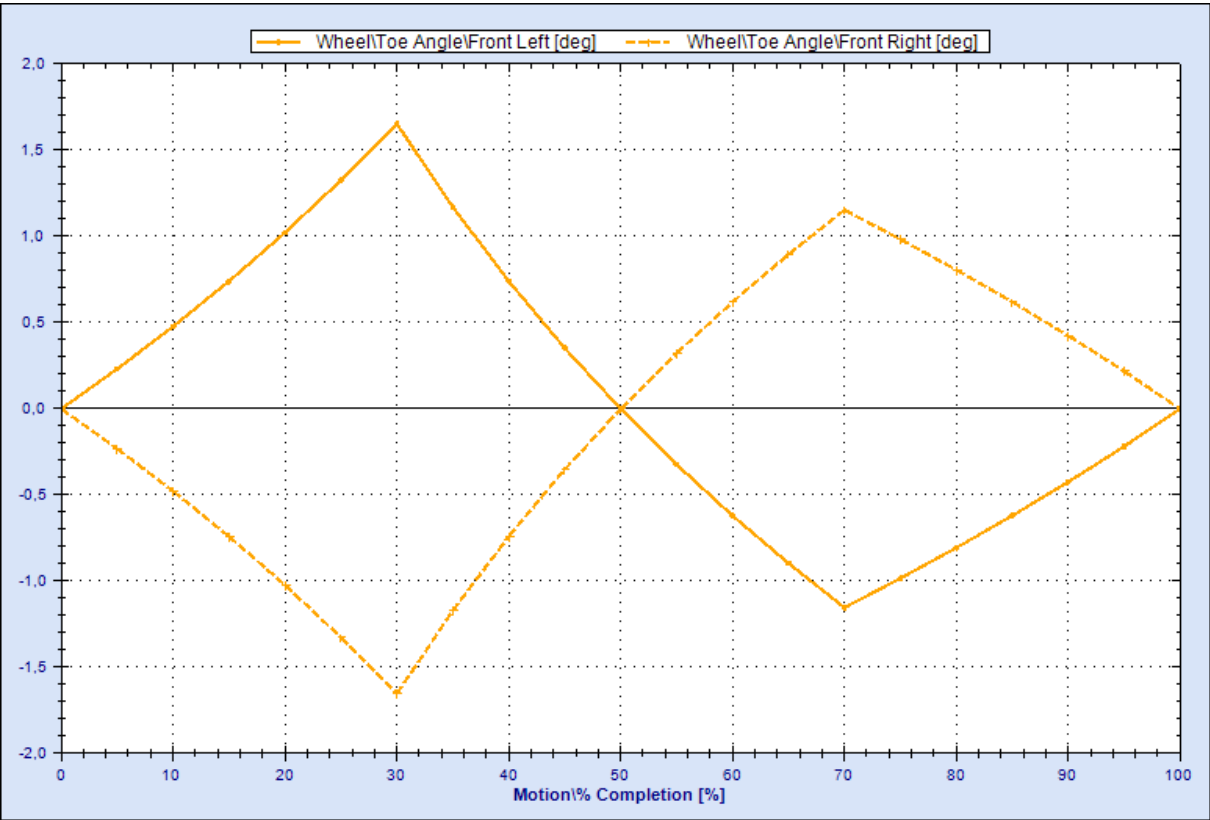


FIGURE 47 – INITIAL TOE CURVE

The corrections on the steering rack and tie rods were made using table 3 from section 11.4 as guidance. The rack was moved down 10 mm to obtain the toe curves in Figure 48.

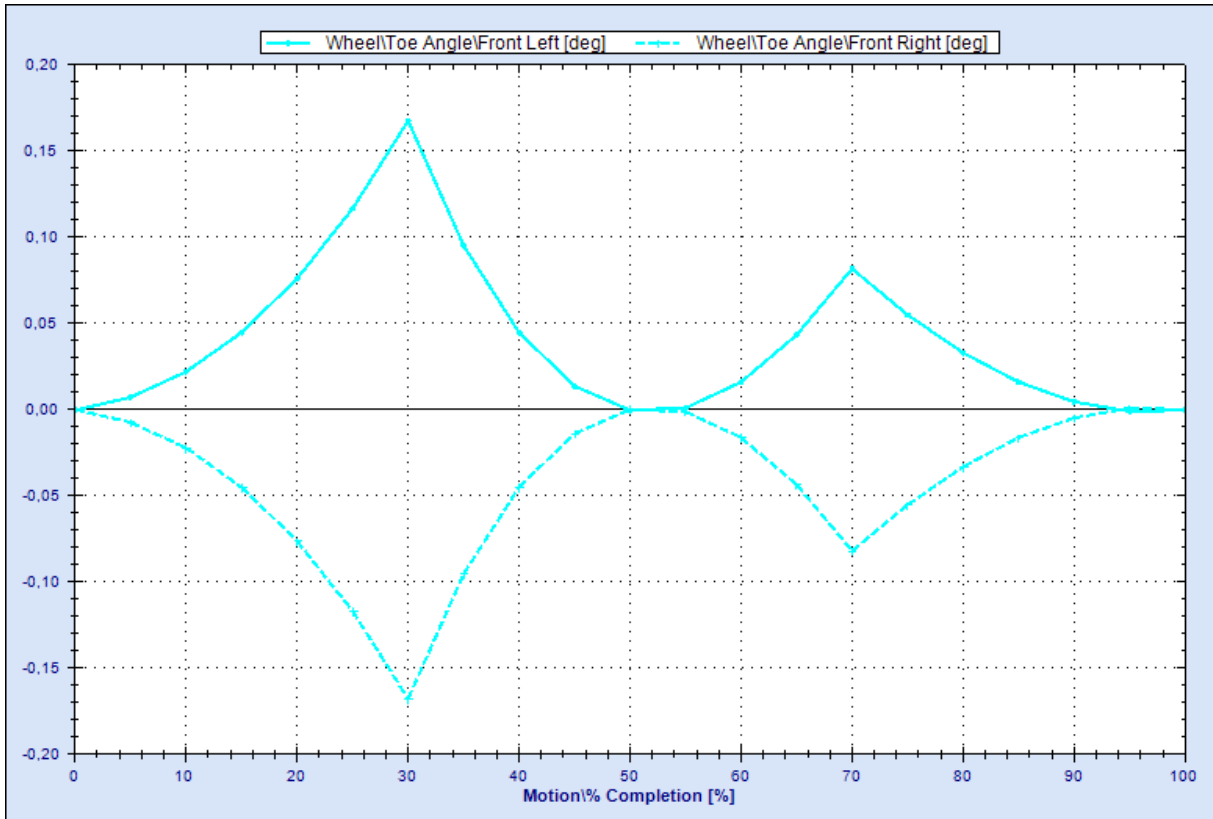


FIGURE 48 – TOE CURVE AFTER 10MM LOWERING RACK 10MM

There is now toe-out on both heave and bump, below 0.2 and 0.1 respectively. This indicates a shortening of the steering rack. 5 mm on each side was tried.

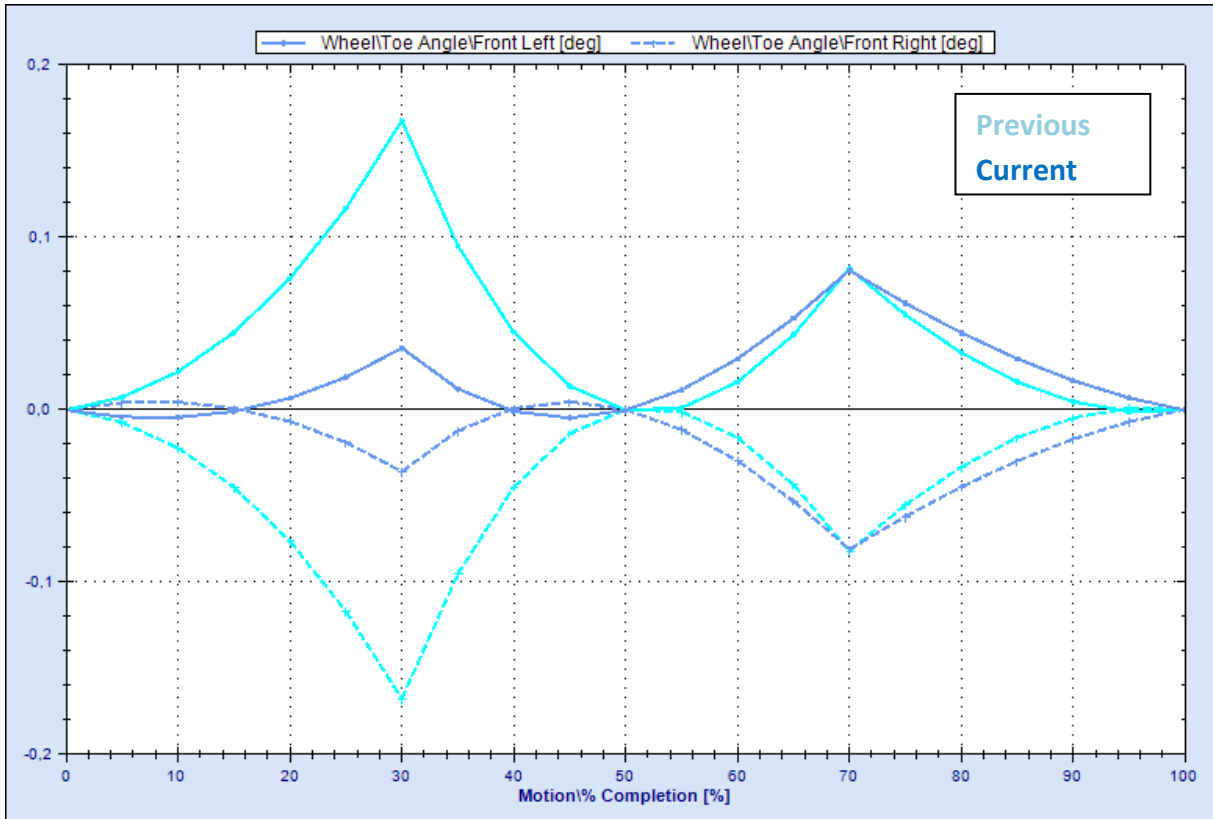


FIGURE 49 – TOE CURVE AFTER SHORTENING RACK 5 ON EACH SIDE

This resulted in unchanged peak toe for bump, while toe for heave is reduced to approximately 0.04. The rack was shortened another 2 mm on each side to reduce the heave to even more.

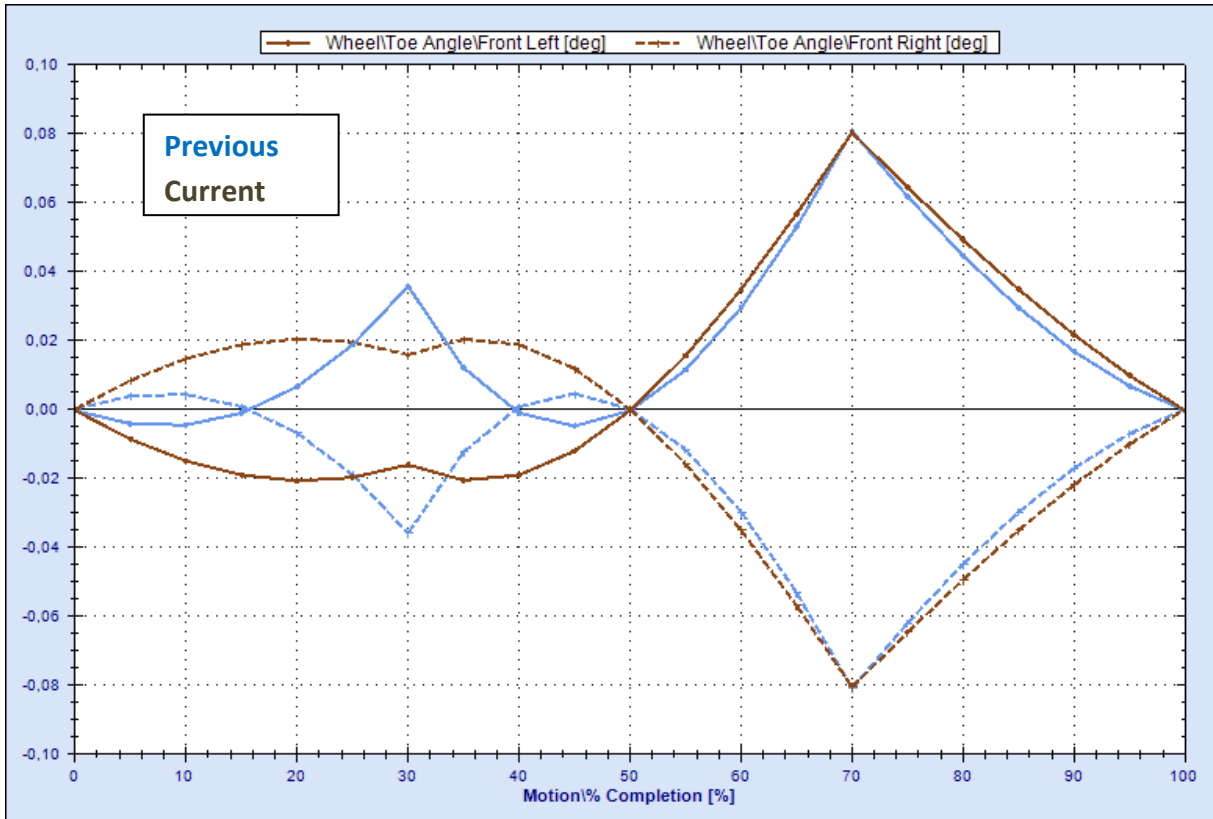


FIGURE 50 – TOE CURVE AFTER ANOTHER 2 MM SHORTENING ON EACH SIDE

The curve now changed to toe-in for heave, without significant changes for bump. This requires slightly raising the rack, 0.5 mm at first.

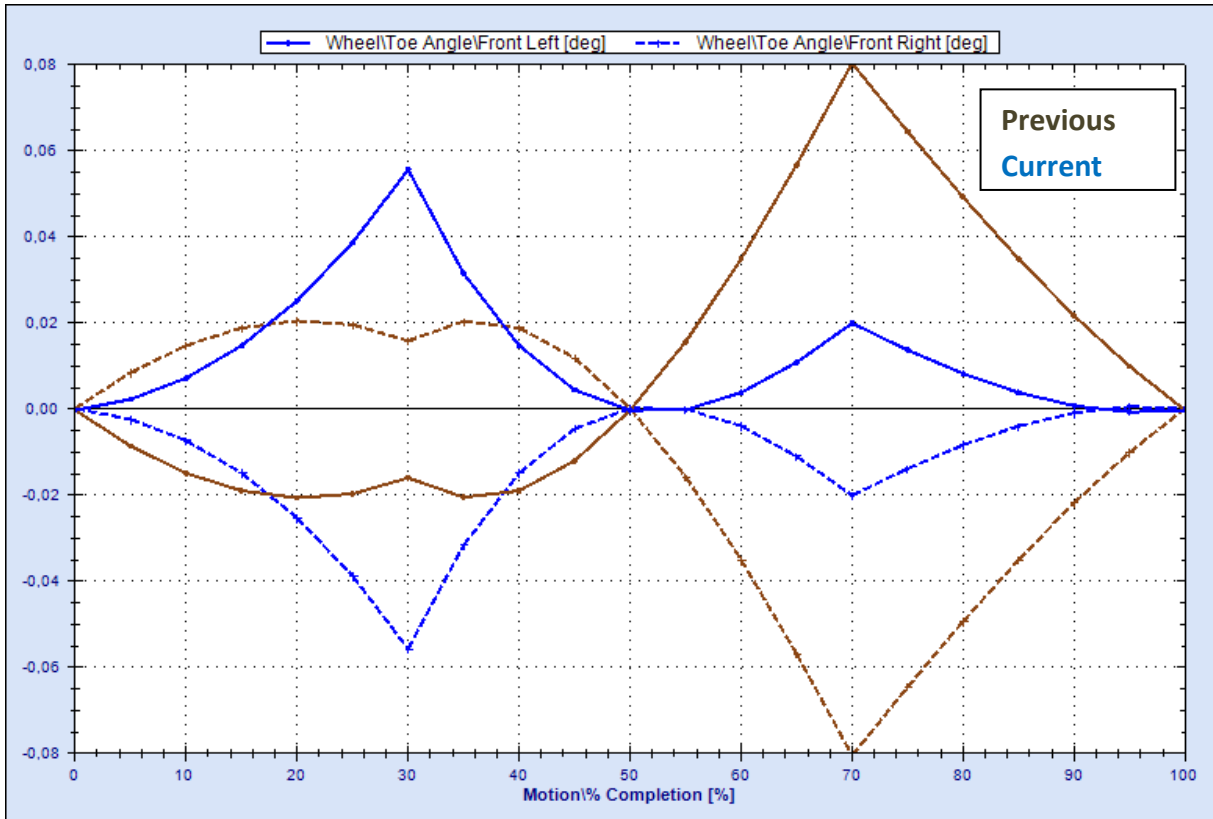


FIGURE 51 – TOE CURVE AFTER RAISING RACK 0.5 MM

This lead to toe-out on both heave and bump and procedure executed earlier was repeated numerous times until the toe curve in Figure 52 was obtained.



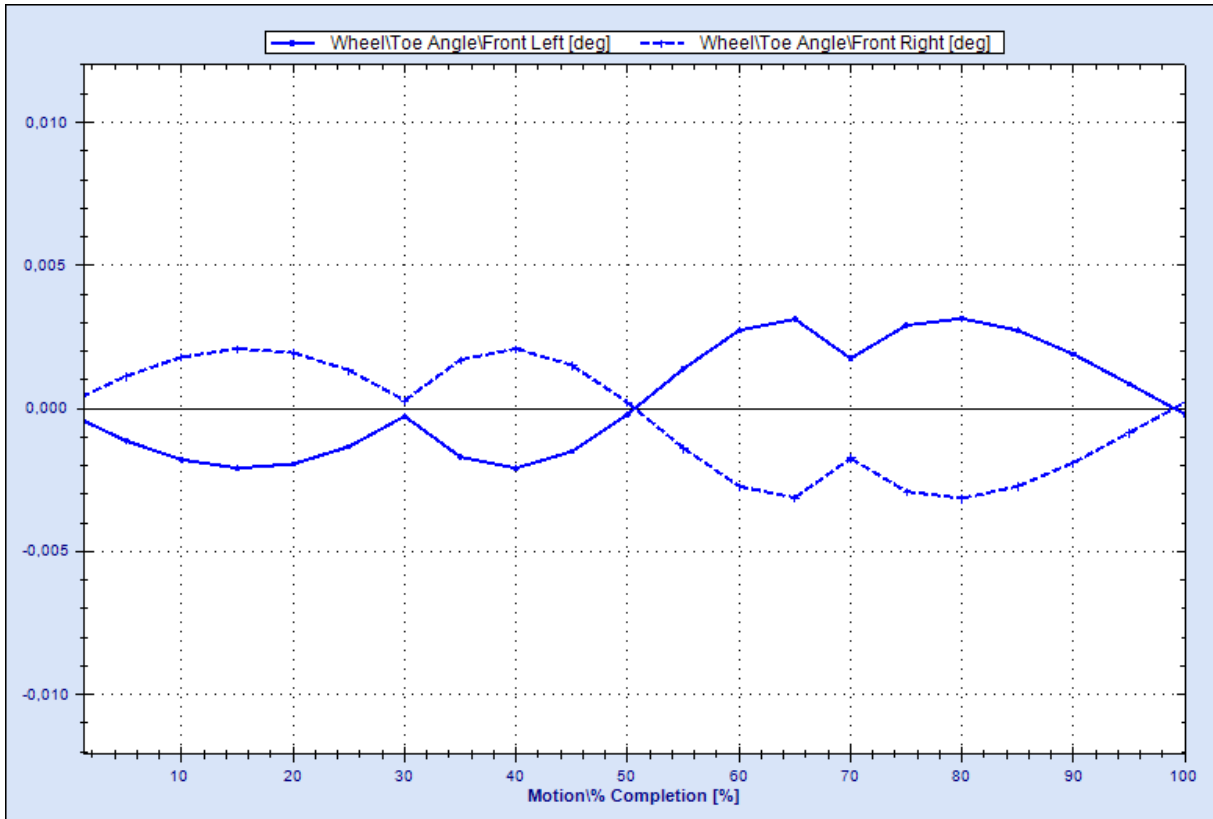


FIGURE 52 – TOE CURVE FOR FINAL TIE ROD LOCATION

The final configuration resulted in a maximum toe of 0.003 degrees, within specification with good margin.

The coordinates for the final rack and tie rod placement is listed in Table 18 below.

TABLE 18 – FINAL TIE ROD LOCATION COORDINATES, [MM]

Point of interest	X	Y	Z
Tie rod inner joint	900	150	240.65
Tie rod outer joint	900	590	200

## 17 FINAL FRONT SUSPENSION GEOMETRY

The final geometry is given by the following parameters:

TABLE 19 – CART DIMENSIONS, [MM]

Measurement	Length
Wheel base	1610 mm
Cart length (tire-tire)	2080 mm
Track width	1305 mm
Cart width (tire-tire)	1483 mm

TABLE 20 – FRONT UPRIGHT GEOMETRY COORDINATES, [MM]

Point of interest	X	Y	Z
Wheel center	805	652.5	235
Upper ball joint	789.5	530	440
Lower ball joint	802.5	595	165
Tie rod outer joint	900	590	200

TABLE 21 – FRAME FRONT SUSPENSION MOUNTS, [MM]

Point of interest	X	Y	Z
Upper control arm - front	860	178	460
Upper control arm - rear	585	178	460
Lower control arm - front	860	165	205
Lower control arm - rear	585	165	225
Tie rod inner joint	900	150	240.65

TABLE 22 – PARAMETER SPECIFICATION

Parameter	Value	Unit
Kingpin inclination	13.3	[degrees]
Scrub radius	18.5	[mm]
Caster angle	2.7	[degrees]
Mechanical trail	5.3	[mm]
Roll center height	84.5	[mm]
Bump steer [max]	0.003	[degrees]
Ackermann	0	[%]
Spindle length	67.7	[mm]

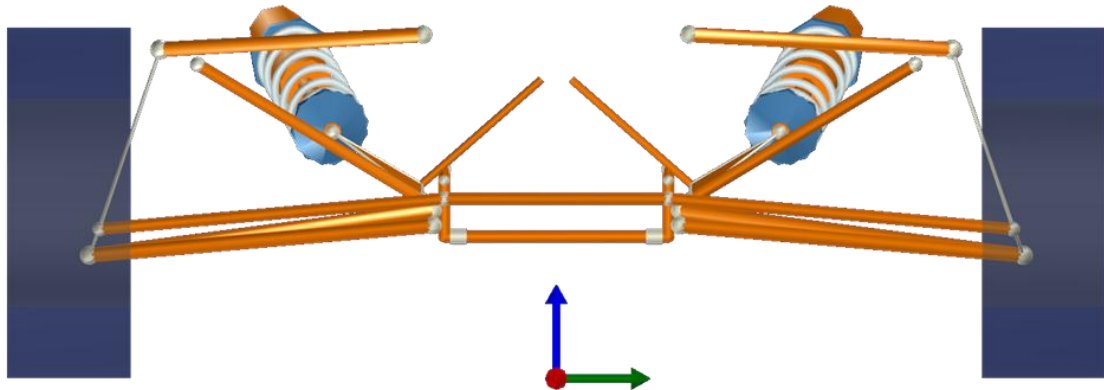


FIGURE 53 – FINAL GEOMETRY, FRONT VIEW

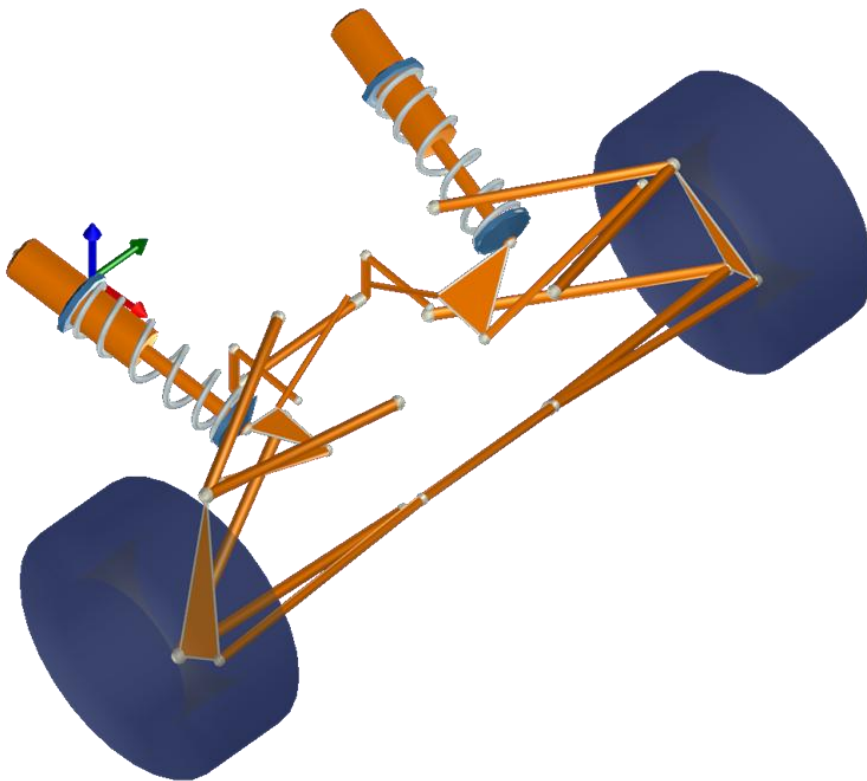


FIGURE 54 – FINAL GEOMETRY, ISOMETRIC VIEW

## 18 KINEMATICS; NEW VS. OLD

The front suspension of a commercially available cross cart was measured, modeled, and simulated for comparison data to the newly developed front suspension design. The suspension geometry of this suspension are listed in Table 23 and Table 24.

TABLE 23 – FRONT UPRIGHT GEOMETRY COORDINATES, [MM]

Point of interest	X	Y	Z
Wheel center	782.5	652.5	235
Upper ball joint	781.5	620	320
Lower ball joint	783.5	650	165
Tie rod outer joint	847.5	637.5	225

TABLE 24 – FRAME FRONT SUSPENSION MOUNTS, [MM]

Point of interest	X	Y	Z
Upper control arm - front	832.5	100	355
Upper control arm - rear	562.5	192.5	355
Lower control arm - front	832.5	100	215
Lower control arm - rear	562.5	192.5	215
Tie rod inner joint	842.5	135	270

TABLE 25 – PARAMETER SPECIFICATION

Parameter	Value	Unit
Anti dive	0	[%]
Kingpin inclination	10.95	[degrees]
Scrub radius	-29.4	[mm]
Caster angle	0.74	[degrees]
Mechanical trail	3.13	[mm]
Roll center height	78.8	[mm]
Bump steer [max]	1.8	[degrees]
Ackermann	14.7	[%]
Spindle length	78.8	[mm]

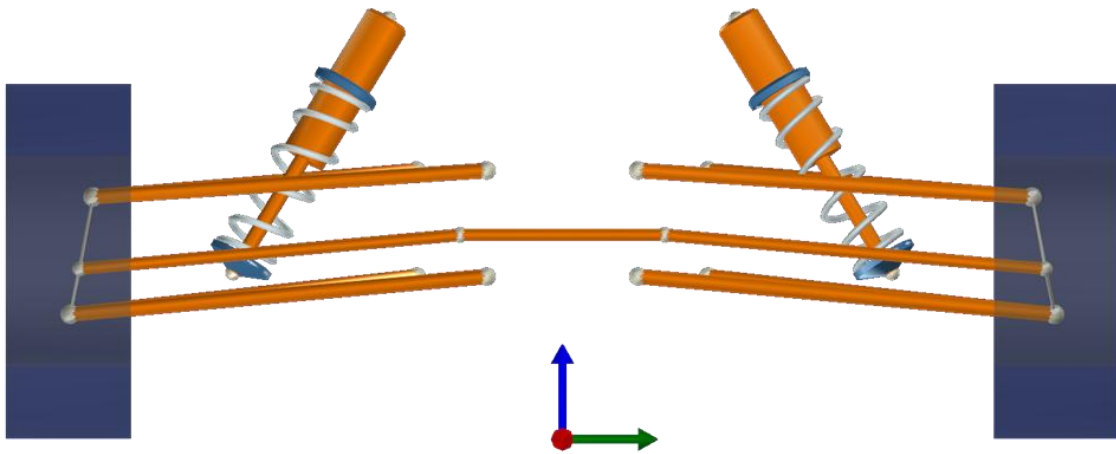


FIGURE 55 – GENERIC CROSS CART GEOMETRY, FRONT VIEW

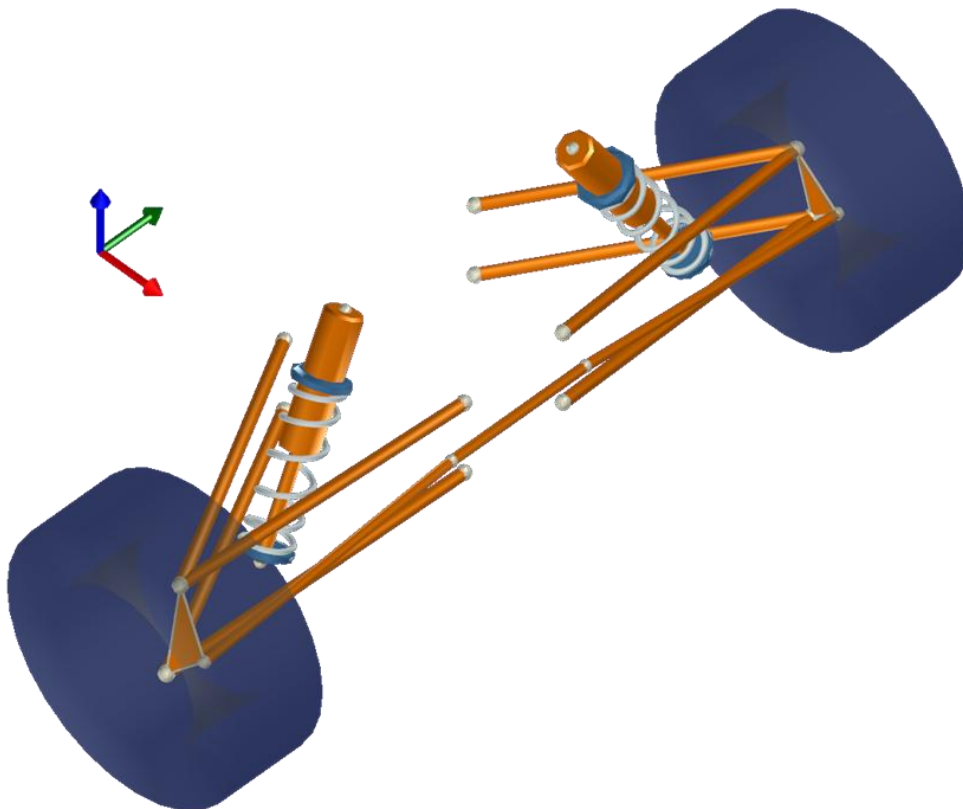


FIGURE 56 – COMMERCIALY AVAILABLE CROSS CART GEOMETRY, FRONT VIEW

The following figures display a comparison of the suspension behavior for the geometry we have developed and the suspension on a commercially available cross cart.

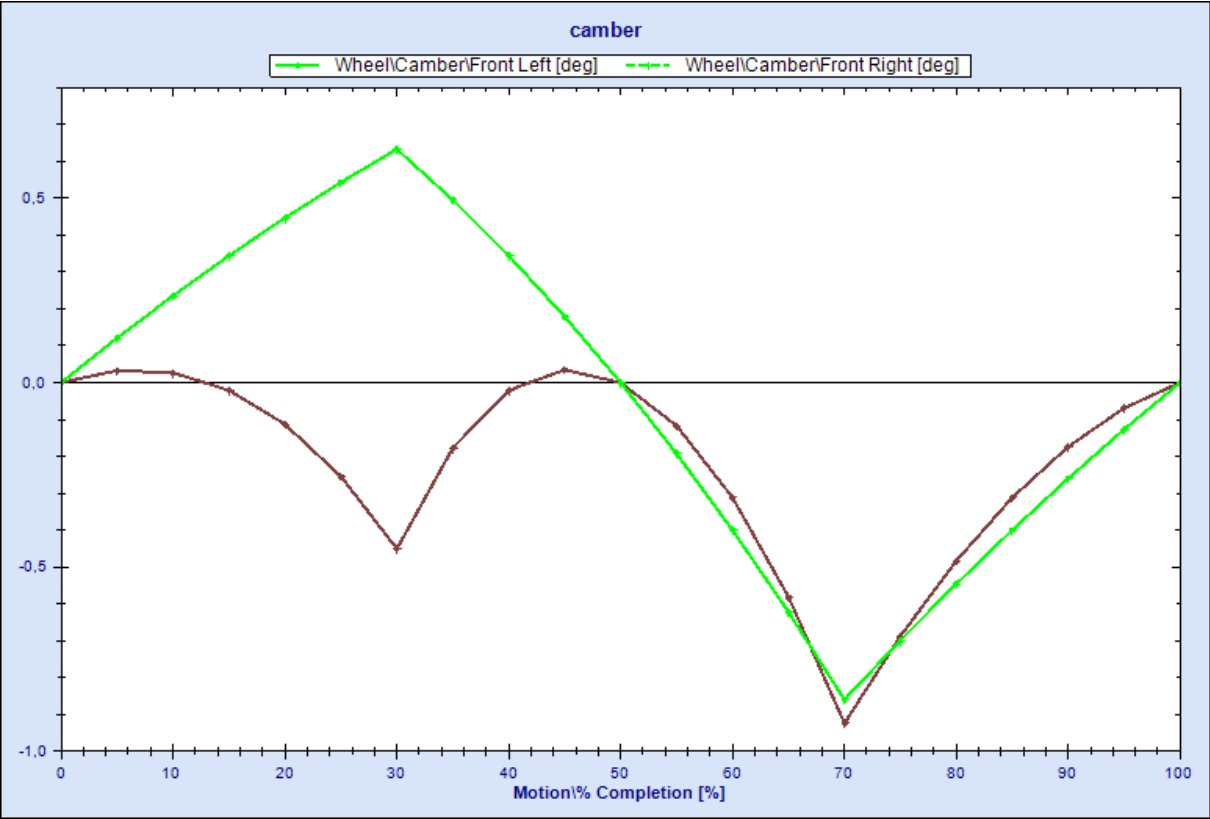


FIGURE 57 – CAMBER CURVE, HEAVE TEST

The camber curve for the commercially available suspension generates 0.65 degrees positive camber for 80mm heave, and -0.83 degrees for 80 mm bump. Our suspension generates - 0.47 degrees in heave and -0.9 degrees in bump.

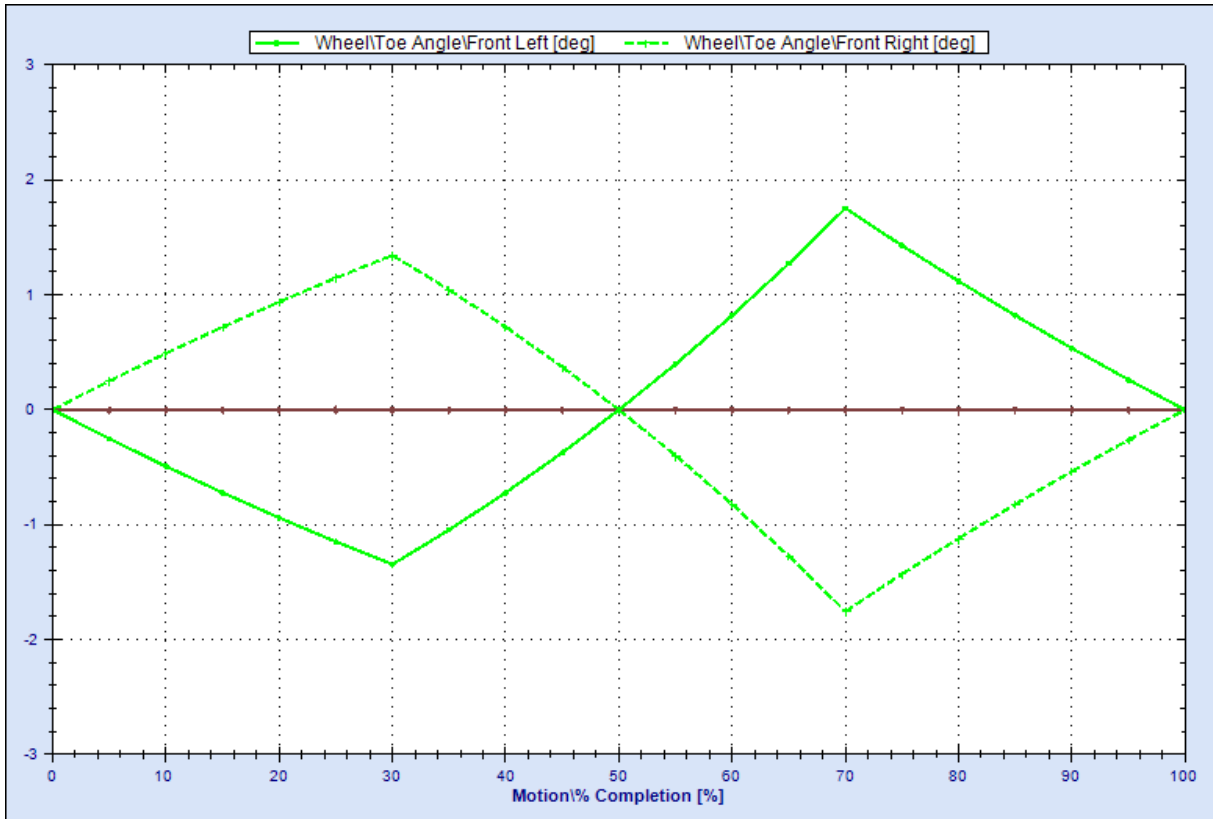


FIGURE 58 – TOE CURVE, HEAVE TEST

The toe curves from the heave test in Figure 58 shows 1.2 degrees toe in for heave and 1.78 degrees toe in on bump for the commercially available suspension. For our suspension the values are 0.002 degrees and 0.003 degrees respectively.

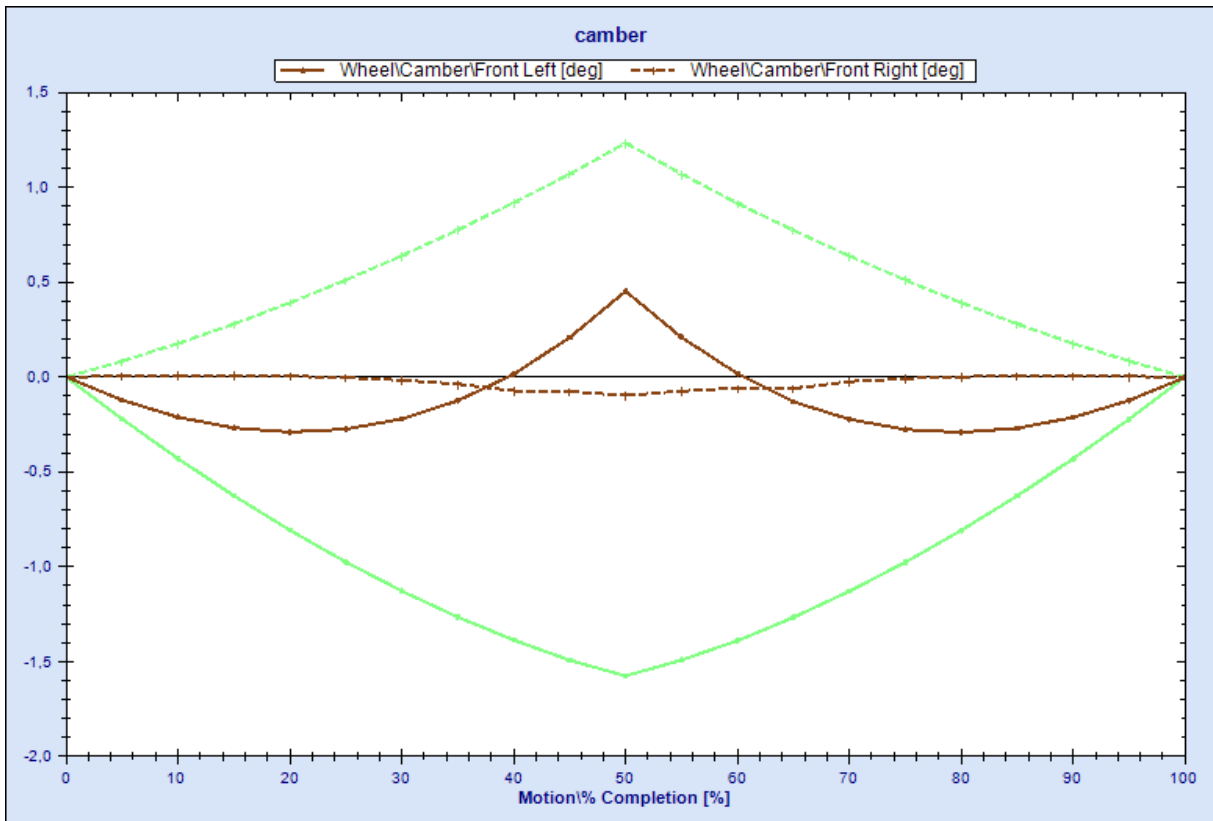


FIGURE 59 – CAMBER CURVE, TURN AND HEAVE TEST

The camber curve from the turn and heave test shows a maximum of 1.6 degrees of positive camber on the inside wheel, and 1.25 degrees negative camber on the outer wheel for the outer wheel, on the commercial cross cart suspension. Our equivalent values are -0.2 for the outer wheel and an inner wheel which crosses from 0.25 degrees peak negative to 0.45 peak positive camber angle.



## 19 SUSPENSION DYNAMICS

### 19.1 SPRINGS

Suspension tuning on any vehicle is a tedious task, with lots of trying and lots of failing. However, one way to minimize the troubles of tuning is to roughly calculate what the different baseline properties of the vehicle's dynamics should be. The bases for these calculations are from the 250ccm cross cart class, with the 260 kg weight minimum including the driver. The minimum weight over the front wheels is 100 kg, with the PSE cart having 118 kg over the front. This gives each front wheel 59 kg's to support. Of these 59 kg's, around 10 kg's are unsprung mass.

Springs have different properties, and their *spring rate* is one of them. The spring rate is a number representing how much the spring compresses for a given load. If a spring is compressed 1 mm from being loaded with a force equal to 1 kg, the spring rate is 1 kg/mm (more commonly used unit is N/m). If the spring is linear it will be compressed 2 mm with 2 kg's of force, 20 mm with 20 kg's of force, and so on. Most springs are however progressive, meaning that the spring rate increases proportionally with the load.

The amount a spring is compressed with a vehicle's weight on top is called the *static compression*, which is determined by the chosen spring rate. It is generally considered wise to set the spring rate such that the static compression does not equal the full suspension/spring travel. After all, there should be room for the suspension to absorb bumps and holes in the road. The static compression shouldn't be too small either, because the wheel needs to be able to stay in contact with the road on hollows and uneven surfaces. This is called *rebound travel*, also needed to keep the inside wheels on the road during sharp cornering.

Another aspect of a spring loaded system (such as a vehicle's suspension) is the *natural frequency*, measured in Hz ( $\frac{1}{s}$ ). When a spring is loaded and the load is removed, the spring will bounce up and down at the spring's natural frequency. The bounces get smaller and die away naturally, but will continue in the same frequency until they stop. The natural frequency can make a vehicle's occupants seem pleasant, the human body favors frequencies around 1 Hz to 1.5 Hz. It can also cause discomfort; frequencies around 0.75 Hz as well as 1.8 Hz are perceived as nauseating and uncomfortable (Rølvåg, 2011). Off-road vehicles such as cross carts have a long suspension travel, along with a substantial static compression which gives it a low natural frequency. The PSE cross cart has a suspension travel of 160 mm, with 80 mm static compression. This gives it a natural frequency of around 1 Hz. This thesis mainly considers the front suspension, but it should be mentioned that the natural frequency should be a little bit higher in the rear than the front, especially on road cars. This is because of the time shift between the front wheels hitting a bump and the rear "catching up", causing a body pitch (Giaraffa, 2010).

When the ride frequency of the system is chosen, the spring rate can be determined from the motion ratio of the suspension, the amount of sprung mass per wheel and the desired ride frequency.

$$f = \frac{1}{2\pi} \sqrt{\frac{K}{M}}$$

EQUATION 10 - RIDE FREQUENCY

$f$  = natural frequency

$K$  = spring rate,  $\left(\frac{N}{m}\right)$

$M$  = mass (kg)

Solved for spring rate, and including motion ratio:

$$K_s = 4\pi^2 f_r^2 m_{sm} MR^2$$

EQUATION 11 - SPRING RATE

$K_s$  = spring rate  $\left(\frac{N}{m}\right)$

$m_{sm}$  = sprung mass (kg)

$f_r$  = ride frequency (Hz)

$MR$  = motion ratio  $\left(\frac{\text{wheel travel}}{\text{spring travel}}\right)$

Using this equation, a baseline spring rate for the PSE cross cart can be calculated. As stated in the requirements specification in section 12, the suspension will have a motion ratio of around 1.

$$K_s = 4\pi^2 * (1 \text{ Hz})^2 * 49 \text{ kg} * 1^2 \cong 1934 \frac{N}{m} = 1,934 \frac{N}{mm}$$

## 19.2 DAMPING

As previously mentioned, springs have a tendency to bounce up and down until something stops them. That something, whether it's an active force working against the motion or just friction or gravity, is called damping. The reason for using damping units on a vehicle is to stop the natural frequency oscillations within a couple of bounces, and not letting them get out of control.

How fast a suspension is excited is called the *input frequency*, the effects of bumps in the road depends on how fast the vehicle is travelling. The shorter the spacing between bumps is, the greater the vertical acceleration inputs into the suspension become. If bumps occur at a certain frequency, the input frequency matches the natural frequency, which greatly increases the amplitude of the motion. Unless damped, this kind of motion quickly escalates into an uncontrollable chaotic system, and can potentially bounce the vehicle off the road. This means that dampers are particularly important in suppressing the suspension motion around the natural frequency, which is where the suspension will move furthest for a given bump input. It is also worth mentioning that no damping actually changes the natural frequency of the system; it only stops the bouncing motion faster.

As the suspension absorbs bumps in the road, the dampers work to stop the motion. While the objective of the suspension is to stop the vertical acceleration of the wheel from passing into the vehicle's body, a stiff damper actually does the opposite; in bump a stiff damper will cause the suspension to transfer more of the acceleration into the body, causing a rough ride. The balance between effective bump absorption and ride comfort is the essence of the correct use of dampers. The trick to achieving this is called *rebound*. When the spring has compressed and is starting to extend back out is the time to apply most of the damping. If the ratio of rebound to bump damping is 2:1, the damping when the spring is extending back out is twice as firm as when the spring compresses. By absorbing most of the movement when the spring is acting away from the body, the dampers don't transfer large amounts of force into poor ride comfort. Spring and damper behavior need to be well matched and adjusted according to the surface the vehicle will normally be driving on. For example, if a low bump damping and a high rebound damping is used, the spring might not have time to extend between each bump and the suspension runs out of travel.

Early types of suspension damping were mainly of the friction type. Old cars often have many kinds of springs, but telescopic dampers are rarely used. Friction damping use components that twist against each other, for example a stack of discs. This type of damping provide a constant decrease in spring extension for each bounce cycle, it does not vary in strength with how fast the suspension is moving, as graphed in Figure 60.

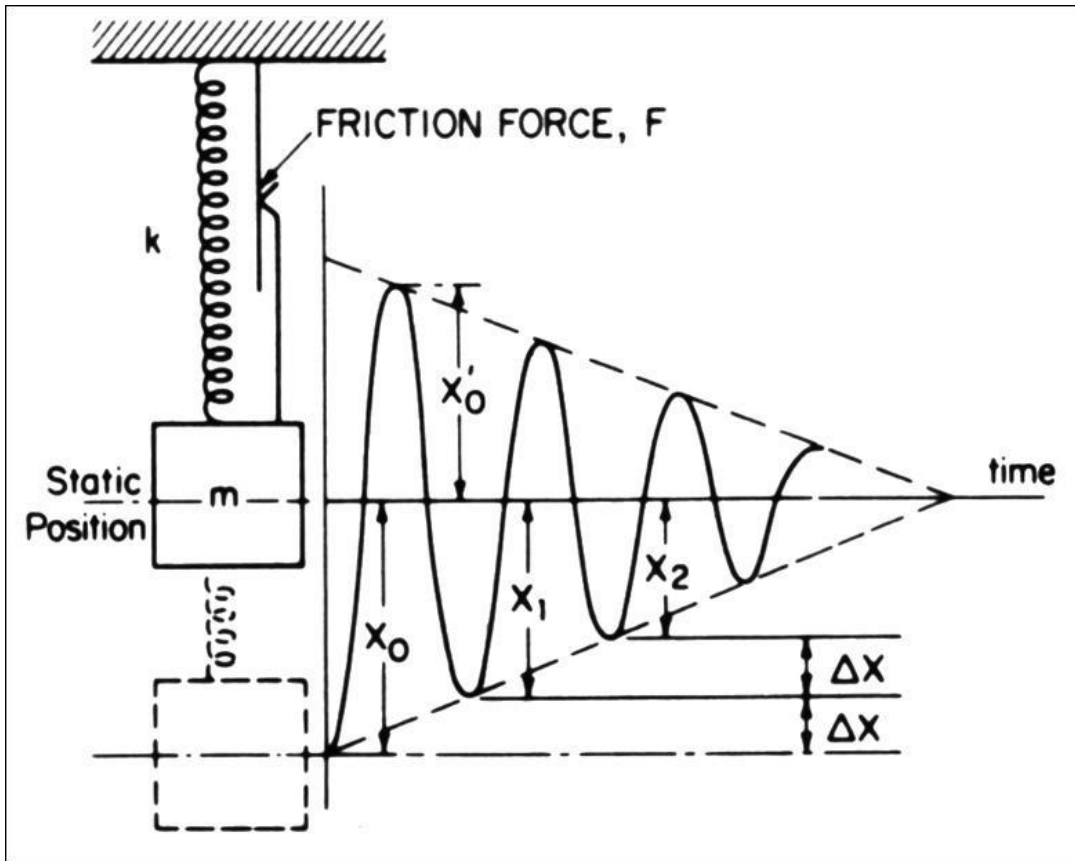


FIGURE 60 – FRICTION DAMPING

All modern dampers are velocity dampers, usually controlled by a liquid flowing through small channels into or out of a reservoir. This makes the damping proportional to the speed of the suspension movement, i.e. faster movement means a more resisting damper, see Figure 61.

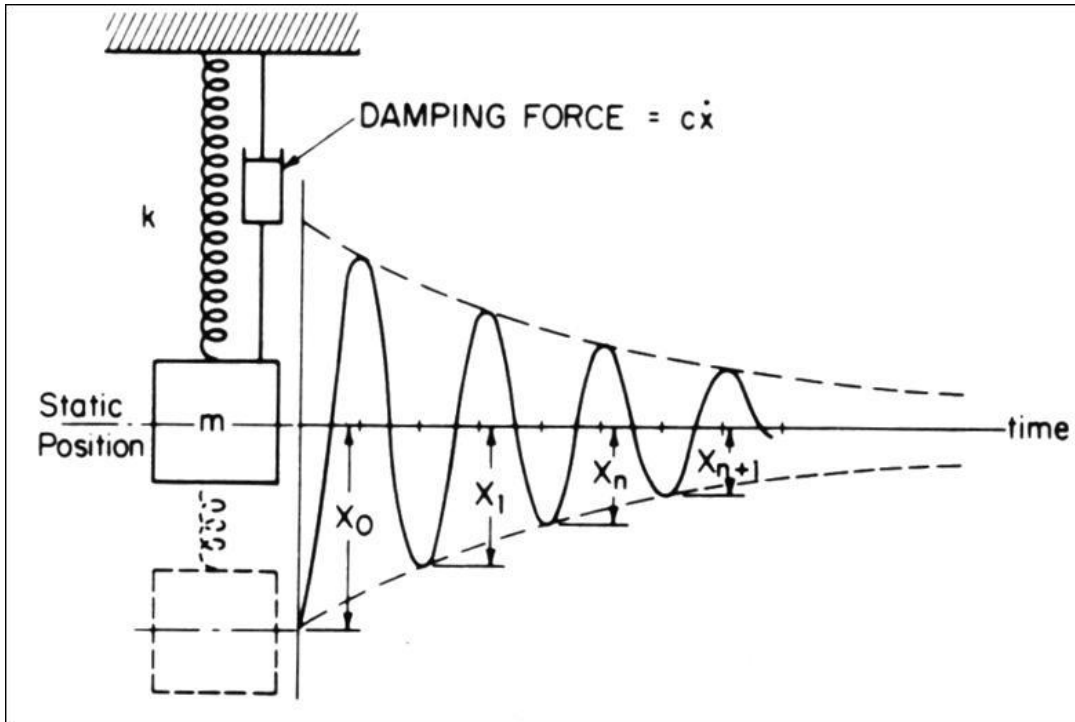


FIGURE 61 – VELOCITY DAMPING

When the damping coefficient of a system is to be calculated, *critical damping* is an important aspect to consider. The critical damping is where the damping has the fastest response time without “overshooting” and making the system respond slowly. This is called over-damping, meaning that the mass of the system has so much damping that it takes a long time to return to its equilibrium (Splung.com, 2012). The opposite of this is under-damping, where the damper is too weak and lets the bouncing motion continue for too long.

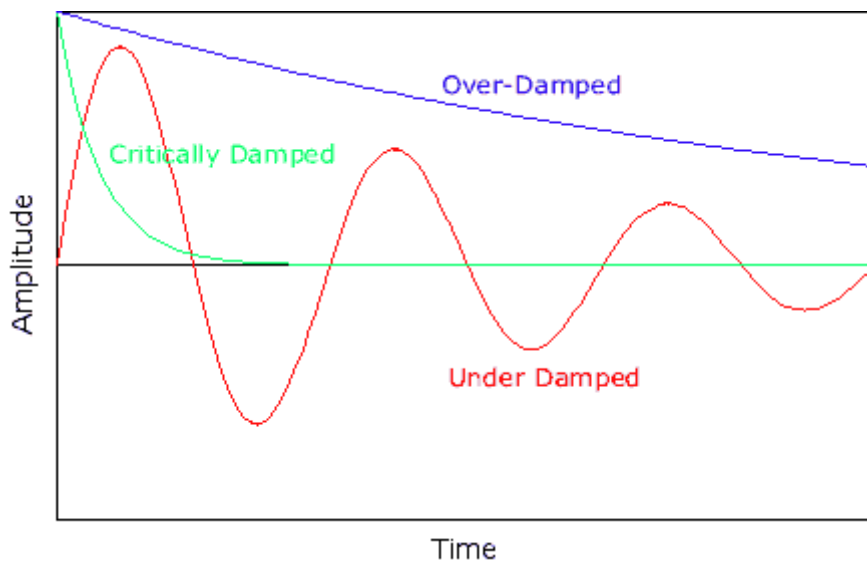


FIGURE 62 – DAMPING TYPES

To calculate the critical damping the following equation can be used.

$$C_{cr} = 2\sqrt{K_w m_{sm}}$$

EQUATION 12 - CRITICAL DAMPING

$$K_w = \text{wheel rate} = \frac{K_s}{MR^2} \left( \frac{N}{m} \right)$$

$$m_{sm} = \text{sprung mass (kg)}$$

Since the motion ratio is 1, the wheel rate is equal to the spring rate;  $K_w = 1,580 \text{ N/mm}$ . In the case of the cross cart, the critical damping follows as below.

$$C_{cr} = 2 \sqrt{1934 \frac{N}{m} * 49 \text{ kg}} \cong 616 \frac{N * s}{m}$$

EQUATION 13 – CRITICAL DAMPING

The damping ratio between the damping force in the system and the critical damping is often used:

$$\xi = \frac{C}{C_{cr}}$$

EQUATION 14 – DAMPING RATIO

From the previous discussion it follows that the type of damping can be expressed as in Equation 15 and Figure 63 (Giaraffa, 2010).

$$\xi < 1, \textit{ underdamped system}$$

$$\xi = 1, \textit{ critically damped system}$$

$$\xi > 1, \textit{ overdamped system}$$

EQUATION 15 - TYPES OF DAMPING

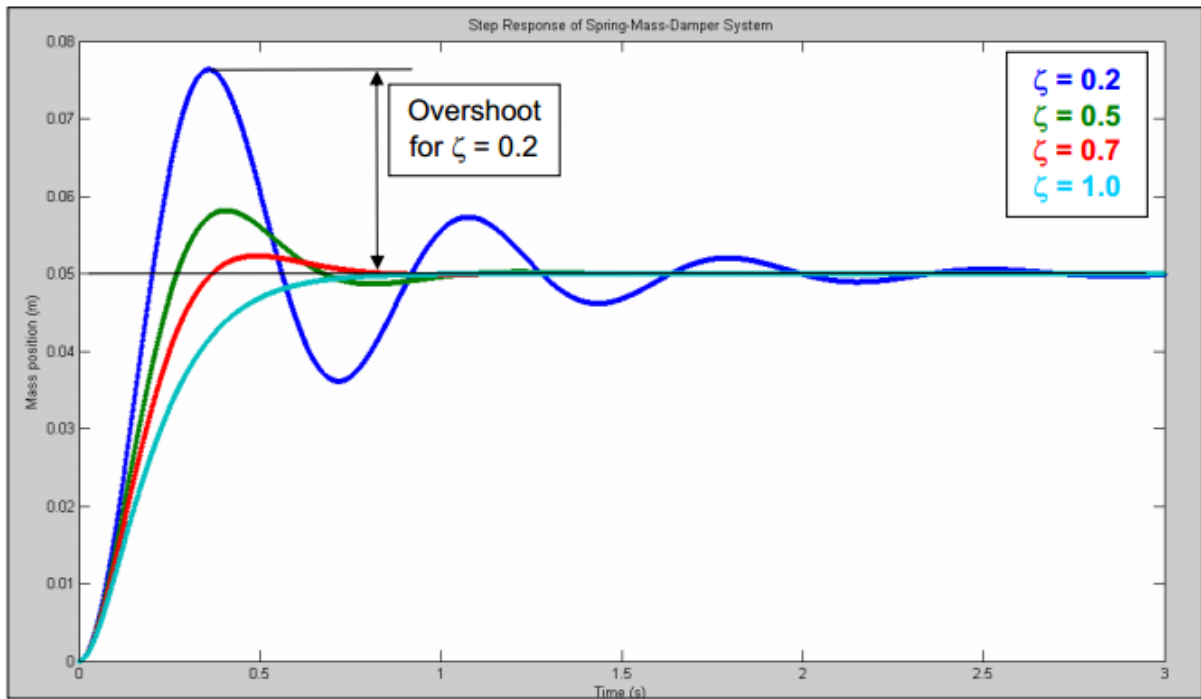


FIGURE 63 – TYPES OF DAMPING

Critical damping is rarely optimal on any driven vehicle, the ride usually becomes much too firm. Passenger vehicles generally use a damping ratio of around 0.25 for maximizing ride comfort. Race cars use around 0.7, to achieve less overshoot and faster response. On a cross cart it is preferable to let the suspension travel a bit, so a rough estimate in this case comes out at around 0.5. The damping coefficient for this setup is shown in Equation 16.

$$C = C_{cr} * \xi = 616 \frac{N * s}{m} * 0.5 = 308 \frac{N * s}{m}$$

EQUATION 16 - DAMPING COEFFICIENT

### 19.3 FEDEM

FEDEM is a computational tool for dynamic simulation of mechanical systems with one or more parts. Each part can be represented by an element model, allowing the analyses to include structural flexibility. FEDEM can be used to investigate movements and vibrations in a system, along with stresses, strains and fatigue components. The tool was made commercially available in 1994, and has since then been used successfully in the design and engineering of wind turbines, car suspensions, industrial robots and drill heads to name a few. FEDEM's strength lies in its unique capacity to quickly calculate large systems and simulate long, complex series of events.

FEDEM gives engineers the opportunity to validate and further develop different aspects of a mechanical system such as a vehicle's suspension. To make this possible, the cross cart suspension was designed in NX 7.5 and element models of the parts exported in a FEDEM-readable format. The setup in FEDEM is simplified because of the exported element models from NX 7.5 also incorporate the part position and orientation in the same coordinate system. When the parts are loaded into FEDEM (in FEDEM, parts are called "links"), the preset position and orientation makes the analysis process a lot easier. To connect two of the links together, a joint of some sort has to be used. To make the model as similar to the preset geometry as possible, joints have to be placed very accurately in the 3D space.

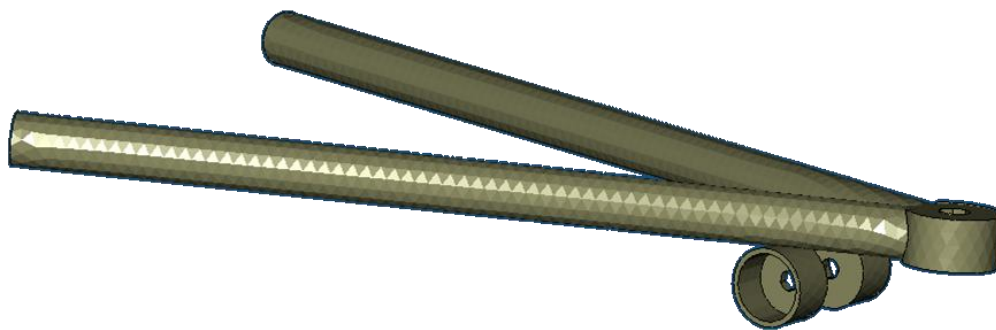


FIGURE 64 – UPPER SUSPENSION ARM

Figure 64 shows a simplified model of the upper arm of the suspension loaded as a link in FEDEM. The actual point where the ball joint in the arm connects to the upright is in the middle of the hole seen on the right on Figure 65. To construct this point a feature called *surface connector* is used. The surface connector can place a point in the center of a circle or a cylinder such in this case. To do this it needs three points along the circle's circumference and optionally the start and end points of the cylinder, as shown in Figure 65.



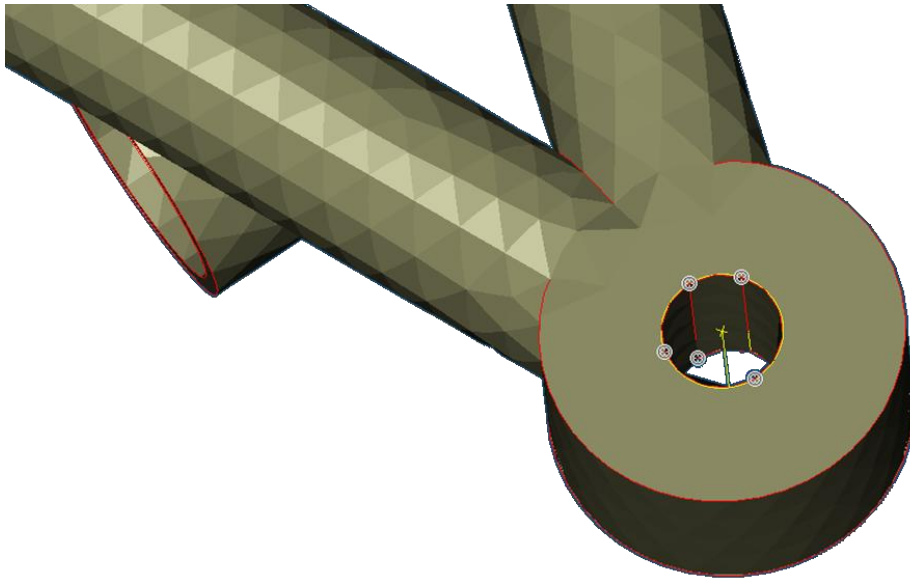


FIGURE 65 – UPPER SUSPENSION ARM DETAIL

This creates a reference able point in the center of the cylinder, called a *triad*. The triad is shown in line view in Figure 66.

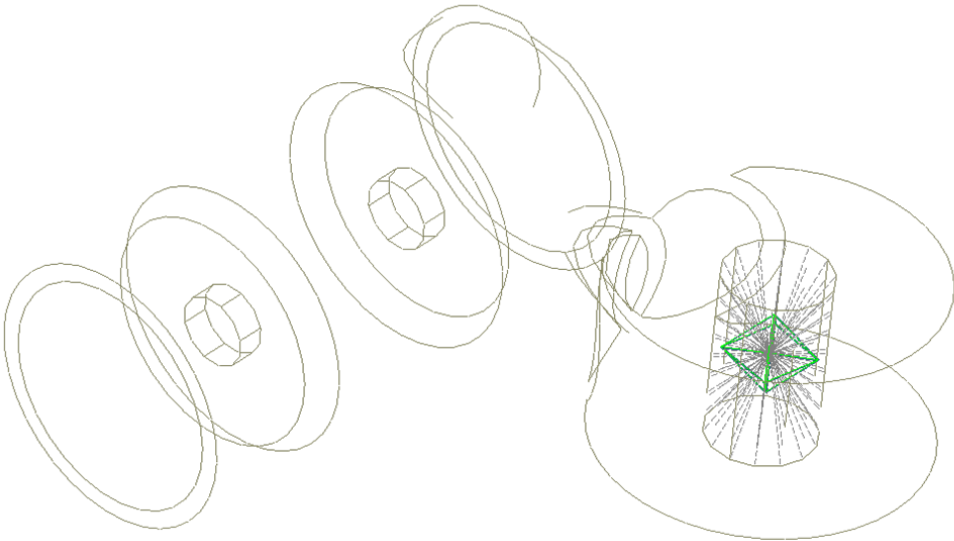


FIGURE 66 – TRIAD

The surface connector feature is used several times on each link, to be able to place the joints needed to connect the links together. Figure 67 shows the upper a-arm with a ball joint placed in the previously mentioned triad. In a typical suspension system the rod ends on the a-arms connecting the suspension to the vehicle body use ball joints to allow the necessary wheel travel. This is also the case in FEDEM. Ball joints can be allowed to move freely around all 3 axes of rotation, or one or more them can be limited or removed entirely.

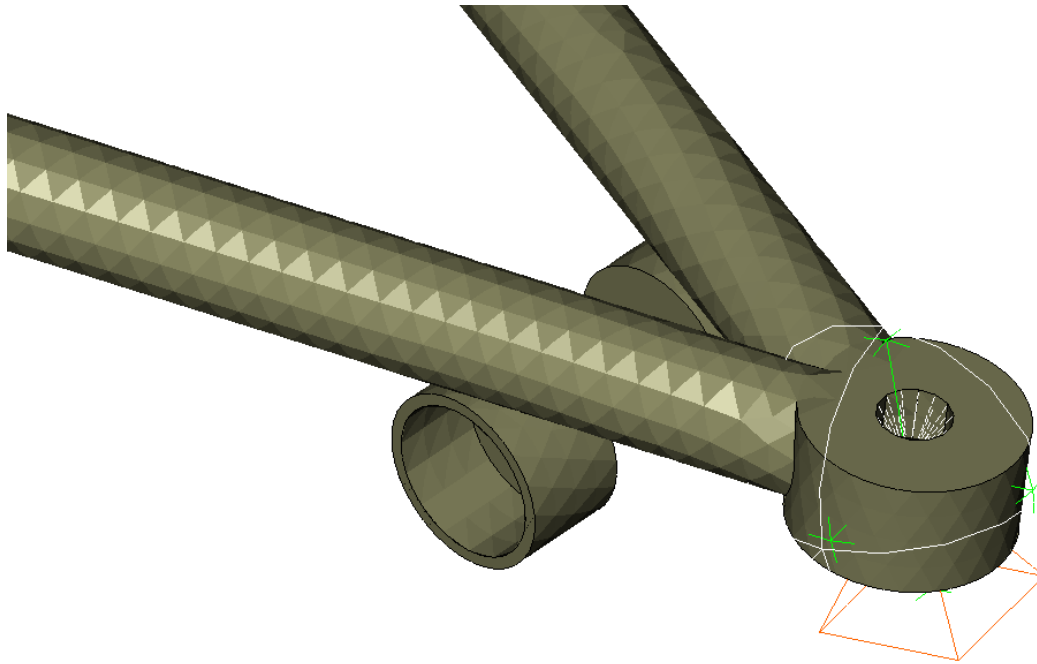


FIGURE 67 – BALL JOINT

The green axis system in the center of the ball joint indicates that the joint is partially connected, in this case to the upper a-arm. To be properly constrained, all joints need to be connected to two or more objects. Attaching links is relatively straight forward; attaching a joint to two links connects the two links with the properties inherent in the joint. Attaching a joint to the reference plane and a link *grounds* the link with a fixed constraint. Links are grounded to simulate being connected to the frame of the vehicle. Figure 68 shows the upper and lower a-arms fully grounded to the specified geometry points via ball joints.

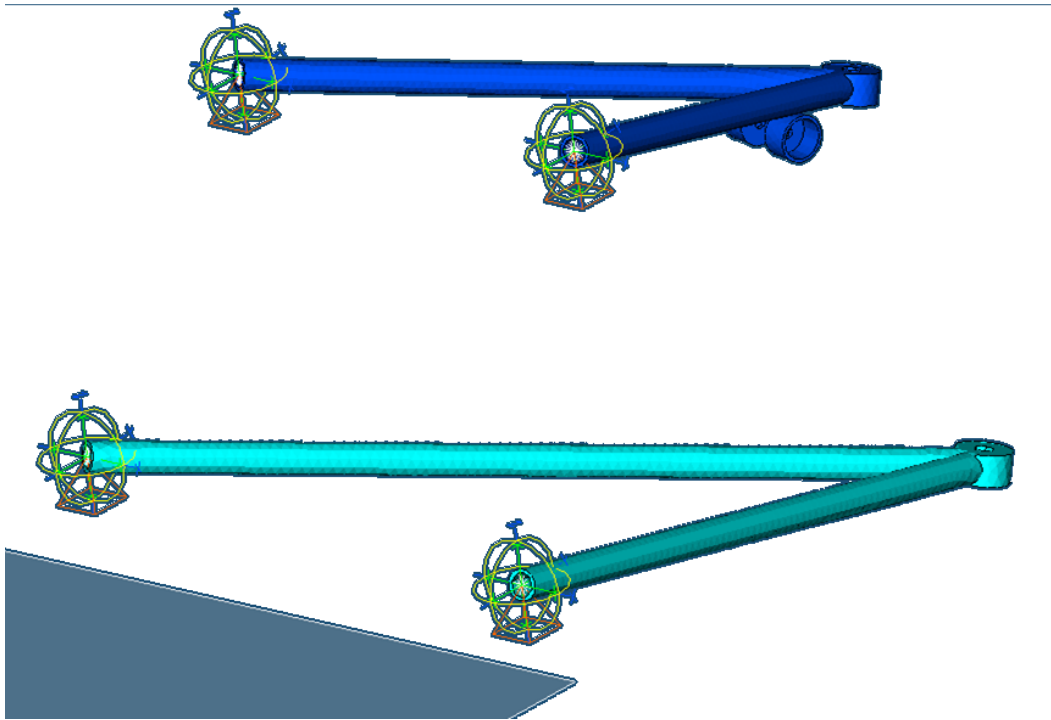


FIGURE 68 – GROUNDED SUSPENSION ARMS

To simplify the analysis process, a few components were not included in the FEDEM model. The wheel, hub, bearing and tire were represented by a “generic part”, with the same weight and stiffness properties. For rotation around just one fixed axis a revolute joint is used, for example in the rotation axis of the pull rod actuated rocker in Figure 69.

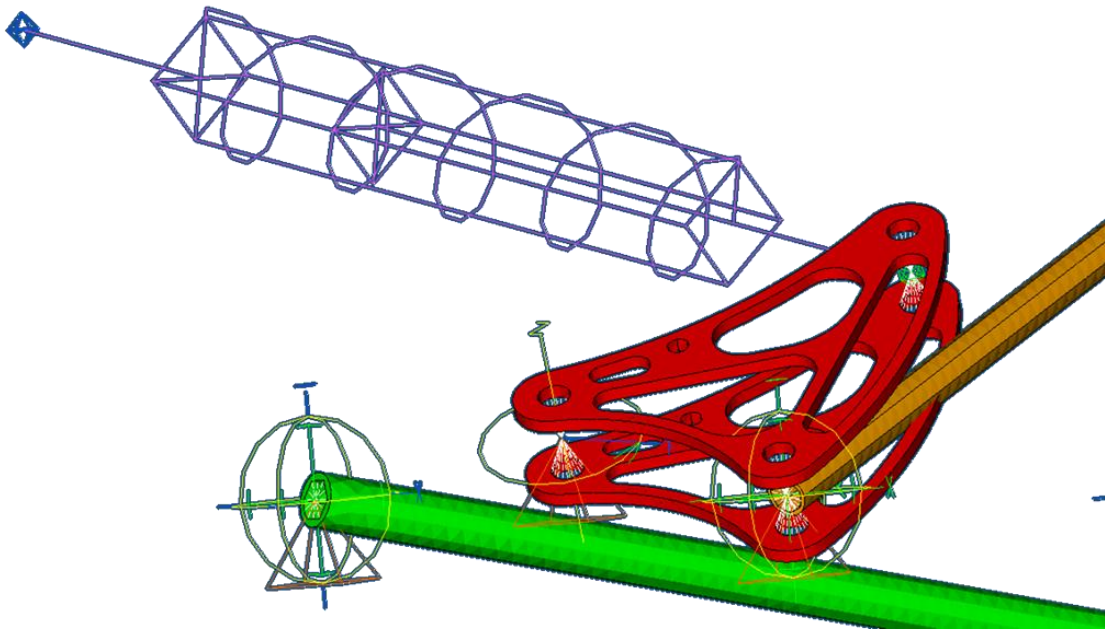


FIGURE 69 – ROCKER

The main purpose of the FEDEM analysis was to validate the baseline spring and damper properties dynamically. It should be mentioned that the various parameters of the

suspension are not optimized, just the baseline is set. Further adjustment and tuning of the suspension setup goes beyond this thesis, and should be carried out if and when it is decided to start further refinement and production of the concept. This includes for example creating realistic functions for variable/progressive spring stiffness.

The suspension was modeled fully extended, to see how the system reacts to being placed on the ground and finding its equilibrium position. This position is ideally the same as the static compression, around 80 mm. The frame and other components of the cross cart are not modeled in the simulation, so the weight of the sprung components needs to be represented by a reaction force in the wheel center. Figure 70 shows the balancing of forces over the front wheels, which indicates that the force on each wheel is approximately 590 N, of which 490 N is from sprung components.

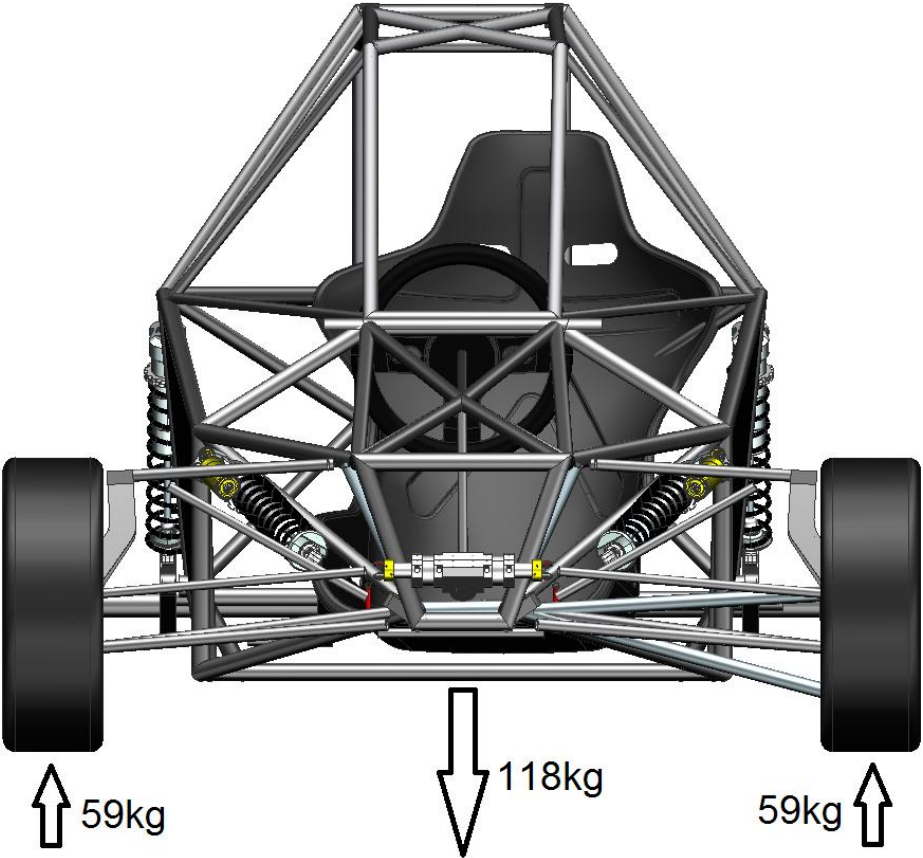


FIGURE 70 – MASS REACTION FORCES, FRONT WHEELS. (ILLUSTRATION)

The force from the 10 kg’s of unsprung components is represented by a point mass of 10 kg in the wheel center.

Figure 71 shows the fully modeled suspension system on one of the front wheels. The spring and damper coefficients are set as previously calculated in sections 19.1 and 19.2.

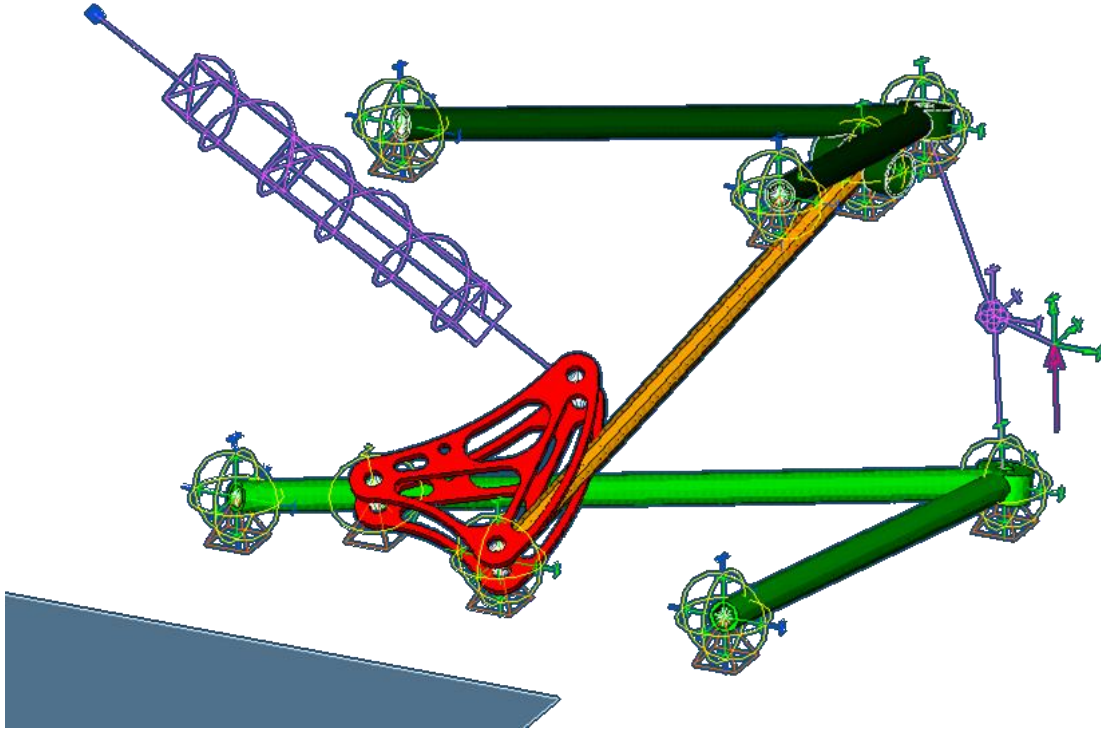


FIGURE 71 – FEDEM SUSPENSION MODEL

At this point the spring is extended fully at 80 mm, which can be specified in the spring properties as *Initial deflection*. This means that when the dynamic simulation starts, the tension in the spring will compress it to a certain extent, despite gravity acting on the unsprung components. The first simulation that was run shows what happens when the suspension is first allowed to settle without the load resulting from being placed on the ground, and then applying that load after 2 seconds. This is shown in the graph in Figure 72 and in video “settle\_start.mpeg”.

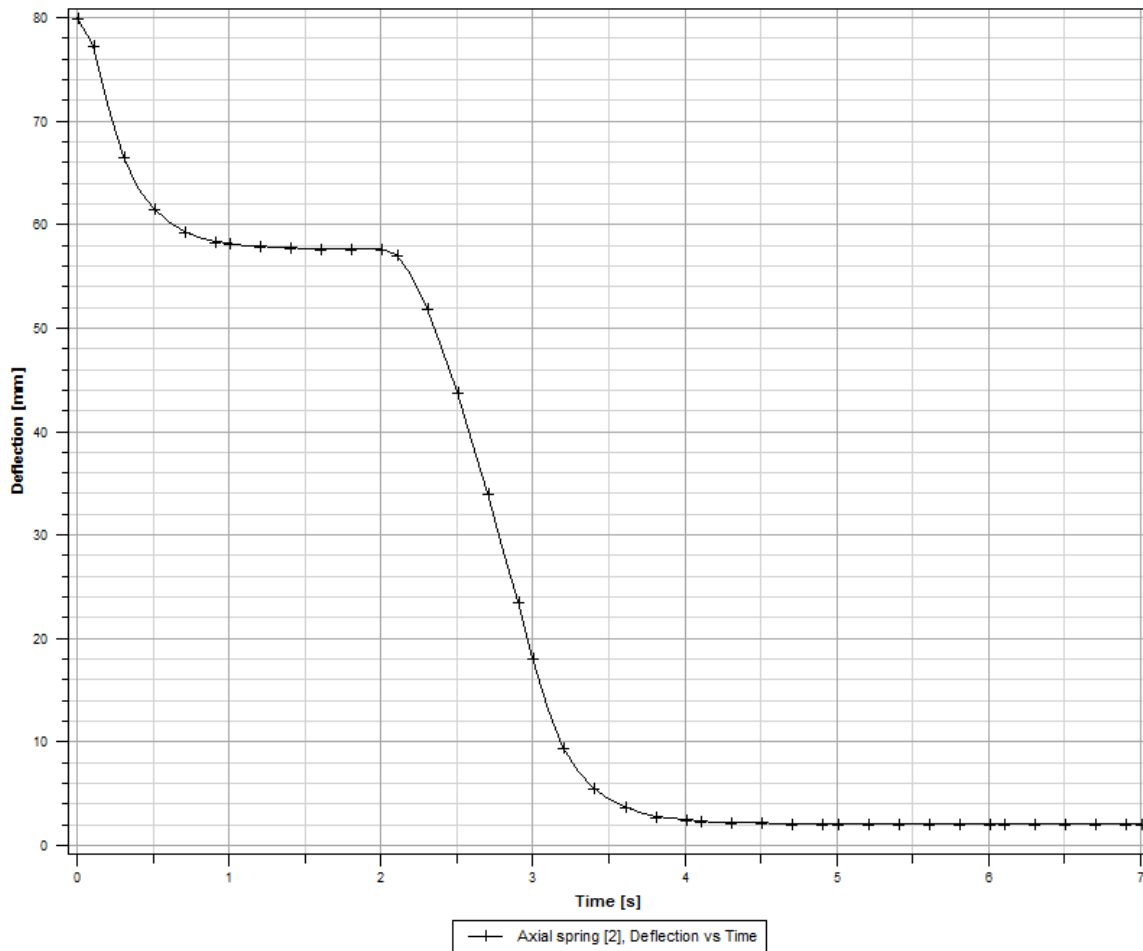


FIGURE 72 – LOAD APPLICATION, STATIC COMPRESSION

The tension in the spring retracts the suspension to 68 mm, 12 mm from the initial deflection. After 2 seconds the “ground force” of 490 N is gradually applied with a ramp function spanning 1 second, resulting in the suspension settling approximately at the center of its travel. The next step is to simulate driving on an uneven surface, and checking how the spring/damper unit copes with continuous excitations. Video “continuous.mpeg” shows repeated violent and fast excitations of the system, with a steady and predictable movement, utilizing the whole spring travel.

It is possible to validate the calculated critical damping by applying a sudden load, simulating a bump in the road.

**Underdamped, C = 100**

In this simulation the damping coefficient is set substantially lower than the calculated value, and as predicted the suspension acts under damped. A large overshoot and the system taking a long time to stop bouncing are signs of this, as shown in Figure 73 and video “underdamped.mpeg”.

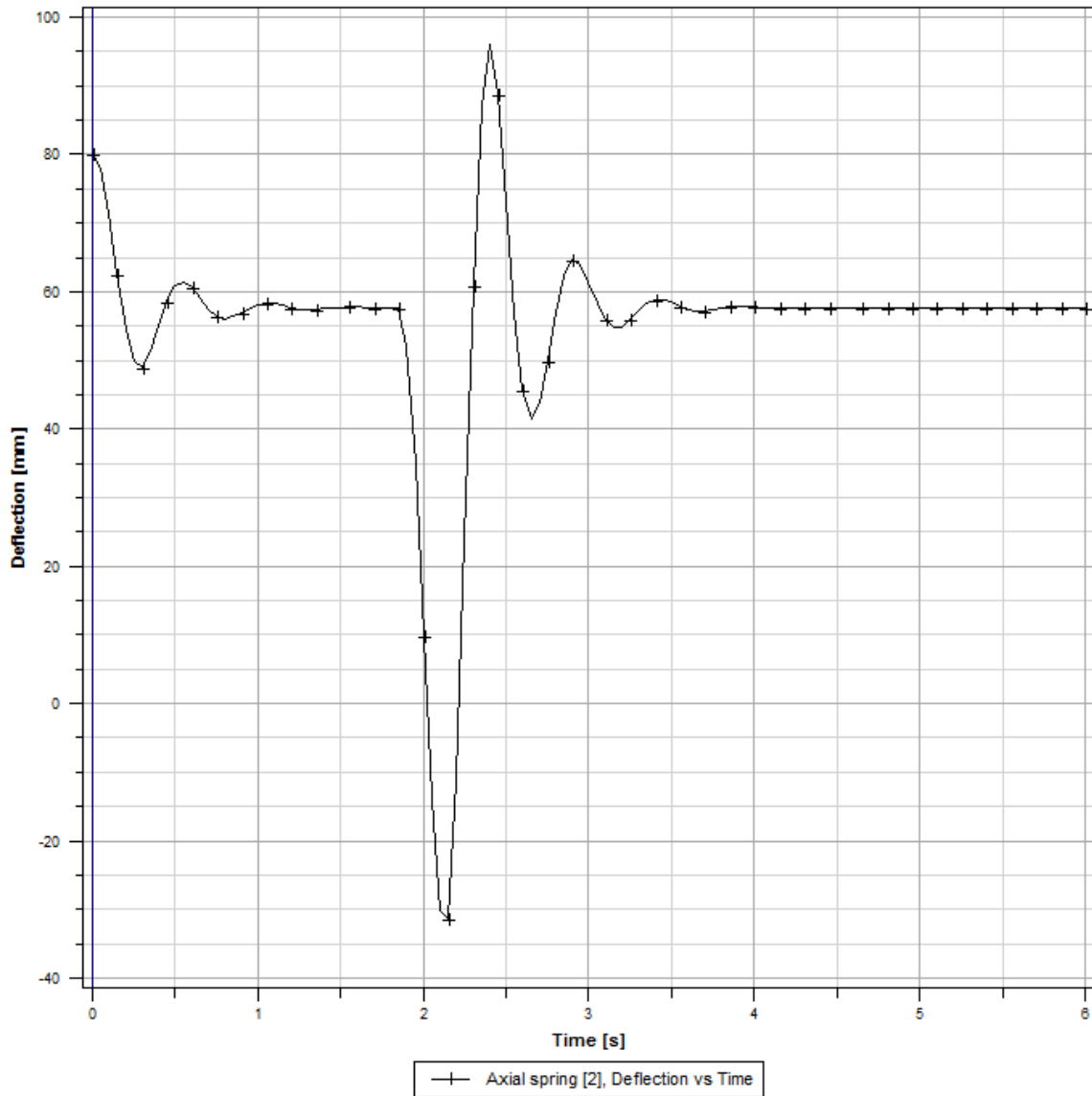


FIGURE 73 – UNDERDAMPED SYSTEM

**Calculated damping, C = 308**

As shown in Figure 74 and video “calculated.mpeg” the system responds well to the calculated damping coefficient, giving a relatively small overshoot while at the same time settling quickly.

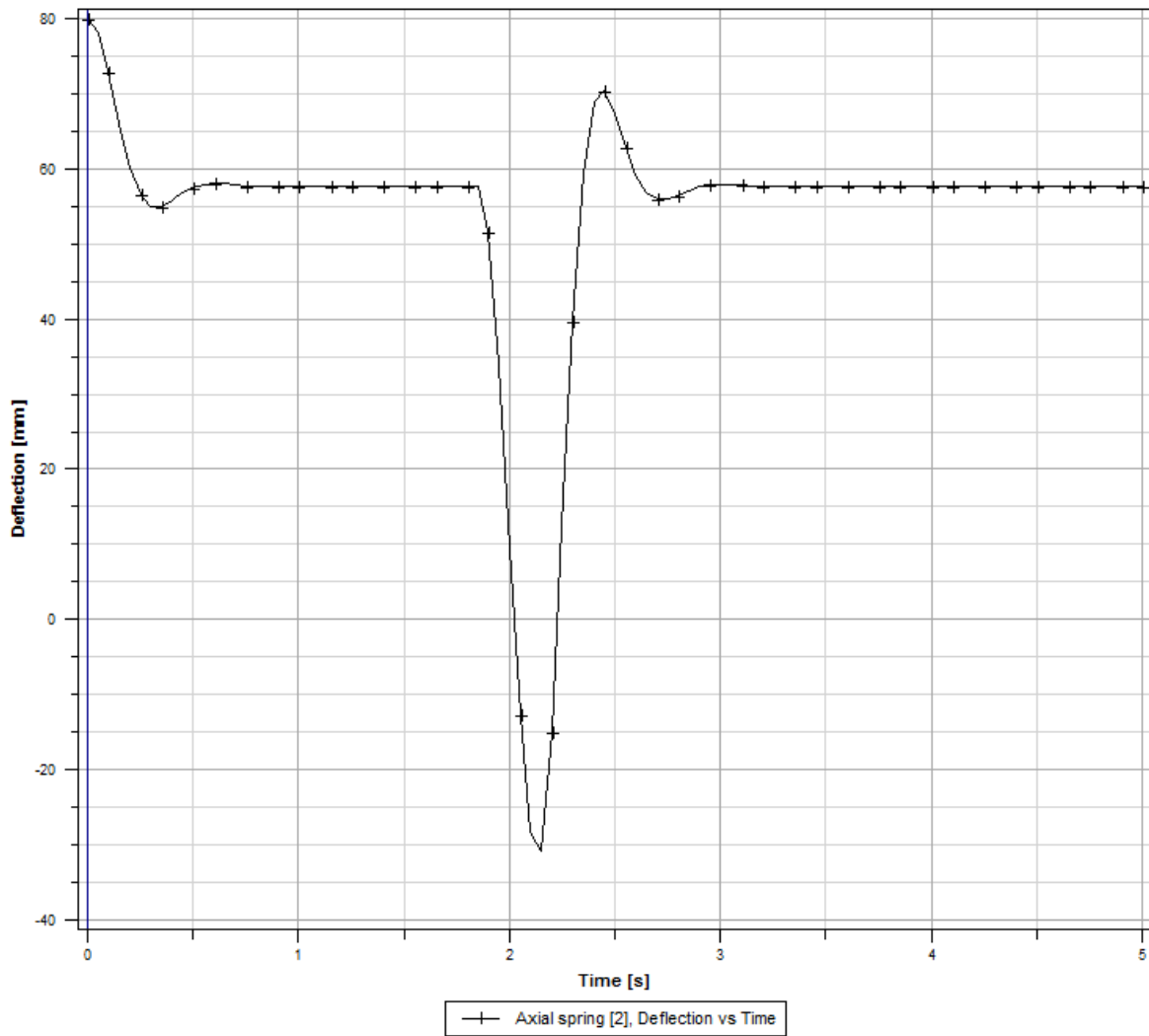


FIGURE 74 – CALCULATED DAMPING

**Critical damping, C = 616**

Figure 75 and video “critical.mpeg” shows the system with the critical damping coefficient in place, coming to rest very quickly and allowing no overshoot.



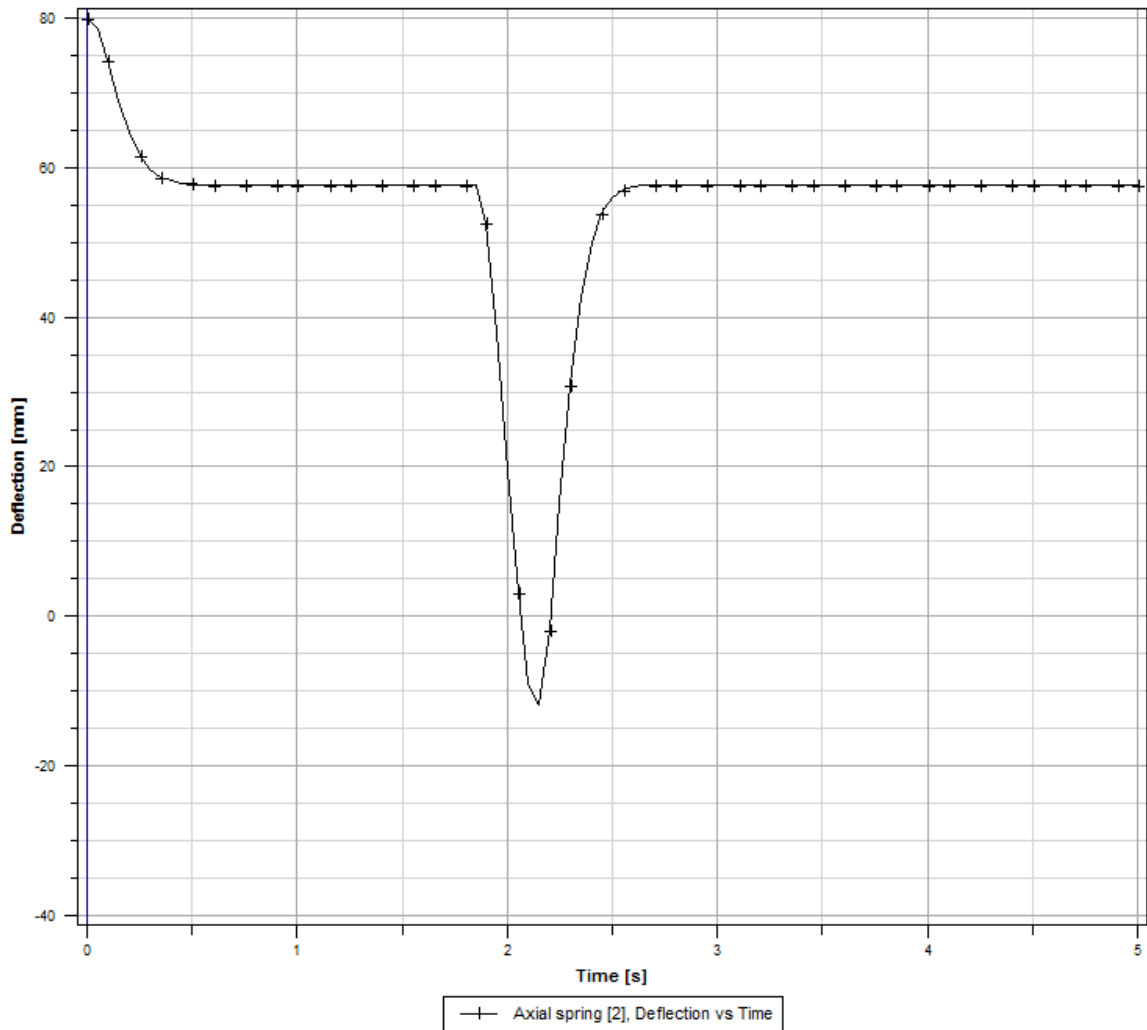


FIGURE 75 – CRITICAL DAMPING

### Overdamped, C = 750

An overdamped system is sluggish and slow in its response in both ways through the suspension travel. An example of overdamping in this system is shown in Figure 76 and video “overdamped.mpeg”. The bump movement is stopped quickly, but the system takes too long to settle and will not be ready for the next bump in time to react it properly.

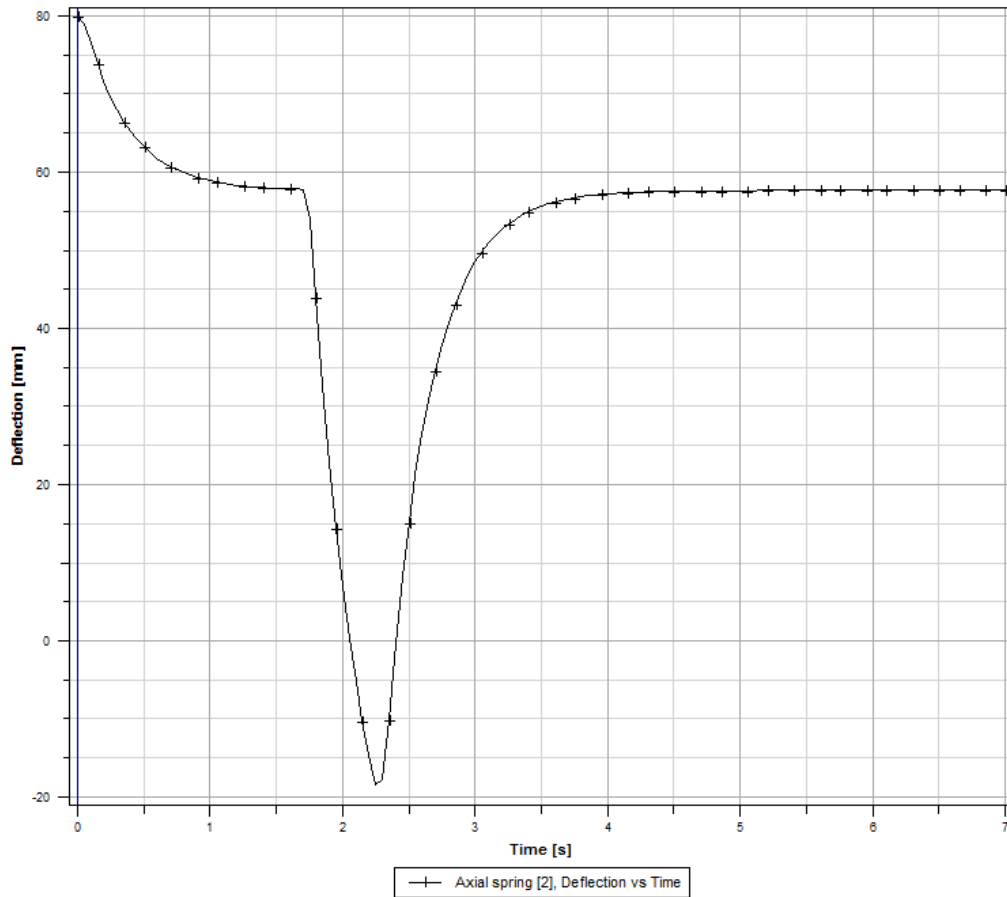


FIGURE 76 – OVERDAMPED SYSTEM

## 20 ANTI-ROLL BAR

In a corner the sprung mass of a vehicle produces a lateral force at the center of gravity (CG) proportional to the vehicle’s lateral acceleration. Since the CG rarely lies on the vehicle roll axis, these lateral forces induce a moment about the roll axis that makes the vehicle’s body roll. This moment is called *roll couple* and is resisted in the suspension roll stiffness. The roll stiffness is determined by the vehicle spring rate and the anti-roll bars (ARB). The ARBs allows an increase in vehicle roll stiffness without the use of stiffer springs which compromise ride quality on rough terrain.

The anti-roll bar is a part of the suspension that reduces a vehicles body roll during cornering. It connects the left and right wheels together through linkages, to transfer loads from one wheel to the other. The ARB increases the suspension roll stiffness and works as an individual unit independent of the springs.

The anti-roll bar intends to force one side of the vehicle to raise or lower to similar heights as the opposite side. It is usually a torsion bar that connects the left and right spring-damper unit through linkages. When the two sides have the same movement, the ARB rotates in its mounts. If the left and right suspension moves relative to each other the ARB is subjected to

torsional loads. The ARB will transfer a percentage of the loads from the heavily loaded wheel to the other. The anti-roll bar stiffness determines the amount of loads transferred, and is proportional to the material stiffness, the second power of its cross sectional area and the inverse length of the lever arms. The rigidity and geometry of the ARB mounting points also affects the load transfer. The stiffer the ARB assembly, the more force is required to move the left and right wheels relative to each other. In other words it increases the force necessary to provoke body roll. (Dixon, 2009)

The anti-roll bar can also be used to tune in the handling balance of a car between over steer and under steer, by adjusting roll stiffness of the front axle relative to the rear or vice versa. Increased proportional roll stiffness on the front axle will increase the total load transfer that the axle reacts and cause the outer front wheel to run at a higher slip angle and the rear wheel at a lower, which causes under steer. An increase on the rear roll stiffness proportion will have de opposite effect and push the vehicle handling towards over steer.

Cross carts are vehicles subject to significant amounts of body roll, which in turn affects the wheel camber when cornering. An anti-roll bar will be incorporated in this front suspension to reduce the camber gain due to body roll. This section discusses and calculates some important factors when considering an implementation. A final decision of whether or not to move further with such a component has not been taken, which is why this section only covers the subject briefly. If more in-depth work is to be done on a later occasion, more thorough research has to be done to eliminate more of the assumptions that form the base of this section. All illustrations and calculations are on a conceptual level.

ARB calculations start with choosing the desired roll gradient. In section 12 it is stated that the maximum body roll should be 2 degrees. With an approximated maximum lateral acceleration of 1.5 g in turns, the roll gradient becomes

$$\frac{\varphi}{A_y} = \frac{2 \text{ deg}}{1,5 \text{ g}} \approx 1,33 \frac{\text{deg}}{\text{g}}$$

**EQUATION 17 – ROLL GRADIENT**

$$\begin{aligned} \varphi &= \text{body roll} \\ A_y &= \text{lateral acceleration} \end{aligned}$$

The equation for calculating the total ARB roll rate is as follows.

$$K_{\varphi A} = \frac{\pi}{180} \left( \frac{K_{\varphi DES} * K_T * \frac{t^2}{2}}{K_T * \frac{t^2}{2} * \frac{\pi}{180} - K_{\varphi DES}} \right) - \frac{\pi K_W \frac{t^2}{2}}{180}$$

**EQUATION 18 – TOTAL ARB ROLL RATE**

$K_{\phi DES}$  is the desired total roll rate; dependent on the vehicle's weight (W) and vertical distance from the roll center axis to the vehicle's center of gravity (H). As mentioned in section 12, the weight of the cross cart is around 260 kg. The roll center is specified as 65 mm above ground, the center of gravity 350 mm.

$$K_{\phi DES} = \frac{WH}{\frac{\phi}{A_y}} = \frac{260 \text{ kg} * (0.350 - 0.065) \text{ m}}{1,33 \frac{\text{deg} * \text{s}^2}{\text{m}}} \approx 55,7 \text{ Nm/deg}$$

EQUATION 19 – DESIRED TOTAL ROLL RATE

$K_W$  is the *wheel rate* of the suspension, calculated as

$$K_W = \frac{\text{spring rate}}{(\text{motion ratio})^2} = \frac{1934 \text{ Nm/deg}}{1^2} = 1934 \text{ Nm/deg}$$

EQUATION 20 – WHEEL RATE

$K_T$  is the *tire rate*, how much the tire deflects under loads. No source was found on the tire rate for the cross cart's tires, so an estimate was set based on typical values for other similar tires.

$$K_T = 140000 \text{ N/m}$$

$t$  is the average track width between front and rear. The track width is specified as 1305 mm both front and rear, meaning that

$$t = 1305 \text{ mm}$$

With all parameters clarified, the total ARB roll rate can be calculated.

$$K_{\phi A} = \frac{\pi}{180} \left( \frac{1934 \frac{\text{Nm}}{\text{deg}} * 140000 \frac{\text{N}}{\text{m}} * \frac{(1,305 \text{ m})^2}{2}}{140000 \frac{\text{N}}{\text{m}} * \frac{(1,305 \text{ m})^2}{2} * \frac{\pi}{180} - 55,7 \text{ Nm/deg}} \right) - \frac{\pi * 1934 \text{ Nm/deg} * \frac{(1,305 \text{ m})^2}{2}}{180}$$

$$K_{\phi A} = 28,49 \text{ Nm/deg roll}$$

The next step is calculating the magnitude of the torque transferred through the ARB when the vehicle rolls. The body roll rate was based on 1.5 degrees of body roll, so the total torque becomes

$$28,49 \text{ Nm/deg roll} * 1,5 \text{ deg body roll} \approx 43 \text{ Nm}$$

**EQUATION 21 – BODY ROLL RATE**

As a base for further calculations the amount of travel on the ARB-link to the rocker was set to be maximum 20 mm. This number is not final, only an estimate. It changes with the position of the link on the rocker relative to the pivot axis. The spring/damper unit moves 80 mm at full extension or compression, and the ARB-link will move 20 mm as it is located a quarter of the distance from the rocker pivot, as seen in Figure 77.

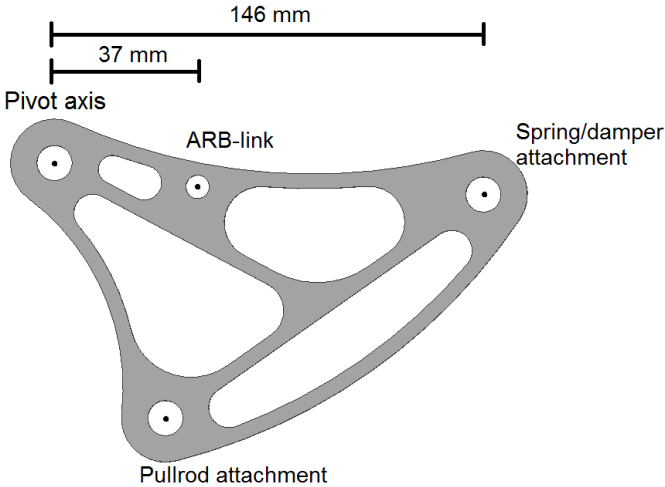


**FIGURE 77 – ROCKER GEOMETRY**

This leads to the knife link moving along an arc as the suspension travels. The important factor to take further is the angle the link moves through, which is the same as the angle of twist in the ARB itself. This twist is what transfers the suspension movement from one side of the vehicle to the other. The arc length is a function of the knife link radius and the angle.

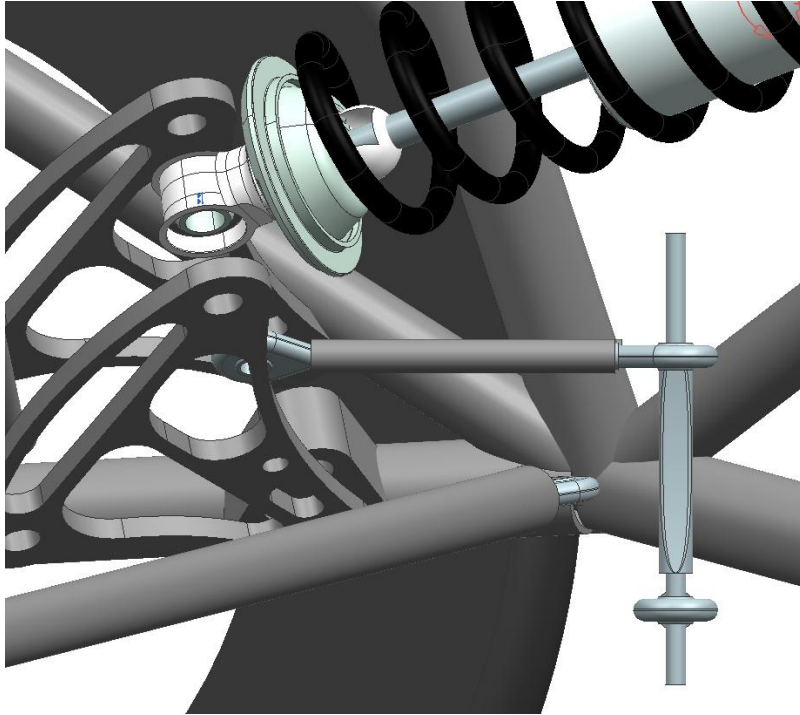


FIGURE 78 – ROCKER LINK AND KNIFE LINK IN SIDE VIEW

The knife link must be long enough to allow the whole ARB to pass under the frame, and is set to 75 mm in this case.

$$L = r * \theta \Leftrightarrow \theta = \frac{L}{r} = \frac{20 \text{ mm}}{75 \text{ mm}} = 0,27 \text{ rad} = 15,3 \text{ deg}$$

The ARB will twist 15.3 degrees to transfer the suspension movement, but should also be allowed to flex to some extent, acting as a torsional spring in the system. The total twist of the ARB is therefore set to 20 degrees, with 4.7 of these resulting in stresses in the ARB torsion bar. Based on these 4.7 degrees of flex, the necessary dimensions of the ARB can be calculated. Angular twist and torsional moment is related through an equation along with the length of the ARB, the shear modulus of the material used and the polar inertia of the cross section. The ARB will be made of steel tubes, and the main torsional rod is 300 mm long to link the suspensions on either side across the underside of the frame.

$$\varphi = \frac{T * L}{G * J}$$

EQUATION 22 – TORSIONAL ANGLE

$$\varphi = \text{angle of twist (rad)} = 4,7 \text{ deg} = 0.08 \text{ rad}$$

$$T = \text{torsional moment (Nm)} = 43 \text{ Nm}$$

$$L = \text{length of ARB} = 300 \text{ mm}$$

The shear modulus (G) of a material is a function of the material's Young's modulus (E) and its Poisson ratio ( $\gamma$ ). The Young's modulus of steel is 200 000 MPa, and the Poisson ratio is 0.3.

$$G = \frac{E}{2 * (1 + \gamma)} = \frac{200000 \text{ MPa}}{2 * 1.3} \approx 77000 \text{ MPa}$$

**EQUATION 23 - SHEAR MODULUS**

In the polar inertia (J) (Irgens, 1999) the necessary parameters to calculate the cross section of the ARB are found.

$$J = \frac{\pi}{2} * (r_o^4 - r_i^4)$$

**EQUATION 24 - POLAR INERTIA**

$r_o = \text{outer radius}$

$r_i = \text{inner radius}$

To make the ARB as small as possible while retaining the necessary properties it was decided to make it a solid rod as opposed to a tube. This means that the inner radius becomes zero and eliminated from the equation.

Rearranging Equation 22 and Equation 24 leads to an equation giving the radius of the rod

$$r = \sqrt[4]{\frac{2 * T * L}{\pi * G * \varphi}} = \sqrt[4]{\frac{2 * 43000 \text{ Nmm} * 300 \text{ mm}}{\pi * 77000 \frac{\text{N}}{\text{mm}^2} * 0.08 \text{ rad}}} \approx 6 \text{ mm}$$

There are large forces at work in suspension systems, and as calculated here the ARB torsion rod should be at least 12 mm in diameter to react them sufficiently. The stresses in the ARB when twisting should also be considered, calculated in Equation 25.

$$\tau = \frac{T}{J} * r = \frac{43000 \text{ Nmm} * 6 \text{ mm}}{\frac{\pi}{2} * (6 \text{ mm})^4} \approx 127 \text{ MPa}$$

**EQUATION 25 - TORSIONAL STRESS**

Basic steel has yield strength of at least 235 MPa, which means that the ARB has a safety factor of at least 1.85. Anti roll bars generally use higher strength steel than is normal in regular structures and vehicles, but the material choice discussion will be left for future work on the project. Further work should be done with regards to fatigue of the ARB components, and the cross section of the knife link to make the stiffness adjustable within specified requirements.

## 21 RESULTS

Table 26 below list the requirements made and the equivalent achieved values.

TABLE 26 – SPECIFIED CRITERIAS VS. ACHIEVED VALUES

Requirement	Specification	Achieved value
Max length (tire-tire)	2100 mm	2080 mm
Max outer width (tire-tire)	1500 mm	1483 mm
Bump steer/ Toe change	Less than 0.05 degree over the full suspension travel	Maximum 0.003 degrees
Ackermann steering angle	Neutral or slightly reversed	0% Ackermann
Scrub radius	15 mm – 40 mm	18.5 mm
Mechanical trail	0 mm – 20 mm	5.3 mm
Kingpin inclination	3 deg – 15 deg	13.3 deg
Caster angle	0 deg – 4 deg	2.7 deg
Minimum suspension travel	Above (+/-) 70mm	(+/-)80 mm
Ground clearance	Above 100 mm	205 mm to lowest mountingoint
Roll steer	Less than 0.4 degrees per degree of body roll	Peak value of 0.225 degrees per degree of body roll
Roll center	50 mm – 100 mm	84.5 mm
Steering ratio	85 mm rack travel per steering wheel revolution	85 mm rack travel per steering wheel revolution
Static camber	0 degrees	0 degrees
Static toe	0 degrees	0 degrees
Wheel camber <sup>2</sup>	-0.5 deg – 0.5 deg	-0.25 deg – 0.45 deg
Wheel steering angle	20 deg – 30 deg	22.5 deg
Anti dive	40% – 50%	50% anti dive <sup>3</sup>
Rocker Motion ratio	Less than 1.2	1.1
Max roll angle	3 degrees	2 degrees

The suspension arms are moved further apart, making the upright larger. This contributes to better load distribution in the suspension, hopefully reducing the stress concentrations that were big problems before. The spring/damper unit attachment is located such that it can easily be integrated in the frame structure longitudinally, significantly reducing torsion loads in the front end of the cross cart. By implementing a pull rod actuated system, the heaviest component in a suspension (spring/damper) has been moved closer to the centre of gravity. This also reduces the unsprung mass substantially.

<sup>2</sup> At maximum turn with maximum bump

<sup>3</sup> Requires 50% front braking



## 22 FUTURE WORK

Petter Solberg Engineering intends to commercialize the cross cart, standardize the carts and make them commercially available. Before this can become reality, final designs of the suspension components needs to be developed and dimensioned. The components need to be integrated with a frame through brackets. A complete assembly of the cross cart should also be analyzed through Fedem to verify the suspension functionality and performance. This will form a base for a prototype. A prototype is necessary because the suspension design primarily consists of compromises, and the performance of the suspension needs to be tested to see if the right choices have been made.

## 23 SUMMARY

The Cross cart suspension geometry for Petter Solberg Engineering has been developed through the use of kinematic and dynamic analysis. A short long arm suspension was chosen due to its ability to achieve desired performance objectives with minimum compromise. A rough geometry was developed using 2D kinematics through the front and side view geometry of suspension systems as described in *Race Car Vehicle Dynamics* by Milliken/Milliken. These were combined to a 3D geometry which was simulated and optimized using OptimumK by OptimumG. The emphasis has been put on handling through rough corners, and all design requirements has been met.

Commercially available cross carts have trouble with breakage of control arms and end rods due to high loads. Our design features a tall knuckle, which significantly reduces the load on the control arms. Anti dive is implemented in the front suspension to geometrically resist this tendency to pitch forward while braking.

Spring and damper actuation is made through a pull rod system. This is to reduce the unsprung mass, and lowering the center of gravity. Calculations on the spring rate and damper coefficient have been made to find a base setup for a future prototype. The calculations are validated through Fedem, which required modeling of prototype components in Siemens NX7.5.

Further work with component design and dimensioning needs to be done before the suspension is ready for prototype production.

## 24 SAMMENDRAG

Det har blitt utviklet et forhjulsoppheng til crosskart for Petter Solberg Engineering ved hjelp av kinematiske og dynamiske analyser. Et Short-Long arm oppsett ble valgt på grunn av at ønskede ytelsesmål ble oppnåelige med minst mulig kompromisser. En overordnet geometri ble skissert ved bruk av 2D kinematikk sett forfra og sideveis etter metoden skissert i *Race Car Vehicle Dynamics* av Milliken/Milliken. Disse ble kombinert til en 3D geometri, og simulert og optimalisert ved hjelp av OptimumK av OptimumG. Ytelse i sving på røft underlag er bli prioritert, og alle design spesifikasjoner er møtt.

Crosskarter som allere finnes på markedet har problemer med kontrollarmer og endeledd som ryker på grunn av høye belastninger. Vårt forhjulsoppheng er utviklet med en høy knoke, som reduserer belastningene betydelig. Anti dive er implementert i forhjulsoppheng for å gi geometrisk motstand mot at karten stuper fremover under innbremsing.

Fjæring og demping blir gjort gjennom et pull rod system. Dette reduserer den uavfjærede massen, og senker tyngdepunktet. Beregninger er gjort på fjærkonstanten og demperkoeffisienten for å finne et grunnoppsett for en fremtidig prototype. Beregningene er verifisert gjennom Fedem av Fedem Technology AS, som krevde modellering av komponentprototyper i Siemens NX7.5.

Videre arbeid med komponentdesign og dimensjonering er nødvendig før hjuloppheng er klar for produksjon av en prototype.

## 25 BIBLIOGRAPHY

AS, F. T., 2011. *FEDEM*. [Online]

Available at: <http://www.fedem.com/nb/programvare/fedem>

Baker, C. S., 2004. *FoES Formula SAE-A space frame chassis design*. [Online]

Available at: <http://eprints.usq.edu.au/39/>

Clarke, P., 2007. *Pat's Column - November*. [Online]

Available at: <http://www.formulastudent.de/academy/pats-corner/advice-details/article/pats-column-november/>

Clarke, P., 2009. *Pat's Column - Space-frame Chassis*. [Online]

Available at: <http://www.formulastudent.de/academy/pats-corner/advice-details/article/pats-column-space-frame-chassis/>

Dictionary, T. F., 2008. *Pushrod - pullrod*. [Online]

Available at: [http://f1-dictionary.110mb.com/pushrod\\_pullrod.html](http://f1-dictionary.110mb.com/pushrod_pullrod.html)

Dixon, J. C., 2009. *Suspension Geometry and Computation*. s.l.:Wiley.

Edgar, J., 2011. *Springs and Natural Frequencies*. [Online]

Available at: [http://autospeed.com/cms/title\\_Springs-and-Natural-Frequencies/A\\_112279/article.html](http://autospeed.com/cms/title_Springs-and-Natural-Frequencies/A_112279/article.html)

Edmund F. Gaffney III, A. R. S., 1997. *Introduction to Formula SAE Suspension and Frame Design*. [Online]

Available at: <http://comp.uark.edu/~jirencis/fsae/resources/SAE%20Paper%20971584.pdf>

Engineering, P., 2012. *About*. [Online]

Available at: <http://psengineering.se/>

Engineering, R., 2011. *Formula Student 2011*. [Online]

Available at: <http://www.racecar-engineering.com/formulastudent/>

Giaraffa, M., 2010. *Tech Tip: Springs and Dampers, Part One*. [Online]

Available at: [http://www.optimumg.com/docs/Springs%26Dampers\\_Tech\\_Tip\\_1.pdf](http://www.optimumg.com/docs/Springs%26Dampers_Tech_Tip_1.pdf)

Giaraffa, M., 2010. *Tech Tip: Springs and Dampers, Part Three*. [Online]

Available at: [http://www.optimumg.com/docs/Springs%26Dampers\\_Tech\\_Tip\\_3.pdf](http://www.optimumg.com/docs/Springs%26Dampers_Tech_Tip_3.pdf)

Giaraffa, M., 2010. *Tech Tip: Springs and Dampers, Part Two*. [Online]

Available at: [http://www.optimumg.com/docs/Springs%26Dampers\\_Tech\\_Tip\\_2.pdf](http://www.optimumg.com/docs/Springs%26Dampers_Tech_Tip_2.pdf)

IC-Kart, n.d. *Klasser*. [Online]

Available at: <http://www.crosskartno.mamutweb.com/subdet207.htm>

IMechE, n.d. *About FS*. [Online]

Available at: <http://www.formulastudent.com/aboutus/Welcome>

International, S., n.d. [Online]

Available at: <http://students.sae.org/competitions/formulaseries/fsae/>

Irgens, F., 1999. *Formelsamling mekanikk*. Trondheim: Tapir akademisk forlag.

Milliken, W. F. & Milliken, D. L., 1995. *Race Car Vehicle Dynamics*. s.l.:SAE International.

NBF, 2012. *Norgesmesterskap i Crosskart 2012*. [Online]

Available at: [http://bilsport.no/uploads/norgesmesterskap\\_i\\_crosskart\\_2012\\_net.pdf](http://bilsport.no/uploads/norgesmesterskap_i_crosskart_2012_net.pdf)

Norges Bilsportforbund, 2012. *Teknisk reglement for crosskart*. s.l.:NBF.

Norskcrosskart.com, 2012. *Hva er crosskart?*. [Online]

Available at: <http://www.norsk-crosskart.com/hva-er-crosskart.html>

NTNU, R., 2011. *Om oss*. [Online]

Available at: <http://www.revolve.no/nb/om-oss>

OptimumG, 2012. *OptimumKinematics Help File*. s.l.:OptimumG.

Reimpel, J., Reimpel, S., Betzler, J. & Betzler, H., 2001. *The Automotive Chassis; Engineering Principles*. 2nd ed. s.l.:Butterworth-Heinemann.

Riley, B., 2000. *Design and Analysis of Vehicular Structures*. [Online]

Available at: [http://rileydynamics.com/m-eng%20web/appendices/riley\\_meng\\_rev2.doc](http://rileydynamics.com/m-eng%20web/appendices/riley_meng_rev2.doc)

Rølvåg, T., 2011. *Car Suspension Theory*. [Online]

Available at: <https://www.dropbox.com/s/9ek0fq2gdcxj7hk/Car%20suspension%20theory.pdf>

SAE, F. & International, S., 2011. *2012 Formula SAE Rules*. [Online]

Available at: [http://www.fsaeonline.com/content/2012\\_FSAE\\_Rules\\_Version\\_90111K.pdf](http://www.fsaeonline.com/content/2012_FSAE_Rules_Version_90111K.pdf)

Soo, A. M., 2008. *Design, manufacturing, and verification of a steel tube spaceframe chassis for Formula SAE*. [Online]

Available at: <http://dspace.mit.edu/handle/1721.1/45320>

Splung.com, 2012. *Damped Oscillations*. [Online].

Staniforth, A., 2010. *Competition Car Suspension*. 4th ed. s.l.:Haynes.

umai1712, S. u., n.d. *Ride Comfort in Cars*. [Online]

Available at: <http://www.scribd.com/doc/86136410/Ride-Comfort-in-Cars>

WRC, F., 2012. *Ford WRC*. [Online]

Available at: <http://www.wrcford.com>

